Engineered Fibre-reinforced Concrete Systems for Bridge Deck Link Slab Applications

by
James F. Cameron

A thesis
presented to the University of Waterloo
in fulfillment of the
thesis requirement for the degree of
Master of Applied Science
in
Civil Engineering

Waterloo, Ontario, Canada, 2014

I hereby declare that I am the sole author of this thesis. This is a true copy of the thesis, including any required final revisions, as accepted by my examiners.

I understand that my thesis may be made electronically available to the public.

Abstract

Rehabilitation and maintenance of the aging transportation infrastructure are of major concern in the Province of Ontario. A large portion of this work is related to the durability of highway bridges around the province. One of the weakest points in a bridge structure from a durability aspect is the expansion joints that can allow harmful elements, such as road salts and contaminants to leak down from the road surface and attack the supporting structure of the bridge. Although expansion joints can be eliminated in the design of a new bridge, such as in an integral abutment bridge, this requires major changes to the supports and structure of the bridge, making it impractical for retrofitting existing bridges. One effective alternative is the replacement of a traditional expansion joint with a link slab. A link slab is a concrete slab used in place of an expansion joint to make the bridge deck continuous while keeping the supporting girders simply supported [1]. Link slabs must be able to resist large force effects both in bending and direct tension while minimizing cracking [2], one solution is to use the high tensile and flexural strength properties of an ultra-high performance fibre-reinforced concrete (UHPFRC) [3]. The UHPFRC mixtures are often proprietary and expensive. The purpose of this research was to evaluate the potential of using common fibre types with standard concrete ingredients in a fibre-reinforced concrete (FRC) as an alternative to UHPFRC in a link slab.

Using a selection of macro fibres commonly used in slab on grade applications for crack control, an optimized FRC mixture was developed following the principals established by Rossi and Harrouche [4]. This mixture was then used with a variety of fibre types to evaluate the structural and durability properties of the FRC. Testing was conducted for fresh mixture properties, compressive, tensile and flexural strength as well as freezing and

thawing resistance, linear shrinkage, environmental and salt exposure along with other durability tests.

Results showed that the concrete mixture used for an FRC link slab should consist of; an equal ratio of fine and coarse aggregate by weight and a higher than normal percentage of cement paste, for optimal workability and a dosage of 1.5% by volume of macro steel fibres. Hooked-end steel fibres resulted in the best performance increase to the FRC of the six fibre types tested. Results also showed that reinforcing cage for an FRC link slab should be designed to ensure that fibres can evenly reach all areas of the link slab form to give homogeneous fibre distribution. Although the FRCs created did not perform to the high level of a UHPFRC, these results show a consistent and effective FRC can be created, for use in a link slab with common fibres and standard concrete materials to provide a less expensive and more widely available FRC link slab than UHPFRC.

Acknowledgments

Special thanks to:

- The Ontario Ministry of Transport for funding and support of this project;
- Holcim Canada, Euclid Chamical, Propex and Fibercon International for their generous donation of testing materials;
- James G. McCants III at Testing, Engineering & Consulting Services, Inc. for assistance with the design of the ASTM C1609 testing apparatus;
- The project advisory committee of Dr. L. Mammoliti, Mr. M. Mahoney and Mr. M. Stanzel for their guidance on this project;
- The centre for pavement and transportation technology (CPATT) for testing equipment;
- Dr. M. Polak and Dr. M. Knight for reviewing and critiquing of this thesis

I would like to show my immense appreciation to my two supervisors Dr. Carolyn Hansson and Dr. Jeff West. Without your assistance and support this project would not have been possible. I have learned so much from the two of you and have gained an experience I will never forget.

Considerable thanks are due to Douglas Hirst, Rob Sluban and Richard Morrison in the University of Waterloo Civil Engineering Structures lab for all their support with sample design, casting and testing. Also, thank you to all the members of SLUG for your support and assistance working in the lab. Thanks to Matt Perrone and Scott Dion for assistance with sample construction and testing during their undergraduate research assistantships.

Thanks to my colleagues Yu (Tony) Hong, Matt Hunt, Mark Cremasco, Brad Bergsma, Tim Bandura and Colin Van Niejenhuis for your reliable help whenever, and with whatever, it was needed, no questions asked.

Thank you to all my friends both at the university and outside of it for their continued support throughout my research and schooling.

Lastly, I would like to thank my parents Jill and David Cameron for all the love and support they have given me over the years and for instilling me with the value of lifelong learning.

Table of Contents

List of Figures

List of Tables

List of Abbreviations

ASTM – ASTM International

CSA – Canadian Standards Association

FRC – Fibre-reinforced concrete

UHPFRC – Ultra-high performance fibre-reinforced concrete

NF – No fibre control concrete

PP – Polypropylene polyethylene FRC

St – Crimped steel FRC

HS – Hooked-end steel FRC

PVA – Polyvinyl alcohol FRC

SS – Deformed stainless steel FRC

BS – Deformed carbon steel FRC

S/G – Sand to gravel ratio

MOE – Relative dynamic modulus of elasticity

MOR – Modulus of rupture

1. Introduction

In the Province of Ontario there are over 2,700 highway bridges owned and maintained by the Ministry of Transport alone [5]. The maintenance and repair of these aging structures is a significant cost to the government each year. One of the biggest impediments to long-term durability of bridge structures in the Province of Ontario is the failure of traditional expansion joints. When the seals in a traditional expansion joint fail, it creates a break in an otherwise continuous bridge deck that will allow water, road salts and other harmful contaminants from the road surface to penetrate the deck and deteriorate the supporting structure of the bridge. One solution to the problems of expansions joints is to replace the joint with a link slab. A link slab is a flexible concrete section that connects the bridge decks in place of an expansion joint and allows for movement through deformation of the link slab. When a link slab is installed it makes the surface of the bridge continuous while the supporting girders remain simply supported. A link slab must be designed to withstand significant force effects with both bending moment and tensile loads. To resist these loads without cracking a link slab is commonly designed with a high volume of steel reinforcement which can make constructing a link slab difficult and costly.

To reduce the need for such a complex steel reinforcement cage, research has been done with ultra-high performance fibre-reinforced concrete (UHPFRC) to allow the concrete to handle higher load effects without cracking [3]. The increased flexibility and tensile resistance of the UHPFRC allows the amount of steel reinforcement required to prevent cracking to be reduced, simplifying the construction of a link slab. These UHPFRC mixtures are often expensive and the materials or mixture designs used are often kept

proprietary. This can become problematic when working with public sector projects that do not allow the specification of proprietary, sole source products that could result in high or unnecessary costs.

The purpose of this research was to determine if a fibre-reinforced concrete (FRC) mixture could be developed, from readily available, non-proprietary materials, which could be used in a link slab with significant structural and constructability benefit with minimal additional cost. Using the common concrete ingredients available in the Province of Ontario, a concrete matrix was developed to test multiple macro fibre types available on the market for their structural properties and durability, as well as the fresh properties of the FRCs they produce. Although not all fibre types could be tested, a variety were selected to represent the majority of possible options in the market to demonstrate what fibre types were the best options for an FRC link slab.

2. Literature Review

2.1. Link slabs

A fundamental problem with any large span bridge is expansion and contraction of the materials. To deal with this, most bridges employ one or more expansion joint to allow the materials to move freely. The problem with these expansion joints is that they become weak points in the deck structure allowing for deterioration to begin [6]. This weakness is due to expansion joints being a break in an otherwise continuous bridge deck surface. When a gap in the deck forms at an expansion joint, it allows water and road salts from the road surface to leak down onto the supporting structure of the bridge. Once the under structure of the bridge is exposed to this destructive environment it will start to cause damage [1], one example of which can be seen in Figure 2.1.

Figure 2.1 – Deterioration under failed expansion joint **[1]**

Once these contaminants start to damage the structure of the bridge it can become a serious problem. Unlike the deck surface that can easily be replaced, if the structure of the bridge is severely damaged it can be a major project to repair. Although expansion joints are highly problematic, they are the most common approach to allow for the expansion and contraction of the bridge due to thermal volume changes and shrinkage over time. To avoid this weakness, an alternative to

traditional expansion joints needs to be considered; one such alternative is a concrete link slab. A link slab can be used to convert an existing, simply supported bridge design to a bridge with a continuous deck over its full length [6] or installed in a new construction application. Although the bridge deck is made to be continuous, the girders remain simply supported making this an easy option for retrofitting existing structures [7] as shown in Figure 2.2.

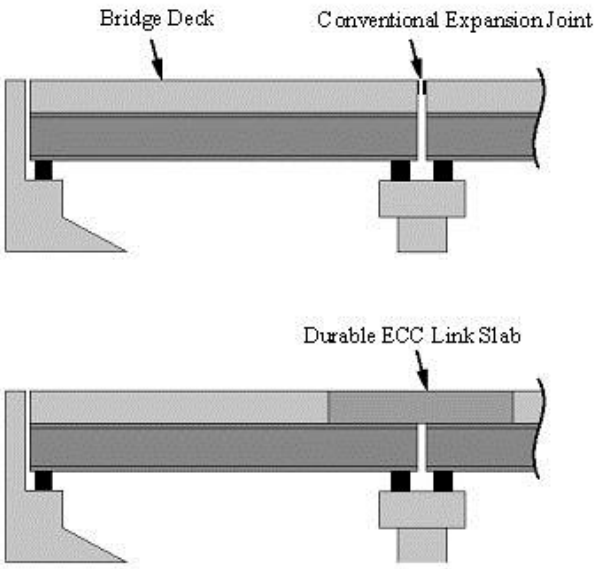

Figure 2.2 – Diagram of conventional expansion joint (top) replaced with a link slab (bottom) **[8]**

To compensate for expansion and contraction of the bridge, a link slab is added in place of a traditional expansion joint. This relatively flexible concrete section is designed to allow the bridge to move and bend under live loads and as the bridge expands and contracts with thermal change [2]. The current method for designing a link slab involves a heavy steel reinforcement cage throughout the link slab. This reinforcement is needed to control cracking in the link slab due to the high forces and moments generated in this area [9]. The addition of fibre-reinforced concrete

(FRC) can be used to reduce the amount of reinforcement required to handle the load as well as reduce the crack propagation and expansion throughout the link slab [3]. This reduction in traditional steel reinforcement can make link slabs easier and less expensive to construct, and the crack controlling properties of FRC will make link slabs more durable over the long-term. FRC should provide smaller crack widths under service loads than regular concrete, as well as, giving the concrete a ductile like behaviour after cracks have formed [10].

2.2. Fibre-reinforced concrete

The properties of Fibre-reinforced concrete can vary greatly based on the type and amount of fibre in the mixture. Some common advantages of fibre-reinforced concrete over traditional concrete are (i) a higher impact resistance [11] [12], (ii) improved strength and toughness [13], (iii) better tensile and flexural resistance [14], and (iv) crack width reduction [15]. The fibres act similarly to traditional reinforcing steel but on a smaller scale, evenly distributed through the concrete increasing tensile and flexural strength [14]. Fibres also bridge cracks restraining growth and propagation throughout the matrix, thereby increasing the toughness and giving the concrete better resistance to cracking [15]. This evenly distributed reinforcement also strengthens the concrete by holding it together under tensile and compressive loads. The addition of fibre to the concrete mixture can, however, increase the voids in the concrete matrix. If too many voids are present, it can weaken the concrete and reduce the effectiveness of the fibres as they are no longer securely anchored [14]. The modern use of fibre-reinforced concrete has

primarily been limited to controlling cracks from thermal and drying shrinkage in on grade floor slabs [16]. More recently, FRCs are being used and investigated for their structural and durability benefits. These two types of applications have very different approaches to the concrete mix design. Floor slabs often have little alterations to mix design and low fibre dosages of 0.5% by volume and lower [17]. The extent of the mix design for this type of FRC can be as little as the addition of a bag of fibres to a standard concrete mixture once the truck arrives on site, followed by the addition of a superplasticizer (high-range water-reducing agent) until the mixture reaches an acceptable consistency and workability [12]. On the other end of the spectrum, mixtures that take advantage of FRCs structural benefits, often referred to as ultra-high performance fibre-reinforced concrete (UHPFRC), have highly developed and strictly specified concrete mixtures that are usually kept proprietary [18]. These UHPFRC mixtures can contain moderate to high volumes of fibre, typically from 1% to 3% and above [13], with little or no coarse aggregate [18]. They often contain other admixtures such as silica fume and fly ash to further modify the properties of the FRC [19].

2.2.1. Fibre options

Most of the basic differences between FRC and standard concrete are common amongst all fibre types but, depending on what material is used as the fibre, different properties of the concrete can be altered and improved. ASTM International has set a standard for the production of FRC that defines all the materials and processes used in production. This standard is C1116/C1116M

Standard Specification for Fiber-Reinforced Concrete [20]. ASTM breaks down FRC in four concrete types based on the kind of fibre used in each type.

Type I refers to concrete that is made with steel fibres including stainless steel or carbon steel. Steel fibres are one of the most common fibre types and have been used in modern construction for many years [21]. Type I fibres are also governed by the ASTM Standard A820. ASTM further classifies steel fibres into five types based on the method used to produce them. The five types are [22]:

Type I: cold-drawn wire – Fibres made from wire that is cut to a specific length

Type II: cut sheet – Fibres cut from sheets of steel

Type III: melt-extracted – Fibres drawn from molten steel and rapidly cooled

Type IV: mill cut – Fibre mill cut from sheets of steel similar to Type II

Type V: modified cold-drawn wire – Type I fibres that have an added surface pattern for better anchorage

ASTM A820 describes the requirements for all steel fibres. Type I and type II fibres are specified by the measured dimensions, diameter or thickness and width, respectively, of the parent material before they are cut, where type III, IV and V are specified by the equivalent diameter of the actual fibres after production. All fibre types are required to pass both tension and bending tests, each on ten randomly selected samples per 4500 kg of material. The tension test

requires that the average tensile strength of the ten samples is at least 345 MPa and that no sample has a tensile strength less than 310 MPa. The bending test requires that at least nine of the ten samples can be bent around a 3.2 mm diameter pin to an angle of 90 degrees without breaking. Additionally, ten samples from every 4500 kg are measured to make sure that 90% of the samples do not vary from the nominal dimensions. Variations allowances are ±10% for length and equivalent diameter and ±15% for aspect ratio. The manufacturer is required to perform and provide proof of the above test unless otherwise specified in the purchase.

Type II FRC is concrete that is made with glass fibres known as glass-fibre-reinforced concrete (GFRC). GFRC is often used in the production of external cladding panels for buildings. Because of the higher tensile and bending strength [23] of the GFRC, the panels can be made thinner with the same effectiveness. This often makes the precast panels much lighter in weight than the standard concrete alternatives, making them easier to install and more cost effective. Glass fibres naturally have a low resistance to highly alkaline environments like concrete and will dissolve rapidly. Because of this, alkali resistant glass fibres were developed to improve the long-term performance in concrete, but these only slow the degradation of the glass fibres [24] so durability can still be a concern.

Type III is concrete reinforced with synthetic fibres such as nylon, polypropylene, polyethylene or carbon. Polypropylene-fibre-reinforced concrete is used in many applications, including decorative precast elements, but can also be used in structural situations to make thin wall elements for buildings or storage tanks [25]. Polyethylene is often used as a replacement for asbestos fibre reinforcement due to its similar properties while being less toxic. These synthetic fibres are made by extruding the material and chopping it into the desired length. Sometimes the surface of the strands is reworked giving them a rougher surface to adhere to the concrete matrix better [25]. If the fibres consist of a chopped polyolefin, such as polypropylene or polyethylene, they are required to meet the ASTM standard D7508 Standard Specification for Polyolefin Chopped Strands for Use in Concrete [26]. This standard states that micro fibres must be 3 – 50 mm in length with an equivalent diameter less than 0.3 mm, while macro fibres can be 12 – 65 mm in length with an equivalent diameter of 0.3 mm or larger . Macro fibres must have a breaking strength of at least 344 MPa. The most common application of these polyolefin fibres is for prevention of shrinkage cracks in large slabs [12] or where watertight concrete is required [27]. Another polymeric fibre that is gaining use in the market is polyvinyl alcohol (PVA). This fibre is often used in UFPFRC for structural applications. PVA fibres have been shown to have a strong bond with the concrete matrix and allow for an extremely flexible and ductile FRC [28]. Another kind of FRC in the type III category is carbon-fibre-reinforced concrete (CFRC). CFRC has extremely high strength in both bending and tension and has

been used in high strength structural elements such as exterior curtain walls. The first implementation of this on a large scale was in Tokyo where panels were able to be one third lighter than even the lightweight precast concrete counterparts [29].

Type IV fibres are any fibres of natural or organic origin. These fibres can come from many natural sources such as wood fibres or plant materials. Organic fibres that are made of cellulose material must meet the ASTM standard D7357 Standard Specification for Cellulose Fibers for Fiber-Reinforced Concrete [30]. Cellulose fibres must specify what organic material they are from, if unknown that must be specified, as well as what processing the material has undergone. Other materials must meet the specifications laid out in C1116 Standard Specification for Fiber-Reinforced Concrete [20] to prove that they are adequately resistant to deterioration within the concrete. In addition to plant fibre, animal fibres such as feathers have also been experimented with recently [31]. Natural fibres were often used as reinforcement in ancient times in some of the earliest forms of concrete. Many ancient cultures are known to have used natural fibres like straw and grass in building materials like adobe or clay bricks [21]. Although, natural fibres are not widely used in modern concrete construction, they are still often used in less developed countries where traditional building methods are used or where modern fibres are not easily accessible [32].

2.2.2. FRC mixture proportioning

Only a few studies have been conducted on how to proportion an FRC mixture and little has been done to develop a standard method for scientifically developing an appropriately proportioned mixture. Very few guidelines exist for the design of FRC. Some recommendations involve reducing the amount of aggregate used in the mixture [13]. Most commonly the large aggregate is reduced but these studies offer no exact way to determine how much aggregate should be removed. Others state that enough paste must be added to the mixture to thoroughly cover all the fibres, as well as, the aggregates to obtain adequate strength for the mixture [33].

One study with a more systematic approach was conducted by P. Rossi and N. Harrouche [4]. The design method that they developed involved two stages to optimize the mixture for FRC. A standard concrete mixture with no fibres is selected as a starting point for the optimization. The desired quantity of fibres is added to the mixture and a workability measurement is taken. The mixture is then repeated but with the ratio of fine aggregate to coarse aggregate, or the sand to gravel ratio (S/G ratio), changed while keeping the total volume of aggregate the same. The S/G ratio is varied until a peak workability of the mixture is observed. Once the optimal S/G ratio is found the workability of the mixture can then be modified to achieve a desired workability for the mixture by increasing or decreasing the amount of paste within the mixture, thereby

changing the workability without changing the water cement ratio or adding a superplasticizer [4].

2.2.3. Challenges with mixing, delivery and installation

One of the most well-known problems with FRC is the problem of placing and finishing the mixtures [12]. When fibres are added to a standard concrete mixture, they have a detrimental impact on the workability of the fresh concrete. This effect can often be as large as a 150 mm decrease of slump when working with some fibre types [34]. To combat the loss of workability, superplasticizer should be used to increase the slump rather than the addition of water, so that the water cement ratio is not increased and the strength of the matrix is not reduced [12]. If the reduction in workability is not solved, it can cause the finished concrete to have poor consolidation, causing strength and durability problems [35]. It is recommended that, when placing FRC, tools such as rakes not be used, as to not artificially orient the fibres in any direction. If vibration is needed, to use an external source of vibration so as to not disturb the uniformity of the fibres [36].

Another problem with FRCs centres on the addition and mixing of the fibres. Some recommendations call for the fibres to be premixed with the aggregates before addition to the truck [36] but this process is not feasible for most concrete batching facilities as existing plants are not set-up for this procedure [37]. Often the fibres are added to the truck once it arrives on site [36]. This can

cause problems with quality control if an inexperienced operator, who has not worked with FRC before, over or under mixes the FRC or adds water to the mix in place of superplasticizer. If an FRC is under-mixed the fibres will not be given a chance to distribute evenly throughout the mixture, leaving areas of higher and lower fibre content and causing varying properties throughout the finished concrete [36]. Conversely, if the fibres are over-mixed, similar problems can be created if the fibres begin to tangle and clump causing there to be areas of the FRC that are almost exclusively fibre with little concrete matrix to hold the FRC together [36]. If fibres are not evenly distributed throughout the mixture there will be observable losses in compressive and tensile strength.

2.2.4. FRC Testing

For the most part testing of FRC is similar to that of regular non-fibre concrete. No special requirements for FRC are specified by ASTM for compressive cylinder testing [38], splitting tensile testing [39], air content testing [40] or slump testing [41]. One test that has been specifically designed to be used to test the properties of FRC is ASTM C1609 Flexural Performance of Fiber-Reinforced Concrete (Using Beam With Third-Point Loading) [42]. This test was developed to determine the post-cracking flexural strength of an FRC. This test uses four-point bending in a closed loop system that runs at a constant rate of midpoint deflection. The resultant load and deflection are recorded up to, and beyond, cracking. With some fibre types and a high enough fibre content, the post-cracking responses can exhibit strain hardening and reach a higher load than

the initial cracking load. Other FRCs can exhibit high levels of sustained load long after the initial cracking of the concrete [42].

3. Experimental procedure

The research approach for this study was divided into three categories, as shown in Table 3.1. The first section was devoted to developing an FRC mixture suitable for use in a FRC link slab. This mixture needed to use commonly available fibres and standard concrete mixture ingredients. The second section was to evaluate as many fibre types as possible for structural benefits to the FRC mixture. The last stage was designed to test the long-term durability properties of the concrete, ensuring that the resulting FRC would perform at least as well as standard concrete over the lifespan of the bridge.

Table 3.1 – Research Approach

	Test	Method	Objective
Mixture optimization	Mixture optimization	Adjustment of S/G ratio and paste %	High workability and reliably consistent
	Compressive and tensile strength testing	Compressive and splitting tensile cylinder tests	Ensure optimized mixture has structural potential
Structural properties	Compressive strength testing	Compressive cylinder tests	Evaluate compressive strength of FRCs
	Tensile strength testing	Splitting tensile cylinder tests	Evaluate tensile strength of FRCs
	Flexural testing of FRC	ASTM C1609 – 4 point flexural test for FRC	Flexural strength, stiffness, ductility
	Flexural testing of FRC beams with steel reinforcement	FRC beams with steel reinforcement tested in flexure	Flexural strength and stiffness, crack control
Material durability properties	Outdoor exposure strain samples	Strain gauged samples in environmental conditions	Evaluate thermal and long-term volume changes
	Linear shrinkage testing	Length change of FRC samples	Evaluate potential shrinkage problems
	Freezing and thawing testing	ASTM C666 – FRC samples exposed to 300 cycles of +4 ° C to -18 ° C to +4° C	Evaluate long-term durability when reputedly exposed to winter conditions
	Rust staining observation	FRCs with carbon steel or stainless steel fibres exposed to road salt solution	Evaluate stainless steel as a potential alternative when rust staining is important

3.1. Mixture design

There are two distinct options when choosing a mixture design for FRC: there are highly engineered ultra-high performance fibre-reinforced concretes (UHPFRC) for structural applications, and then there are FRCs made by adding low doses of fibres to a standard concrete mixture to reduce shrinkage cracking. The problem with the first of these is they often come with a high cost and proprietary or secret ingredients, making them less than ideal for widespread use. On the other hand, adding low doses of fibres in standard mixtures may reduce cracking, but typically cannot be relied upon for increased mechanical properties. For this reason, a selection of common fibres were combined with available concrete mixture materials to develop an FRC that would have significant increases in mechanical properties while retaining the ability to be produced at an average Ontario ready mix or precast concrete plant without any major modifications.

3.1.1. Fibre types

The fibres selected for the study were primarily chosen based on those commonly used in Ontario. Other, less common fibre types, specifically, the polyvinyl alcohol and stainless steel fibres, were added to the study to investigate their potential benefits. Only macro fibres were selected for the study, due the need for them to bridge large cracks and provide greater beneficial properties in structural applications. All fibres selected conform to ASTM C1116 [20], are either Type I or Type III fibres for use in concrete and are commercially available products. Details of all fibre types are shown in Table 3.3.

3.1.1.1. Polypropylene polyethylene fibre

The polypropylene polyethylene fibre is a Type III synthetic fibre as described in ASTM C1116. The fibre was supplied by Euclid Chemical and is marketed as TUF-STRAND SF®. This fibre is a macro synthetic fibre made from a polypropylene polyethylene copolymer. The addition of the polyethylene to the fibre gives the fibre additional anchorage in the concrete. As the fibre is mixed into the concrete, the polyethylene begins to fibrillate or fray from the main fibre creating a larger surface area to bond with the concrete. This fibre is shown in Figure 3.1.

3.1.1.2. Crimped steel fibre

The crimped steel fibre is classified as a Type I steel fibre under ASTM C1116 and is further classified by ASTM A820 as a Type II sheet cut steel fibre. It has a deformed 'zig-zag' appearance as shown in Figure 3.2. Samples of this fibre were supplied by both Euclid and Propex. The fibres from the two suppliers were dimensionally and compositionally indistinguishable. A summarized version of the composition obtained with X-ray fluorescence (XRF) is shown in Table 3.2.

Table 3.2 – Crimped steel fibre composition analysis from XRF (weight %)

Supplier	Alloy	Mo	Fe	Mn	Cr	S	P	Si
Propex	Iron/CS	< LOD	98.739	0.883	0.009	0.022	0.027	0.263
Euclid	Iron/CS	0.008	98.742	0.809	0.074	0.030	0.025	0.186

3.1.1.3. Hooked-end steel fibre

The hooked-end steel fibre is classified as a Type I steel fibre under ASTM C1116 and a Type I drawn wire fibre under ASTM A820. This

fibre was supplied by Propex and is marketed under the name Novacon 1050®. The fibre has the appearance of steel wire with bent up ends to anchor it in the concrete as shown in Figure 3.3.

3.1.1.4. Deformed carbon steel fibre

The deformed carbon steel fibre is classified as a Type I steel fibre under ASTM C1116 and is further classified by ASTM A820 as a Type II sheet cut steel fibre. This fibre was supplied by Fibercon International Inc. and is sold under the name CAR25CDM. The fibre has a flat straight shape with stamped deformations along its length as show in Figure 3.4. This fibre was selected due to its dimensional similarity to the following stainless steel fibre supplied by the same company.

3.1.1.5. Deformed stainless steel fibre

The deformed stainless steel fibre is classified as a Type I steel fibre under ASTM C1116 and Type II sheet cut steel fibre under ASTM A820. This fibre is dimensionally the same as CAR25CDM from Fibercon International Inc., but is made from a 430 grade stainless steel instead of low carbon steel. This fibre is shown in Figure 3.5.

3.1.1.6. Polyvinyl alcohol (PVA) fibre

The PVA fibre is classified by ASTM as a Type III synthetic fibre. The fibre is made from polyvinyl alcohol and has an appearance as shown in Figure 3.6. This fibre is produced by Nycon and is called PVA – RF 4000.

Figure 3.1 – Polypropylene polyethylene fibre

Figure 3.2 – Crimped steel fibre

Figure 3.3 – Hooked-end steel fibre

Figure 3.4 – Deformed carbon steel fibre

Figure 3.5 – Deformed stainless steel fibre

Figure 3.6 – Polyvinyl alcohol (PVA) fibre

Table 3.3 – Fibre properties (as reported by manufacturer)

Name	Length (mm)	Aspect Ratio	Specific Gravity
Polypropylene polyethylene	51	74	0.92
Crimped steel	50	45	7.7
Hooked-end steel	50	50	7.7
Deformed carbon steel	25	41	7.7
Deformed stainless steel	25	41	7.7
Polyvinyl alcohol (PVA)	30	45	1.3

3.1.2. Mixture optimization

Initially, two commonly available fibres were selected for the mixture optimization: the crimped steel fibre and the polypropylene polyethylene fibre. An initial mixture design was selected from a common highway bridge concrete mixture used in Ontario. This mixture was then modified following a method based on that outlined by P. Rossi and N. Harrouche [4], where an initial mixture with fibre added is chosen and then incrementally modified to optimize the workability. This is done by first holding constant the cementitious content, total aggregate content, fibre volume and water/cementitious (w/c) ratio while varying the ratio of fine aggregate to coarse aggregate, or the ratio of sand to gravel (S/G). The workability is then determined by a slump test and the optimum ratio is selected as that exhibiting the highest workability. To further adjust the workability, the amount of cement paste in the mixture is adjusted until the desired workability is achieved. This adjustment is made by increasing or decreasing the amount of water and cementitious materials added to the mixture, while keeping the w/c ratio and the optimum S/G ratio constant. This mixture optimization procedure was carried out for 1% and 2% by volume of the crimped steel fibre and polypropylene polyethylene fibres and a no fibre control mixture. Shown in Table 3.4 is a sample mixture optimization for the 1% polypropylene polyethylene FRC with the selected S/G ratio in bold face. All mixtures carried out in the optimization procedure are shown in Appendix A.

Table 3.4 – Optimization mixtures for the 1% polypropylene polyethylene FRC (per cubic metre)

		S/G ratio				Paste percentage (%)			
	Units	0.7	1	**1.5**	2	26.75	30.0	32.5	35.0
Gravel	kg	1042	886	**709**	591	709	677	653	629
Sand	kg	730	886	**1063**	1181	1063	1016	980	944
GU cement	kg	263	263	**263**	263	263	295	320	345
Slag	kg	88	88	**88**	88	88	99	107	115
Fibre	kg	10	10	**10**	10	10	10	9	9
Air entrainer	mL	235	235	**235**	235	235	235	235	235
Superplasticizer	mL	333	333	**333**	333	900	1009	1093	1177
Total water	L	157	157	**157**	157	157	176	190	204
Slump	mm	0	3	**5**	0	0	40	90	180

With each batch mixed in the optimization phase, cylinders were cast to perform both compression testing and splitting tensile strength tests. This information was used to determine if the optimized mixture would have significant structural properties to be considered for further testing. Once an optimized mixture was found for fibre type and dosage, it was seen that the optimal proportions were similar across all mixtures. For simplicity it was assumed that the same mixture proportions could be used with all six fibre types for material property tests. The optimal S/G ratio was found to be in the range of 1-1.5 and as a result a ratio of 1 was selected to reduce the volume of sand required and minimize the change from the original mixture. A paste percentage of 35% was selected for the FRCs because it gave adequate workability without the need for a superplasticizer. A dosage of 1.5% fibre volume was selected as an upper limit on what would be commercially used, while still maintaining the benefits of a high fibre content. The mixtures used for further material properties testing are shown in Table 3.5.

Table 3.5 – Optimized mixtures used in FRC material property testing (per cubic metre)

Mix	Units	No fibre	1.5% Polypropylene polyethylene	1.5% Crimped steel	1.5% Hooked-end steel	1.5% PVA	1.5% Deformed stainless steel	1.5% Deformed carbon steel
Gravel (19mm)	kg	828	781	781	781	781	781	781
Sand	kg	828	781	781	781	781	781	781
GU cement	kg	319	344	344	344	344	344	344
Slag	kg	107	115	115	115	115	115	115
Fibre	kg	0	14	116	116	20	116	116
Air entrainer	mL	237	233	233	233	233	233	233
Total water	L	190	204	204	204	204	204	204
S/G	-	1.0	1.0	1.0	1.0	1.0	1.0	1.0
Paste %	-	32.5	35	35	35	35	35	35

3.2. Material preparation

3.2.1. Concrete mixing

One of two concrete shear pan type mixers was used for mixing each of the concrete batches. One mixer had a capacity of approximately 0.2 cubic metres (large mixer), shown in Figure 3.7, while the other had a capacity of 0.05 cubic metres (small mixer), shown in Figure 3.8. Each mixture was designed to have an optimal volume for either the large or small mixer to ensure that adequate mixing of the material was achieved.

Figure 3.7 – Large lab mixer

Figure 3.8 – Small lab mixer

3.2.2. Concrete casting

All specimens were cast in accordance with ASTM C192 [43]. Moulds were either made of wood, steel or plastic depending on the sample type. External

vibration was used to give optimal compaction of the concrete. The external vibration was provided by a vibration table, on which moulds were placed for 10 to 15 seconds after each lift of concrete was added. Samples were then finished with a magnesium float and covered with wet burlap and plastic. After 24 hours, samples were de-moulded and placed in a high humidity curing room until testing. This procedure was followed for all samples unless otherwise stated.

3.3. Fresh properties

Fresh properties were tested to establish the workability of the mixture, and to give an indication of whether the concrete was mixed and proportioned correctly and met Provincial air content requirements.

3.3.1. Slump testing

A slump test was conducted on each batch of concrete produced following ASTM C143 [41] or CSA A23.2-5C [44]. Slump was tested to determine the workability of the concrete. Some slump tests were conducted before and after fibres were added in the preliminary optimization phase to gain a better understanding of the effects of fibres on workability. Thereafter, slump was only tested after the fibres were added.

3.3.2. Air content testing

Air content testing was conducted in accordance with CSA A23.2-4C [44] on all concrete mixes produced. The air content was measured and recorded to assess

the consistency of the concrete mixture as well as to ensure the concrete would meet Provincial specifications of 5-8% air entrainment [45].

3.4. Structural properties

The structural properties of the various FRC mixes were evaluated to determine useful properties that can be applied to design. Compressive and splitting tensile strength was tested as well as the flexural properties of both reinforced and unreinforced FRC.

3.4.1. Compressive strength testing

Compressive strength testing was completed on three samples for every batch of concrete produced in accordance with ASTM C39 [38]. Cylindrical samples were cast in D100 x 200 mm plastic moulds and were placed directly into the high humidity curing room. When samples were de-moulded, they were again placed in the high humidity room until testing at 28 days. This curing method was followed for all samples, except during the optimization phase, where samples were cured wet for two weeks and set out in ambient conditions for the remaining two weeks to better simulate real world conditions.

At 28 days, the sample ends were ground flat and parallel, then samples were placed in a hydraulic testing machine and tested until failure. Failure load and strength were automatically determined and recorded by the testing machine.

3.4.2. Splitting tensile strength testing

Splitting tensile strength testing was completed on three samples for every batch of concrete. Samples were cured in the same way as explained in 3.4.1 for the compressive strength samples. At 28 days the sample lengths were measured and recorded, and samples were placed in a splitting tensile testing apparatus as shown in Figure 3.9. This was then positioned in the hydraulic testing machine and tested until failure, with the machine automatically recording the peak load from which the tensile strength was calculated.

Figure 3.9 – Splitting tensile testing apparatus

3.4.3. Flexural testing of FRC

Samples were cast in 150 x 150 x 500mm wooden moulds, to create samples as shown in Figure 3.10, in accordance with ASTM C1609 [42]. A testing support set-up was designed and fabricated within ASTM C1609 guidelines, with

modifications currently recommended by the committee that are yet to be adopted by ASTM and with advice from the personal experience of M. Mahoney [46] and J. McCants [47]. Concrete mixtures were cast with 1.5% by volume of each of the six fibres described above, in addition to a no fibre control mixture. Samples were moist cured for 28 days and tested in a 100 kN capacity hydraulic test frame as shown in Figure 3.11. Control of the frame was done by a closed loop system with displacement transducers mounted at the midpoint of the concrete specimens. Data from a load cell as well as the displacement transducers were automatically collected by the computer system. The rate of displacement was adjusted based on the guidelines in ASTM C1609 and the test was run until the displacement reached approximately 4mm so that data were collected at least to the displacement equal to 150^{th} of the span length ($L/150$). After the test was completed on three of each FRC type, one sample was replaced in the test frame and loaded to the point of total separation to allow the fracture surface to be examined.

Figure 3.10 – ASTM C1609 beams in moist curing

Figure 3.11 – ASTM C1609 test set-up in testing frame

3.4.4. Flexural testing of FRC beams with steel reinforcement

Three sets of two beams were cast with embedded reinforcing steel cages as shown in Figure 3.12. Each beam measured 150 mm by 100 mm and 1.9 m in length. The beams contained two 10M steel reinforcing bars at a depth of 100 mm with shear reinforcement stirrups outside of the maximum moment zone to

prevent premature shear failure. A reinforcement depth of 100 mm was selected because it resulted in similar reinforcement and effective depth to overall depth ratios of that used in a link slab constructed by the ministry of transport in Ontario.

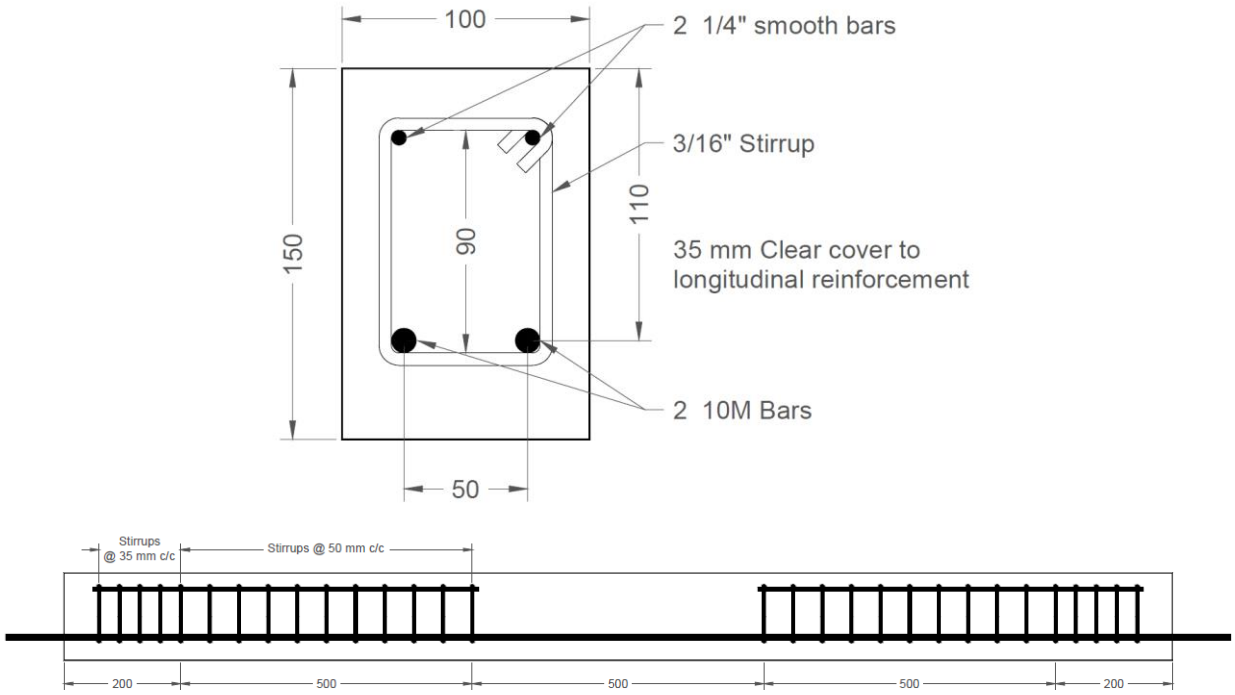

Figure 3.12 – Reinforced FRC flexural beam layout (mm) (NTS)

These cages are shown in Figure 3.13 before they were installed in the moulds and in Figure 3.14 after they were placed in the moulds. Each set of two beams was cast with a different concrete mixture: one control standard concrete with no fibres, one FRC with 1.5% by volume polypropylene polyethylene fibres and one with 1.5% by volume hooked-end steel fibres. After the concrete was added to the moulds, a handheld pencil vibrator was used to provide both internal and external vibration to the beams to assure proper consolidation of the beams.

The beams were then wet cured under burlap for one week and then removed from their moulds and stored in ambient interior conditions until testing.

Figure 3.13 – Reinforcement cages for reinforced FRC beams

Figure 3.14 – Forms used for reinforced FRC beams

Tests were conducted 28 days after casting of the reinforced FRC beams. The beams were tested sequentially in a four point hydraulic testing frame with load points spaced at 500 mm as shown in Figure 3.15. Each beam was then tested at a constant displacement rate of 1 mm per minute with displacement measured at the centre point of the beam. Additionally, the test was paused at regular load intervals and photographs of the crack pattern were taken along with crack width measurements using a crack microscope. The tests were continued until a point when an obvious condition of failure was observed.

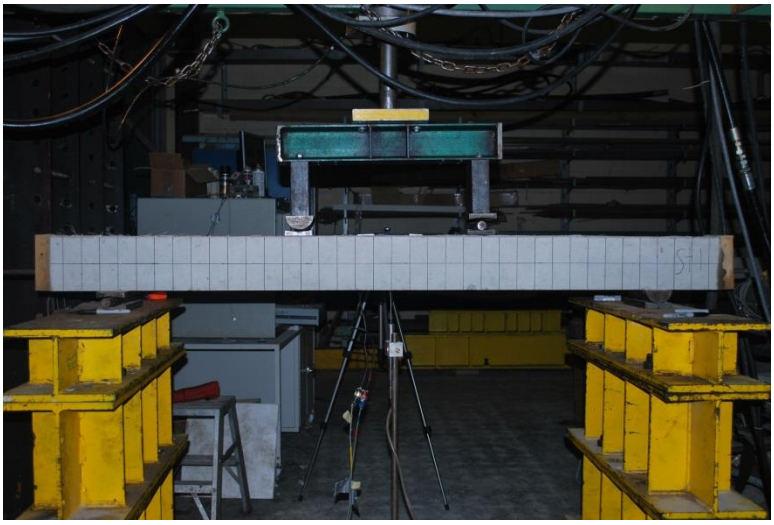

Figure 3.15 – Reinforced FRC beam test set-up

3.5. Material durability properties

3.5.1. Outdoor exposure strain samples

Samples were cast to measure the effects of long-term environmental exposure on FRC. These samples measured 330 x 457 x 254mm (13 x 18 x 10”) and had a 50mm (2”) deep ponding well cast into the top surface of the sample as shown in Figure 3.16. Each sample had two or three embedded vibrating wire strain gauges with thermistors that were placed at mid height prior to casting.

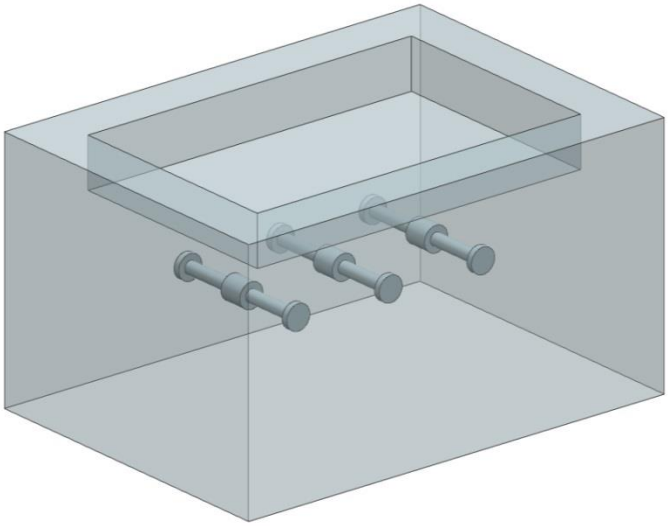

Figure 3.16 – Design of outdoor exposure samples with embedded strain samples

The concrete mixture used was the standard non-optimized mixture with either 0.5% crimped steel fibres or 0.5% polypropylene polyethylene fibre added or a control mixture. These mixtures are shown in Table 3.6.

Table 3.6 – Concrete mixtures used in outdoor exposure strain samples

	Units	No Fibre	Crimped steel FRC	Polypropylene polyethylene FRC
Gravel (19mm)	kg	1060	1060	1060
Sand	kg	730	718	723
GU cement	kg	266	266	266
Slag	kg	89	89	89
Crimped steel fibre	kg	0	45	0
PP fibre	kg	0	0	5
Air entrainer	mL	237	237	237
Water reducer	mL	800	800	800
Superplasticizer	mL	900	900	900
Water	L	159	159	159

Due to the long-term nature of this experiment, samples were cast early in the research period and, as a result, have a much lower dosage of the fibres than other mixtures tested. Because optimized mixture had yet to be carried out basic manufacturer's recommendations were used for selecting a fibre dosage. Two samples were cast with each mixture type and were cured under burlap and plastic for 7 days before being moved to an exposed outdoor location where they were subjected to the natural elements and temperature conditions of Southern Ontario. The ponding well of one sample of each type was filled with sodium chloride (NaCl) (analysis shown in Appendix B) road salt brine while the other was filled with water. The ponding wells were refilled or replenished when necessary. Strain and temperature measurements were automatically collected hourly by a data logger starting from approximately 2 hours after

concrete placement up to 96 weeks of exposure, excluding the time taken to move samples outside and reconnect the gauges.

3.5.2. Linear shrinkage testing

Shrinkage samples were cast from each of the batches used for the ASTM C1609 samples. Steel moulds were used with dimensions of 75 x 75 x 254 mm, shown in Figure 3.17, to cast samples with embedded stainless steel gauge studs at each end as shown in Figure 3.18.

Figure 3.17 – Linear shrinkage mould

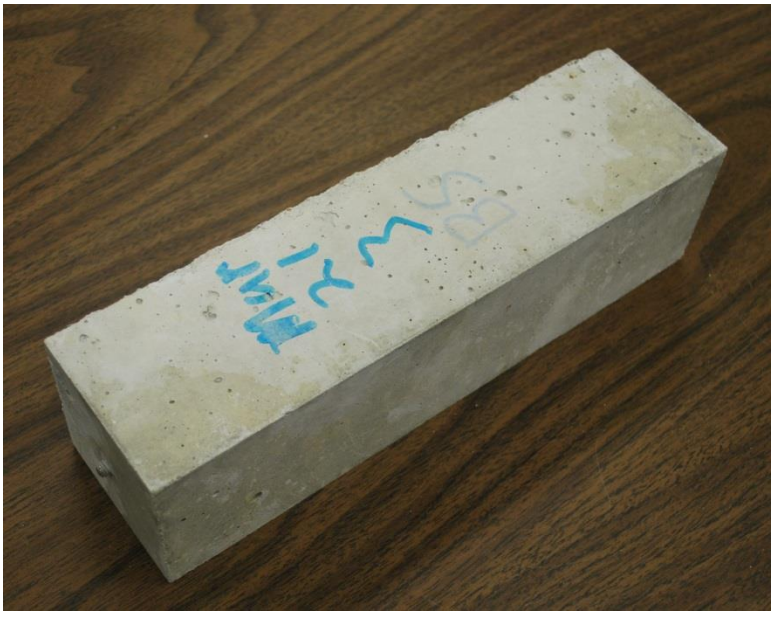

Figure 3.18 – Linear shrinkage sample

Test Method LS-435, Rev. No. 23 [48] provided by the Ontario Ministry of Transportation was followed where possible. LS-435 is similar to ASTM C157. Samples were de-moulded at approximately 24 hours from the time of casting, a length reading was taken and the samples were placed in a lime ($Ca(OH)_2$) saturated water bath as described in LS-435. At 7 days of age, the samples were removed from the bath and the initial "zero length change" reading was taken with a length comparator as shown in Figure 3.19.

Figure 3.19 – Measurement of length change with length comparator

Samples were then stored in a sealed container for the reminder of the test except when measurements were taken. Length change measurements were taken at 1, 7, 8, 14, 21, 35, 56 and 112 days of age with an additional measurement at 224 days if time allowed within the duration of the research.

3.5.3. Freezing and thawing cycle testing

Samples for freezing and thawing testing according to ASTM C666 [49] were cast from the same concrete mixture as the samples for the ASTM C1609 tests. Steel moulds were used to cast samples 76 x 102 x 406 mm (3 x 4 x 16") in size. Samples were stored in a high humidity room or in saturated lime water until time of testing. Initial weight and fundamental frequency measurements were taken and recorded before samples began the freezing and thawing cycles. Samples were then submerged in water and were placed in a freeze-thaw chamber, as shown in Figure 3.20.

Figure 3.20 – Freeze-thaw chamber with samples

The chamber was set to cycle between +4°C and -18°C and back to +4°C approximately every 3 hours. The internal temperature of a concrete dummy specimen was recorded every 10 minutes with an automatic data logger. After 7 days (approximately 50 freezing and thawing cycles), the samples were removed and their weight and fundamental frequency measurements were again taken and recorded. The fundamental frequency was measured with an

ultrasonic frequency testing unit within the range of 1 to 5 kHz, shown in Figure 3.21.

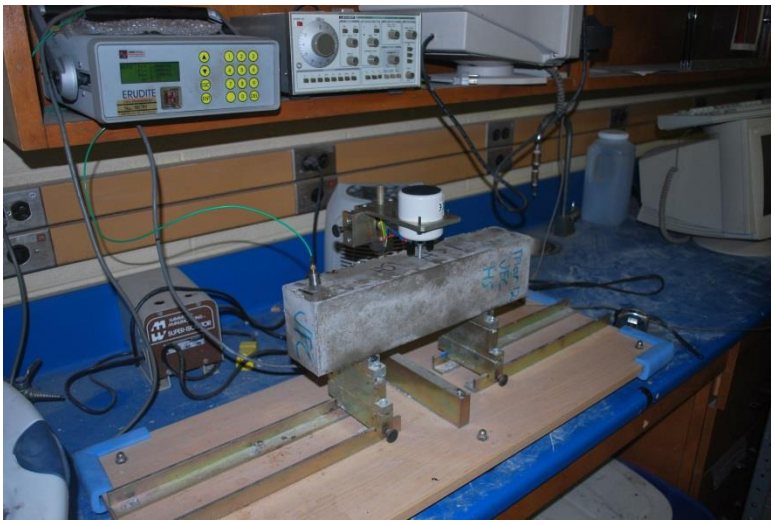

Figure 3.21 – Ultrasonic testing set-up for fundamental frequency

After measurement, samples were replaced in the chamber and measurements were repeated every 7 days, until 300 freezing and thawing cycles had been completed.

3.5.4. Rust staining observation

A common problem with steel fibres is the spotted rust staining that appears on the surface of the concrete after time. To evaluate if this problem could be avoided by using stainless steel fibres, a qualitative test was developed. Two standard D100 x 200 mm cylinders were cast, one containing the deformed carbon steel fibres the other containing the deformed stainless steel fibre with the same dimensional properties. Each cylinder was cut in half to expose an internal surface as well as the cast outer surface. The half cylinders were placed together in a bath of calcium chloride ($CaCl_2$) anti-icing road salt solution as

shown in Figure 3.22. Analysis of calcium chloride solution is shown in Appendix B. The cylinders were then observed and photographed over time to observe differences in the rust staining of the surfaces.

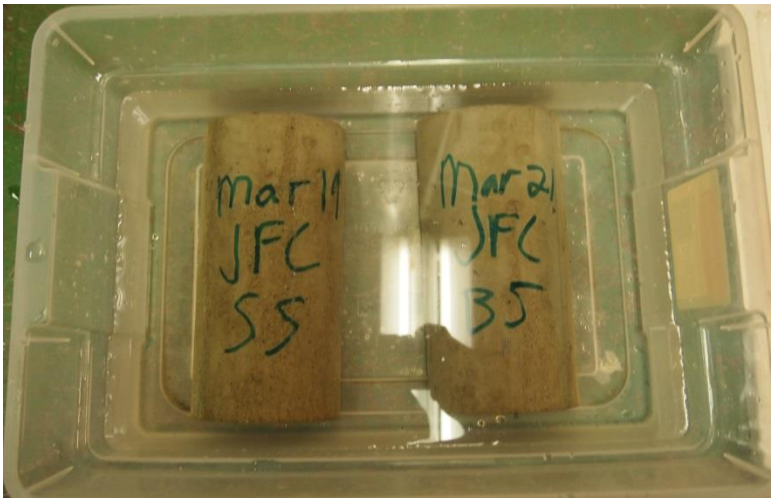

Figure 3.22 – Half cylinders in salt solution

4. Results

4.1. Mixture design

4.1.1. Mixture optimization

The mix design optimization was carried out based on a standard mix for non-FRC concrete that is currently used in the province of Ontario for bridge construction. The two proportions that were varied in the optimization process were the sand to gravel (S/G) mass ratio and the volume paste percentage. These were found to be 0.7 and 26.75% respectively for the standard mixture. The selected testing values for the S/G ratio were the initial 0.7 increasing to 1, 1.5 and 2. The values of paste content were chosen as 26.75%, 30%, 32.5% and 35% paste.

4.1.1.1. Slump testing

Using the results of the slump test, the optimal sand to gravel (S/G) ratio was selected for each fibre type. The results of the slump tests on the optimization mixes are shown in Table 4.1 for the no fibre mixture, polypropylene polyethylene (PP) FRC and the crimped steel (St) FRC.

Table 4.1 – Slump values for S/G ratio optimization (mm)

S/G	No Fibre	1% PP FRC	2% PP FRC	1% St FRC	2% St FRC
0.7	30	0	0	0	NA
1	45	3	NA	35	90
1.5	0	5	0	0	70
2	0	0	NA	0	60

After each sand gravel optimization set was conducted, an optimal ratio was selected from the mix with the peak slump. Peak slump was observed for most mixes to be in the range of 1 to 1.5 sand gravel ratio

as seen in Table 4.1. Once an appropriate S/G ratio was selected, shown for each mixture in Table 4.2, it was used in the next test where the percentage of paste in the mixture was varied and the increase in slump was recorded for each mix as shown in Table 4.2.

Table 4.2 – Slump values for paste percentage optimization (mm)

Paste	No Fibre	1% PP FRC	2% PP FRC	1% St FRC	2% St FRC
S/G	1.0	1.5	1.5	1.0	0.7
26.75%	0	0	0	30	5
30.0%	70	40	20	150	120
32.5%	175	90	NA	230	170
35.0%	NA	180	140	NA	185

As can be seen in Table 4.2, as the paste content increased, the slump and workability of the mix also increased. Some mixes in the paste percentage sets were not done to save time if a reasonable trend was established. These are designated in the table by "NA".

4.1.1.2. Air content testing

Air content tests were conducted on each batch made in the optimization phase to establish how changing the variables would affect the air content of the FRC mixes. The air contents for each FRC mix are show in Table 4.3.

Table 4.3 – Air content for FRC optimization

S/G	No Fibre	1% PP FRC	2% PP FRC	1% St FRC	2% St FRC
0.7	2.5%	3.5%	5.0%	5.0%	4.5%
1	4.0%	5.0%	NA	3.5%	7.0%
1.5	7.0%	6.5%	8.0%	9.0%	8.0%
2	7.0%	11.0%	NA	6.0%	7.0%
Paste	No Fibre	1% PP FRC	2% PP FRC	1% St FRC	2% St FRC
26.75%	6.0%	9.0%	8.0%	3.5%	4.0%
30.0%	4.5%	5.5%	5.0%	6.0%	5.0%
32.5%	4.5%	7.0%	NA	6.5%	5.5%
35.0%	NA	7.0%	9.0%	4.0%	6.0%

4.1.1.3. Compressive strength testing

Compressive cylinder tests were conducted 28 days after casting of each batch in the optimization phase. Cylinders were wet cured for two weeks and cured in ambient conditions for the remaining two weeks to simulate real world casting conditions. The average compressive strength of three specimens for each concrete mixture is shown in Table 4.4 with full results shown in Appendix C.

Table 4.4 – Average 28 day compressive strength for FRC optimization mixes (MPa)

S/G	No Fibre	1% PP FRC	2% PP FRC	1% St FRC	2% St FRC
0.7	53.08	58.46	37.59	64.09	45.98
1	49.57	52.42	NA	54.66	42.61
1.5	56.21	52.64	48.69	59.65	42.46
2	51.34	50.89	NA	58.27	40.90
Paste	No Fibre	1% PP FRC	2% PP FRC	1% St FRC	2% St FRC
26.75%	57.92	50.70	48.69	55.11	45.13
30.0%	53.82	50.52	49.57	50.30	41.27
32.5%	51.01	48.06	NA	50.93	38.87
35.0%	NA	47.48	40.57	53.39	41.02

4.1.1.4. Splitting tensile testing

Splitting tension cylinders were tested at 28 days alongside the compressive cylinders from their respective mixes. Cylinders were cast and stored in the same manner as the compressive cylinders. The average splitting tensile strength was calculated with the equation given in ASTM C496 as:

$$T = \frac{2P}{\pi l d}$$

Where:

T is the splitting tensile strength in MPa

P is the maximum load at failure in N

l is the length of the cylinder in mm

d is the diameter of the cylinder in mm

Three cylinders from each mixture were tested in the splitting tensile testing apparatus and the average splitting tensile strength of each mixture is presented in Table 4.5 with full results shown in Appendix D.

Table 4.5 – Average 28 day splitting tensile strength for FRC optimization mixes (MPa)

S/G	No Fibre	1% PP FRC	2% PP FRC	1% St FRC	2% St FRC
0.7	4.32	4.98	4.53	7.15	5.49
1	4.18	4.82	NA	5.72	5.15
1.5	4.16	5.43	5.26	6.93	5.52
2	3.83	4.96	NA	5.84	4.68
Paste	No Fibre	1% PP FRC	2% PP FRC	1% St FRC	2% St FRC
26.75%	3.90	5.08	5.26	5.87	5.93
30.0%	3.88	4.63	5.06	4.98	5.42
32.5%	4.24	4.60	NA	5.68	5.44
35.0%	NA	4.58	4.28	5.34	5.29

4.2. Structural properties of FRC with selected fibre types

After optimization, a fibre dosage of 1.5% by volume was selected with a sand gravel ratio of 1:1 and a high 35% paste percentage to achieve optimal workability and strength for all fibre type. The selected mixes are shown in Table 3.5. Samples were cast to evaluate further the structural properties of the FRC mixes. The fibre types tested were polypropylene polyethylene, crimped steel, hooked-end steel, PVA, deformed stainless steel and deformed carbon steel to evaluate as many of the commercially available fibre products as possible for potential benefits.

4.2.1. Flexural testing of FRC

ASTM C1609 flexural testing was conducted on six FRC mixtures and a control mixture of no fibre concrete. The ASTM C1609 test is specifically designed to test the post-cracking behaviour of the FRC. Because the control mixture did not have fibres, it did not exhibit any post-cracking behaviour. The full load deflection curve for the no fibre control concrete is shown in

Figure 4.1 while Figure 4.2 shows the data on the same abscissa scale as for the other fibre types to allow comparison.

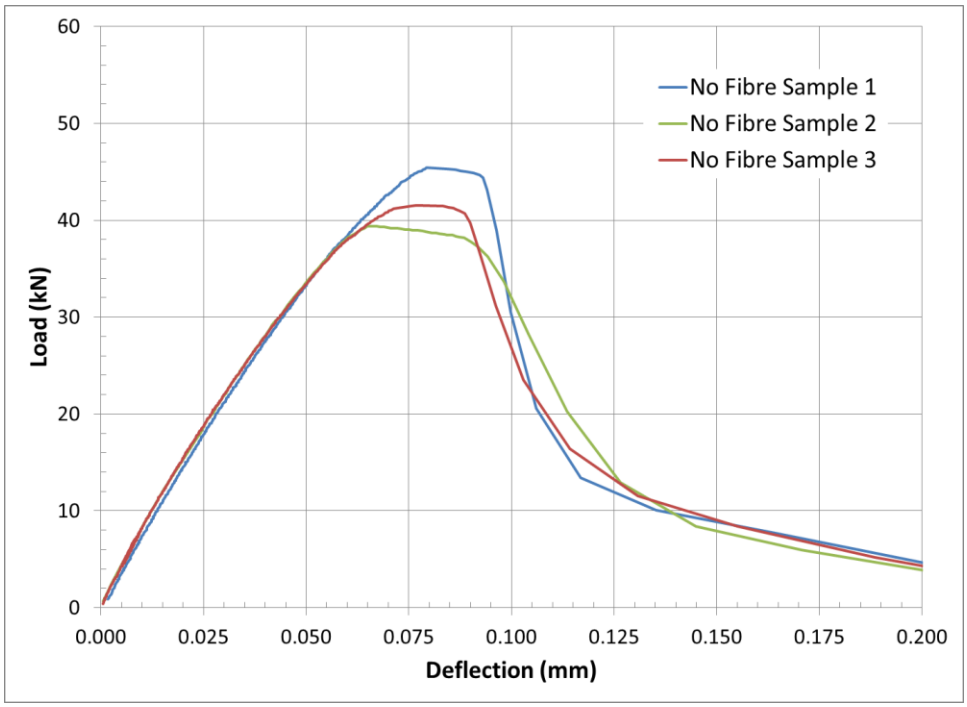

Figure 4.1 – Flexural load deflection curves for no fibre control

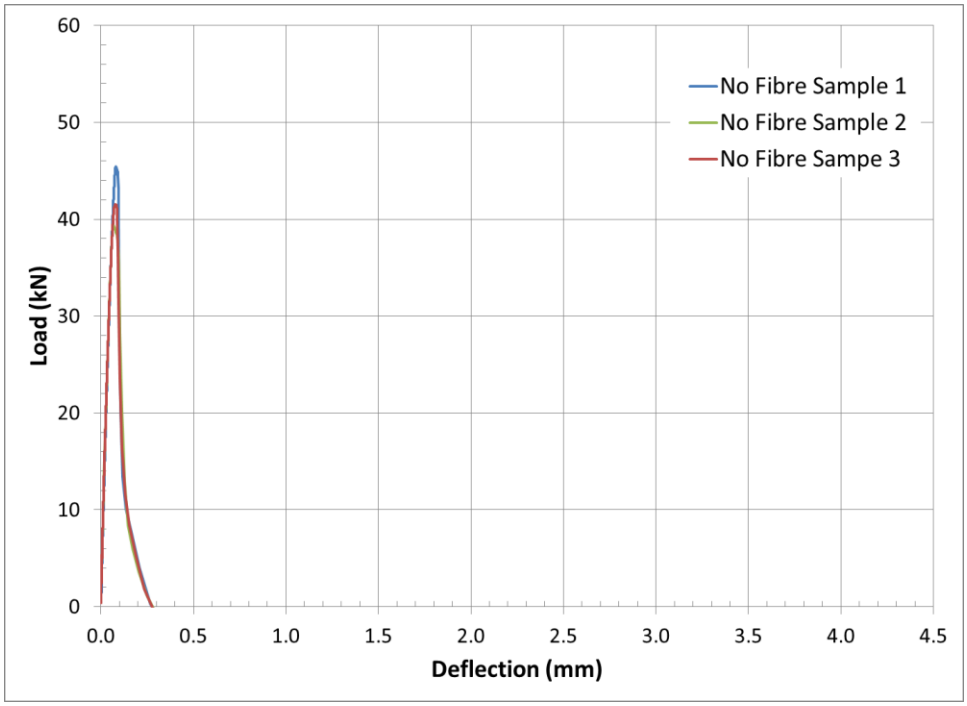

Figure 4.2 – Flexural load deflection curves for no fibre control (common scale)

The first set of flexural testing was conducted on the no fibre control concrete, the polypropylene polyethylene and crimped steel FRCs. The load deflection curves for these FRCs are shown in Figure 4.3 and Figure 4.4 respectively. The polypropylene polyethylene FRC displays a larger initial load drop after cracking but with a flat post-cracking response, whereas, the crimped steel fibre shows a more gradual and consistent decline in strength over the post-cracking region. The polypropylene polyethylene FRC shows a large drop off immediately after cracking in all three samples which were believed to be a result of a slow reaction of the frame to respond when the beams crack because, when the tuning of the frame was adjusted to a faster response rate, this drop was not seen in other samples. The actual response is believed to follow a more direct transition from the peak load to the sustained load region.

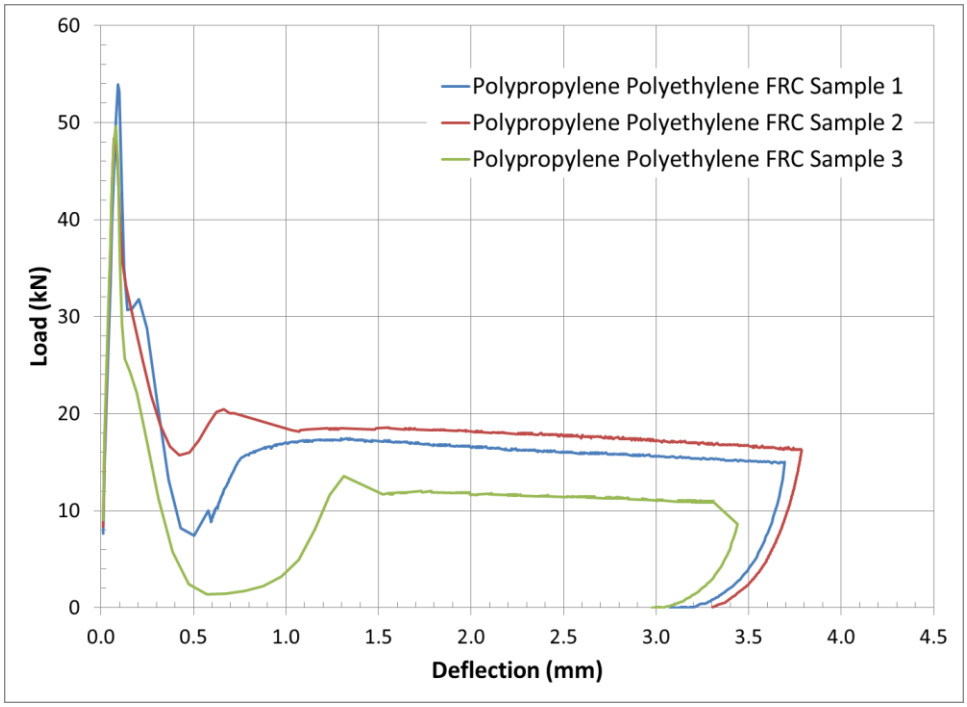

Figure 4.3 – Flexural load deflection curves for polypropylene polyethylene FRC

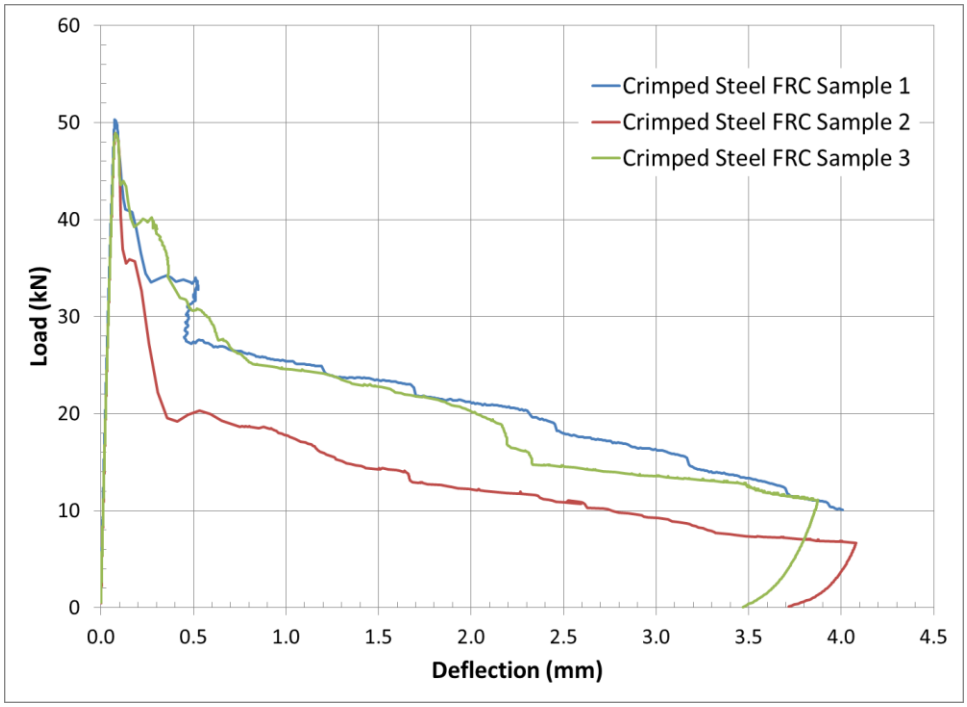

Figure 4.4 – Flexural load deflection curves for crimped steel FRC

Figure 4.5 through Figure 4.8 show the load deflection curves for the hooked-end steel, PVA, deformed stainless steel and deformed carbon steel FRC samples.

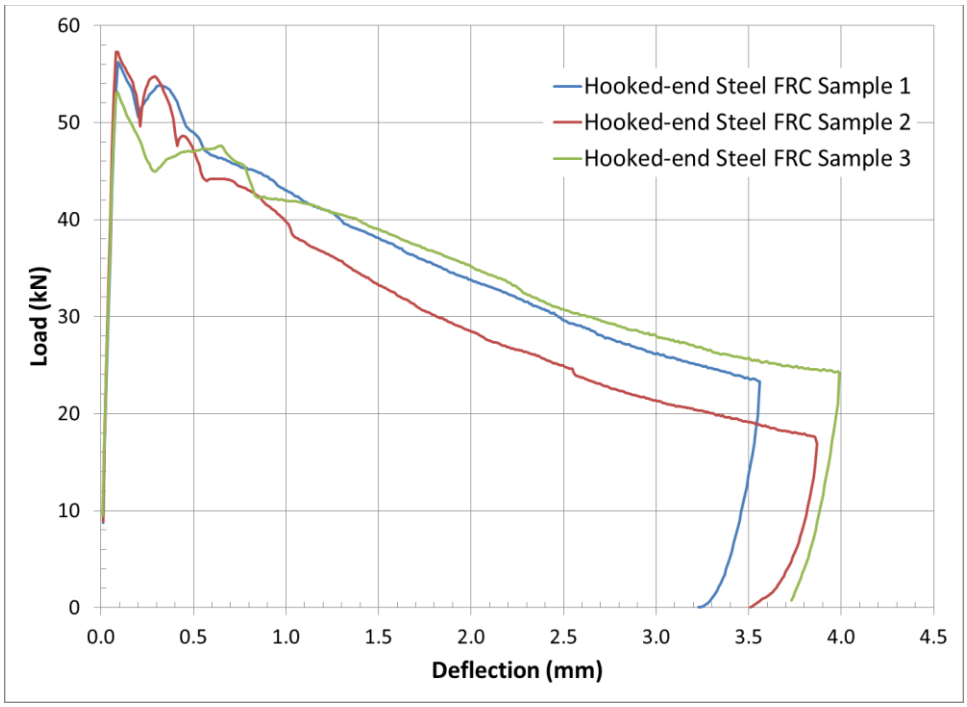

Figure 4.5 – Flexural load deflection curves for hooked-end steel FRC

When testing the flexural beams for the PVA FRC, problems with the constancy of the power supply to the lab because of a local storm caused one of the samples and the backup samples to fail without complete data collection. As a result there are only two load deflection data sets shown for the PVA FRC in Figure 4.6.

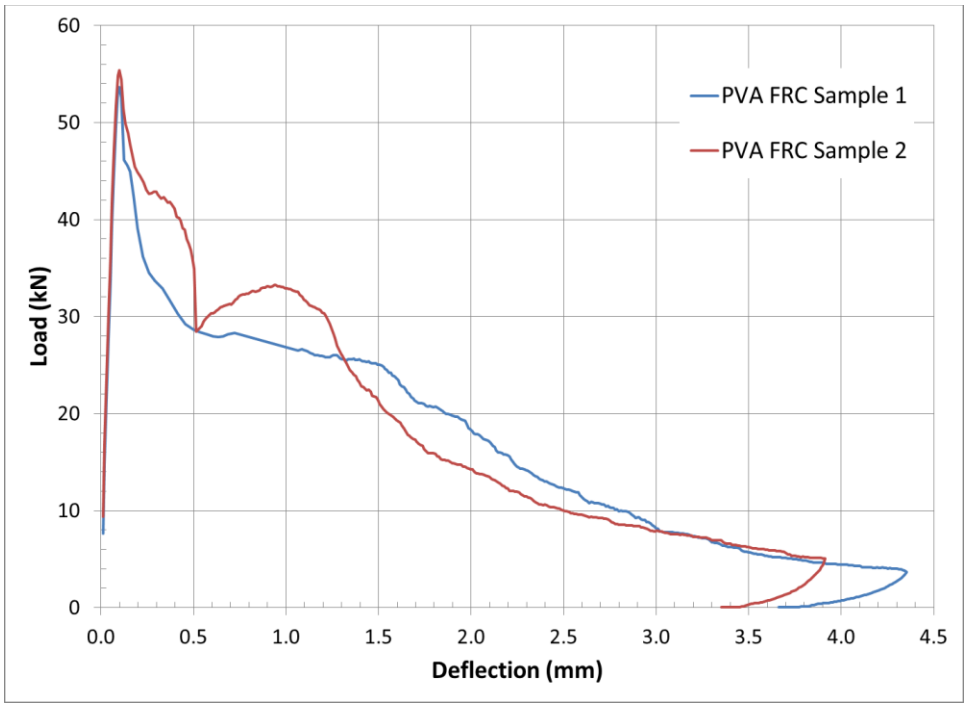

Figure 4.6 – Flexural load deflection curves for PVA FRC

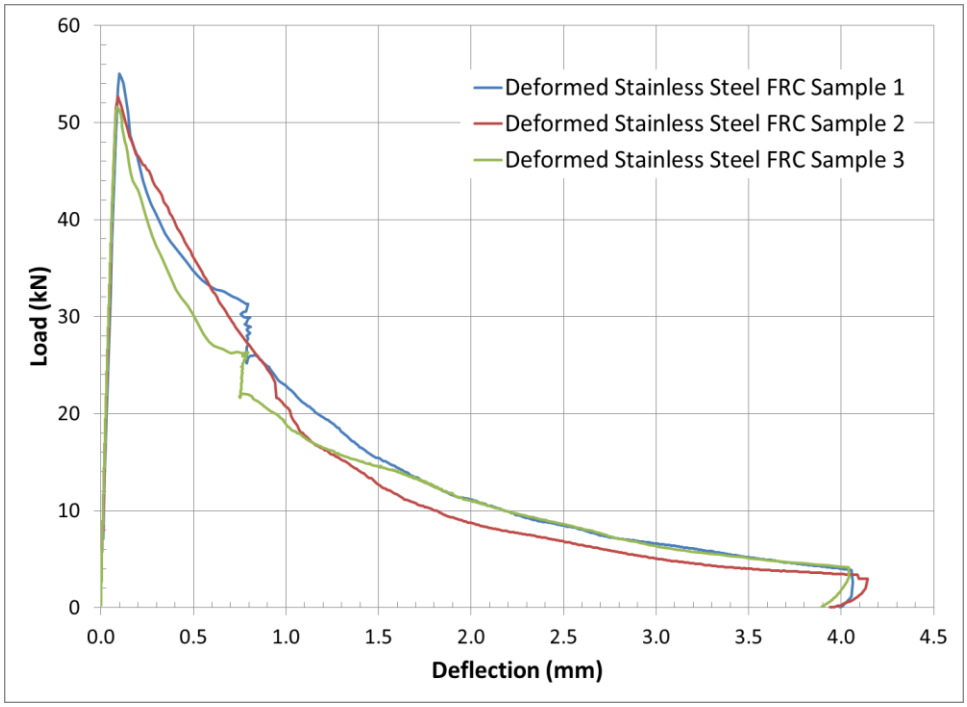

Figure 4.7 – Flexural load deflection curves for deformed stainless steel FRC

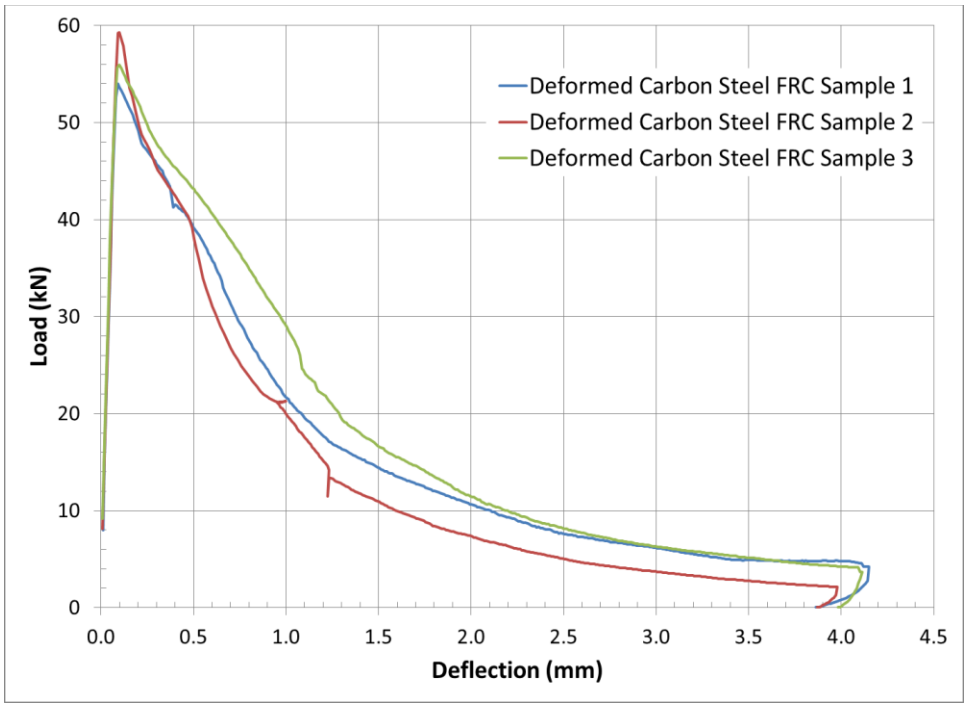

Figure 4.8 – Flexural load deflection curves for deformed carbon steel FRC

Figure 4.9 show representative samples load deflection curve from each mixture together for comparison.

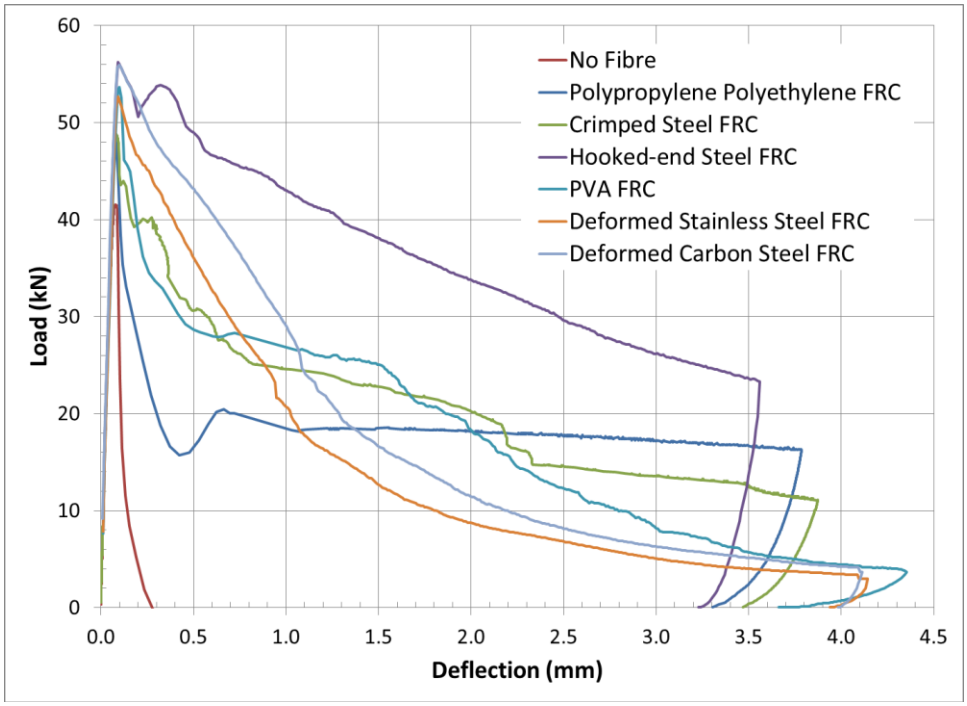

Figure 4.9 – Flexural load deflection curves of representative samples

Figure 4.9 indicates that the hooked-end steel FRC has the highest post-cracking response over the testing period and that the deformed stainless steel FRC and the deformed carbon steel FRC with the same nominal dimensions, show similar flexural responses. Both of these are again evident in Table 4.6, which shows the average numerical results specified by ASTM C1609 with full results shown in Appendix E:

P_1, P_{600} and P_{150} are the first cracking load, the load at $L/600$ (0.75mm) and $L/150$ (3mm)

f_1, f_{600} and f_{150} are the flexural strengths corresponding to P_1, P_{600} and P_{150} calculated with equation:

$$f_x = \frac{P_x L}{bd^2}$$

Where:

f_x is the flexural strength at x (MPa)

P is the load at x (N)

L is the span length (mm), 450mm

b is the width of the sample (mm), 150mm

d is the depth of the sample (mm), 150mm

Two other numbers that are reported in Table 4.6 are T_{150} and $R_{T,150}$. T_{150} is the toughness and is the tabulated area under the load deflection curve up to L/150 in joules. A graphical representation of P_1, P_{600}, P_{150} and T_{150} is shown in Figure 4.10 on a schematic data set.

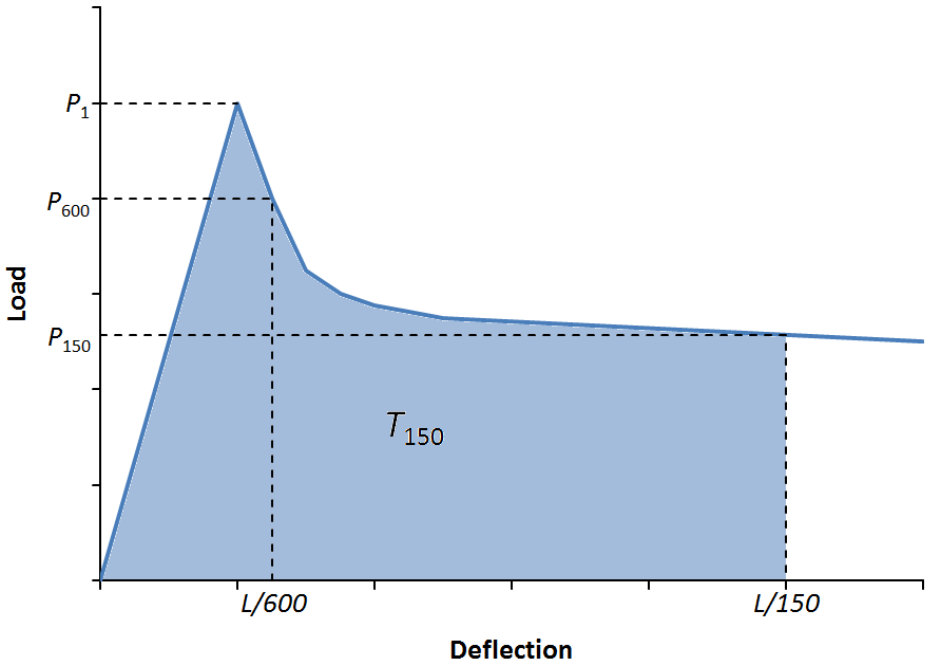

Figure 4.10 – Graphical representation of P_1, P_{600}, P_{150} and T_{150}

$R_{T,150}$ is the equivalent flexural strength ratio and allows samples of different size to be easily compared to each other. This is calculated from the following equation:

$$R_{T,150} = \frac{150 \times T_{150}}{f_1 bd^2} \times 100\%$$

Where:

$R_{T,150}$ is the equivalent flexural strength ratio (%)

T_{150} is the toughness up to $L/150$ (j)

f_1 is the flexural strength at cracking (MPa)

b is the width of the sample (mm), 150mm

d is the depth of the sample (mm), 150mm

Table 4.6 – Average ASTM C1609 numerical results

	Units	NF	PP	St	HS	PVA	SS	BS
P_1	kN	42.30	51.19	49.38	55.50	54.17	52.94	56.31
P_{600}	kN	NA	17.70	23.73	44.80	30.30	28.56	30.00
P_{150}	kN	NA	16.34	12.90	24.84	7.75	5.84	5.25
f_1	MPa	5.73	6.93	6.69	7.52	7.34	7.17	7.63
f_{600}	MPa	NA	2.40	3.21	6.07	4.10	3.87	4.06
f_{150}	MPa	NA	2.21	1.75	3.37	1.05	0.79	0.71
T_{150}	Joules	NA	55.71	64.44	113.00	68.88	56.23	59.95
$R_{T,150}$	-	NA	35.9%	42.8%	66.9%	41.7%	34.8%	35.1%

4.2.1.1. Compression and splitting tensile strength testing

Cylinders were cast to test both the compressive and splitting tensile strength of the concrete mixes tested in the C1609 flexural test. The average compressive and splitting tensile strength results are shown in Table 4.7, with full results in Appendix F, as well as in Figure 4.11 on a plot of compressive versus splitting tensile strength.

Table 4.7 – Average 28 day compressive and splitting tensile strengths for flexural testing FRC mixtures

FRC type	Compressive strength (MPa)	Splitting tensile strength (MPa)
No fibre	42.76	3.81
Crimped steel	43.89	5.21
Polypropylene polyethylene	41.31	4.50
Hooked-end steel	48.90	6.34
PVA	41.02	4.59
Deformed stainless steel	45.70	5.55
Deformed carbon steel	48.32	5.54

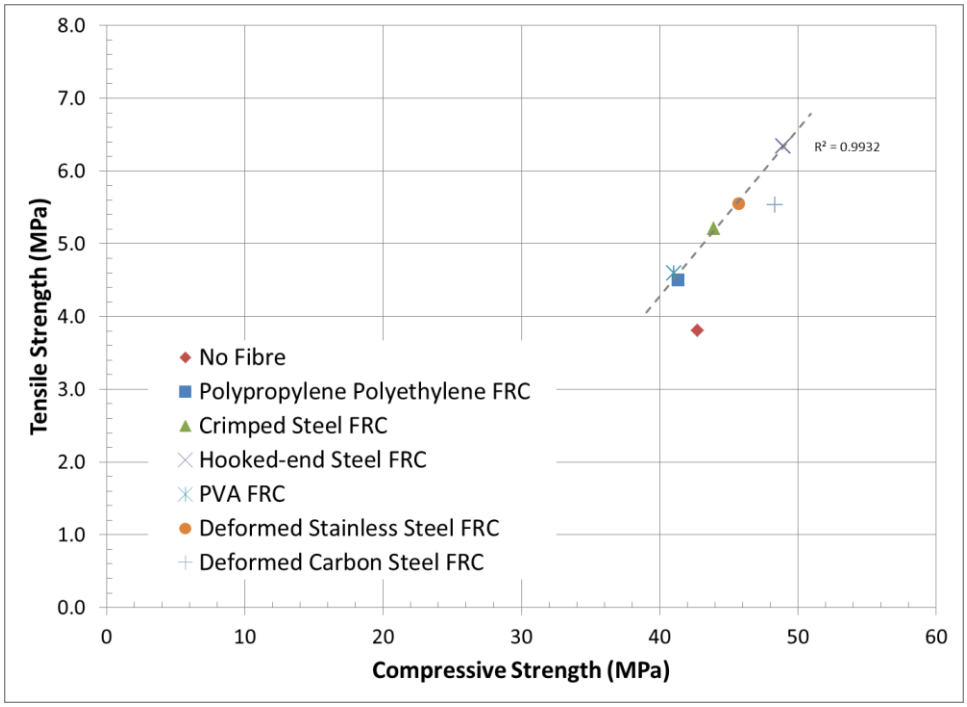

Figure 4.11 – Compressive vs. splitting tensile strength

As is shown in Figure 4.11 the addition of the fibres has an effect on the compressive strength of the concrete mixture but has a greater effect on the splitting tensile strength. The four steel (crimped steel, hooked-end steel, deformed stainless steel, deformed carbon steel) fibres have the greatest effect on both strength properties while the synthetic fibres (polypropylene polyethylene, PVA) have a lesser effect on the concrete mixture. These data also apply to the concrete used for shrinkage and freezing and thawing testing.

4.2.2. Flexural testing of FRC beams with steel reinforcement

Beams were cast with embedded steel bars to assess how FRC would perform in a structural application. Figure 4.12 shows load deflection curves for each

of the three concrete mixtures used for the test. Full details of these mixtures can be seen in Table 3.5. As can be seen, the post yielding response of each beam was increased with the addition of fibres as well as an initial stiffening of the elastic phase.

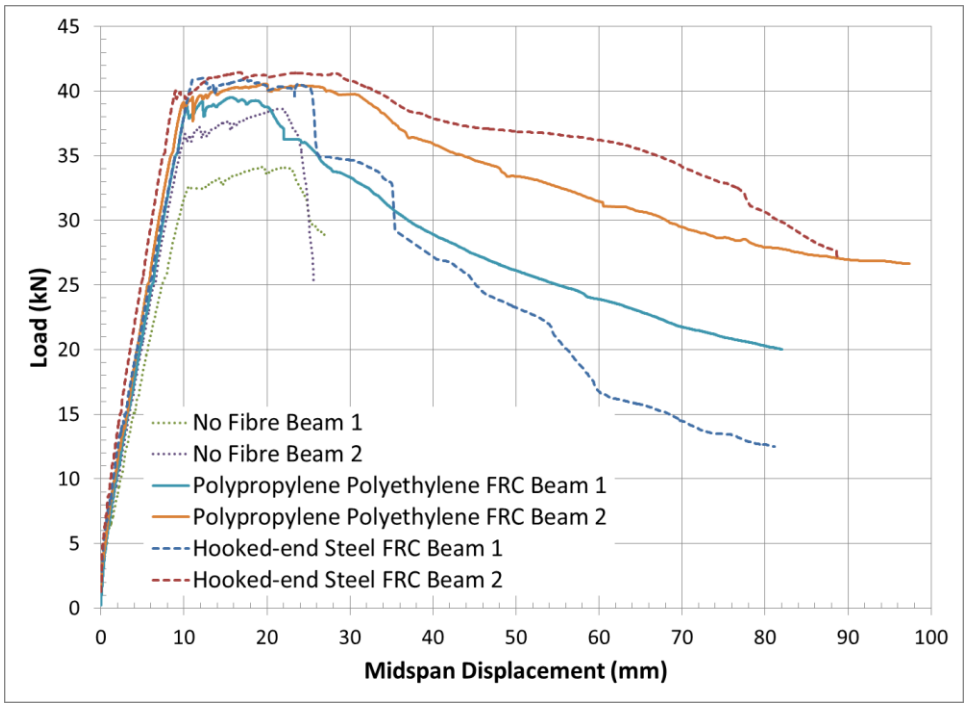

Figure 4.12 – Reinforced FRC beams load vs. deflection curves

As the beams were tested, the crack patterns on the surface were marked at standard intervals. Figure 4.13 through Figure 4.18 show the progression of the crack patterns at selected load levels.

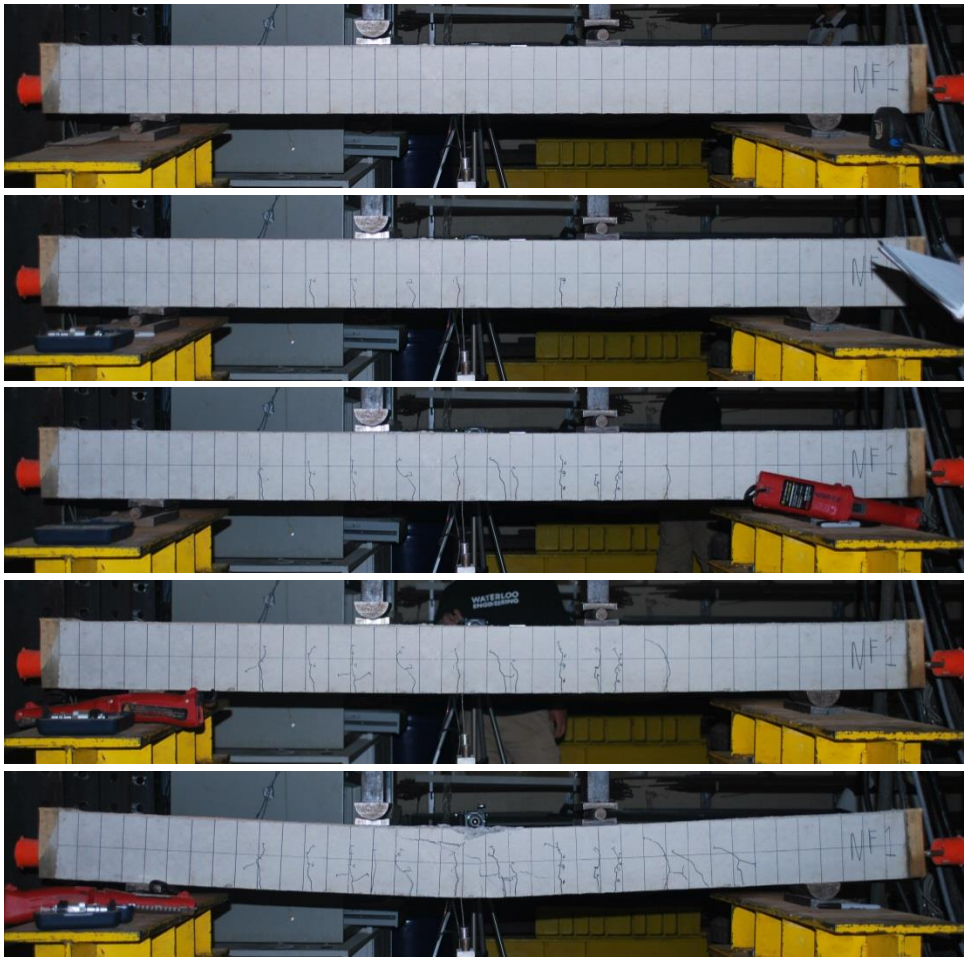

Figure 4.13 – No fibre reinforced flexural beam 1

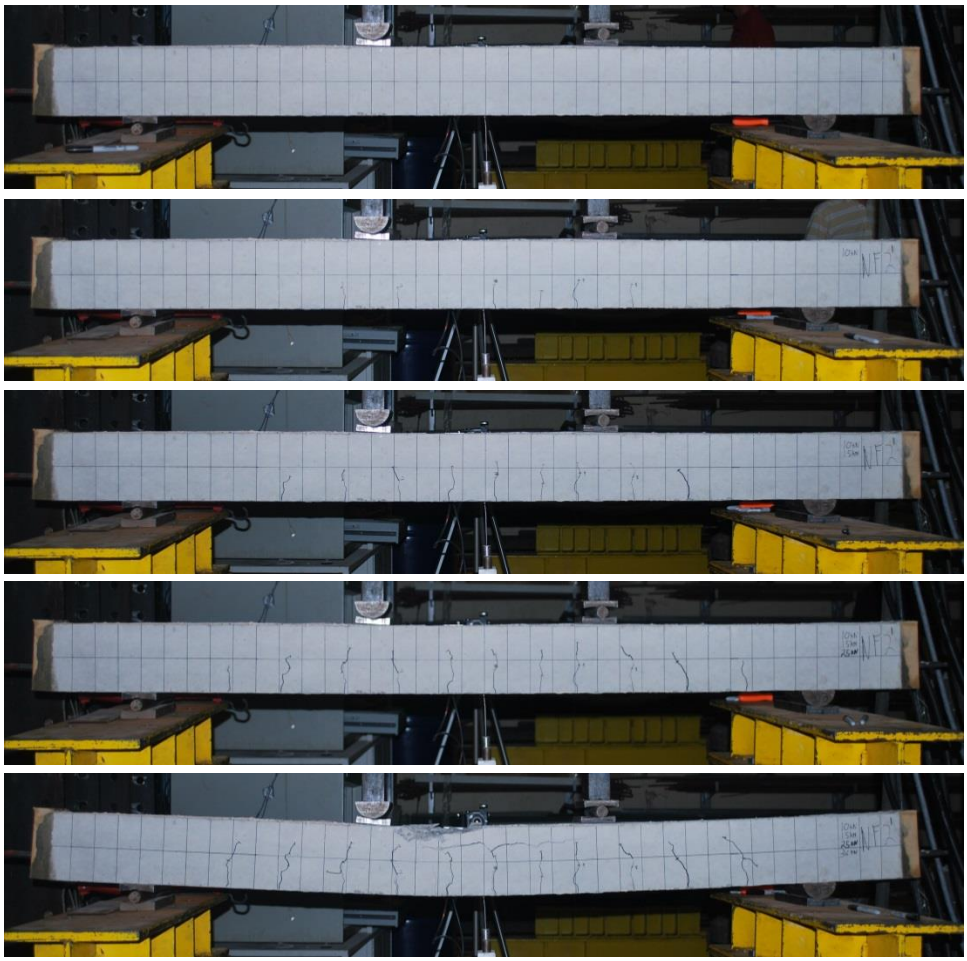

Figure 4.14 – No fibre reinforced flexural beam 2

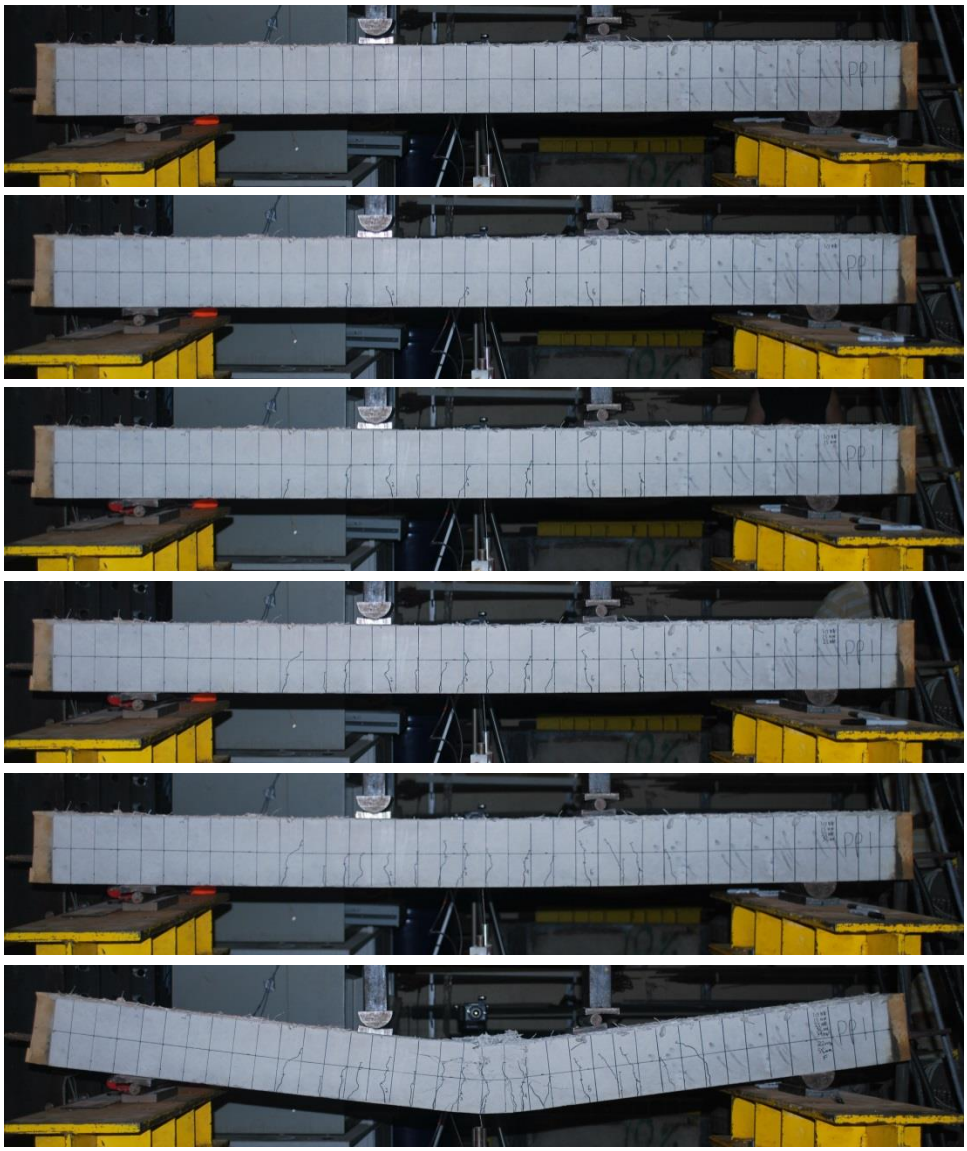

Figure 4.15 – Polypropylene polyethylene FRC reinforced flexural beam 1

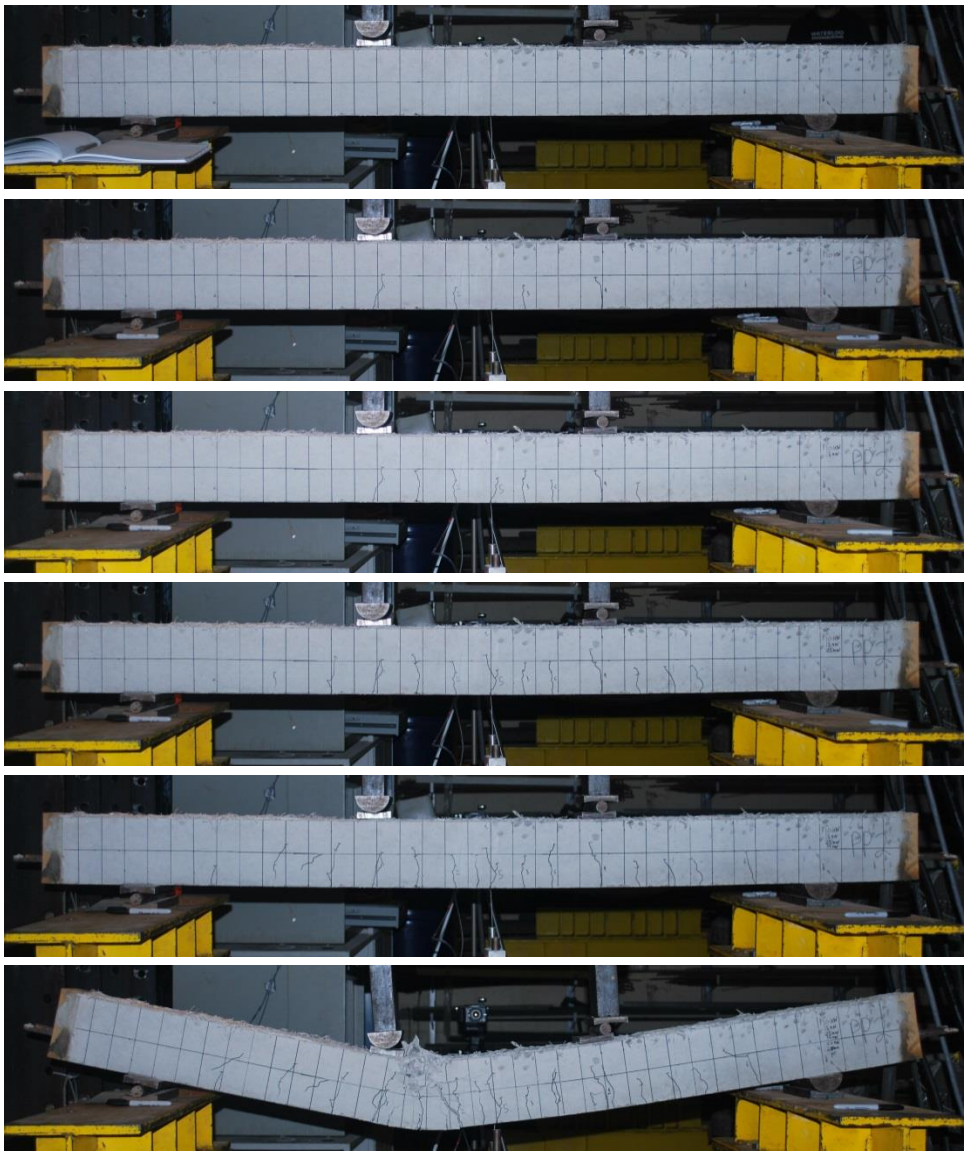

Figure 4.16 – Polypropylene polyethylene FRC reinforced flexural beam 2

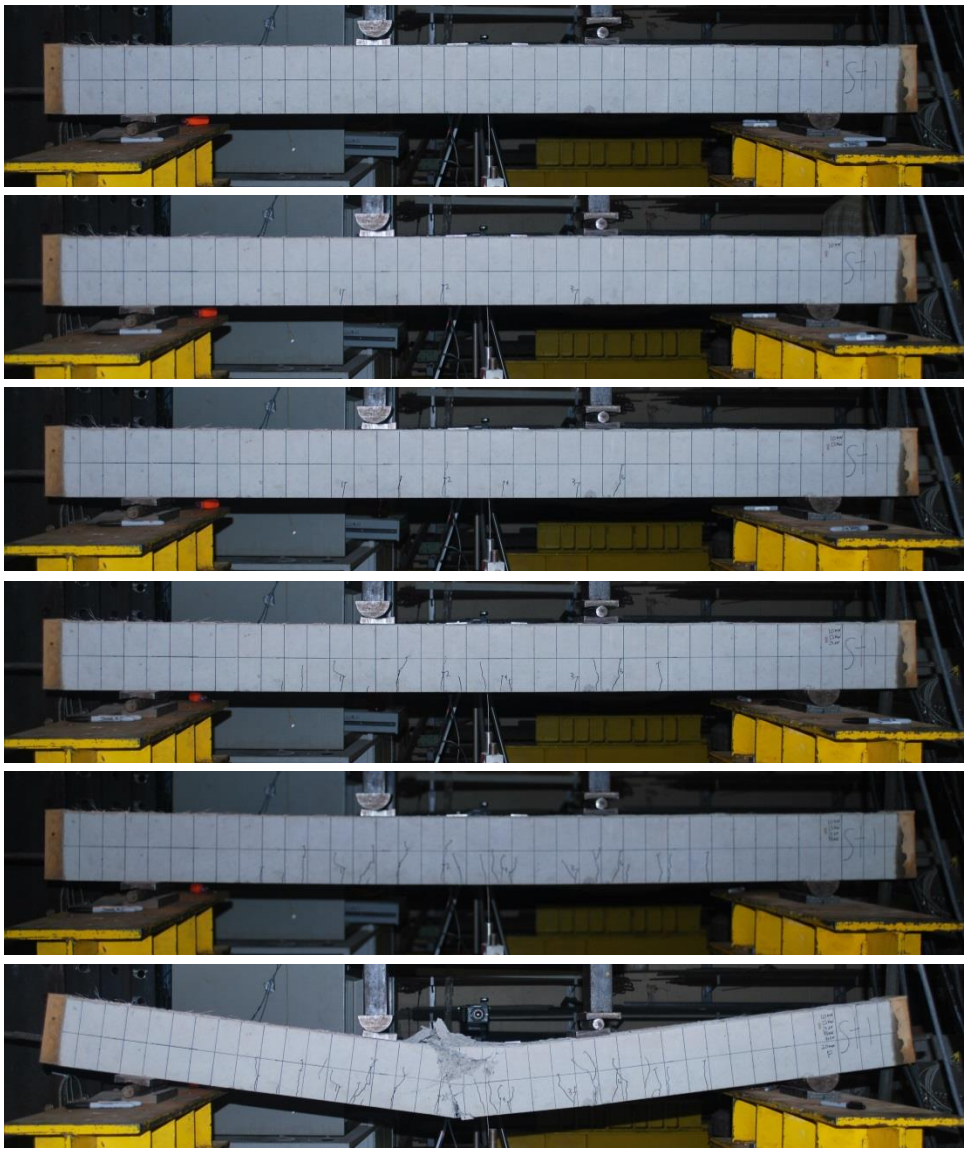

Figure 4.17 – Hooked-end steel FRC reinforced flexural beam 1

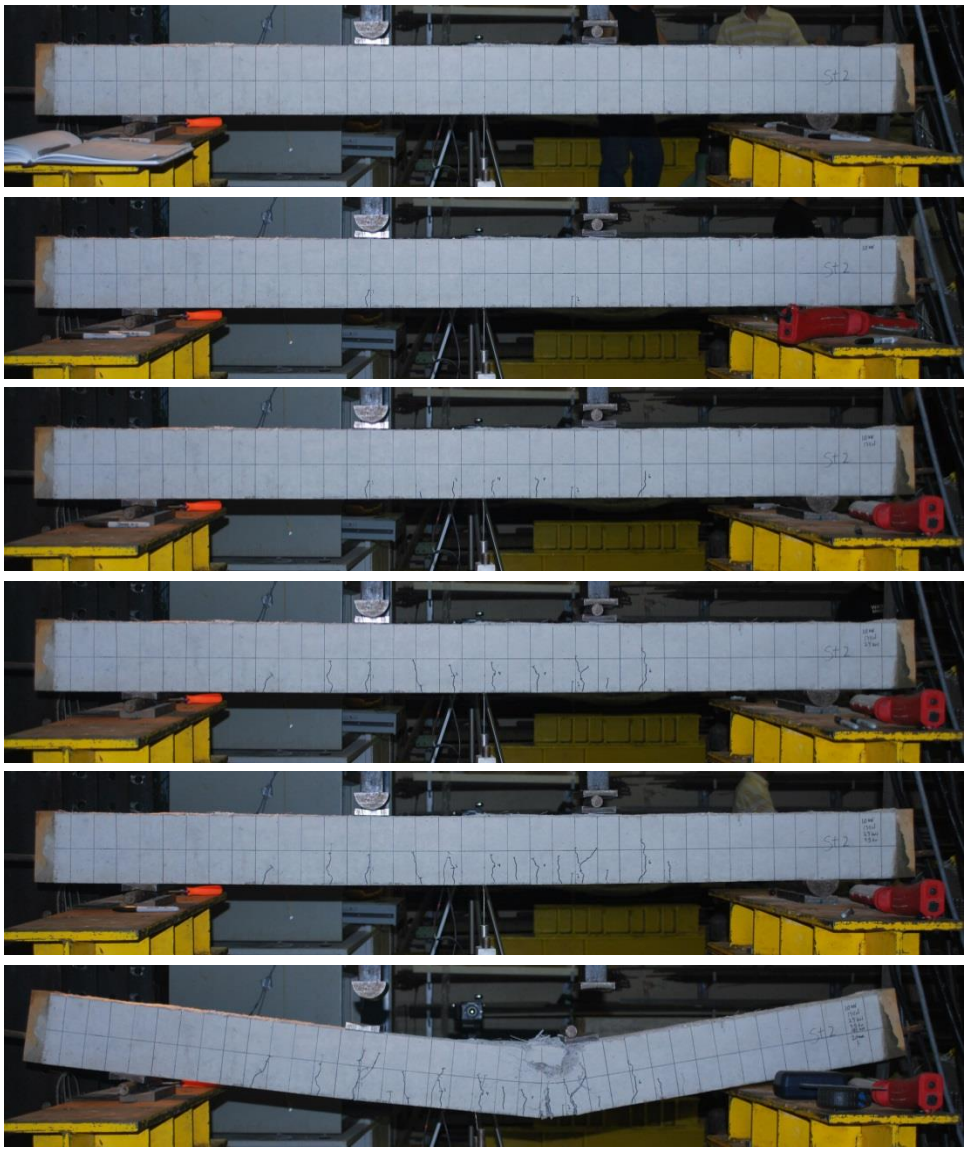

Figure 4.18 – Hooked-end steel FRC reinforced flexural beam 2

Along with the above photographs, crack width measurements were taken at each load interval shown. These are displayed in Table 4.8 and Figure 4.19 with all crack measurement data shown in Appendix G.

Table 4.8 – Average crack widths (mm) at selected bending moments for reinforced FRC beams

Applied Load (kN)	10	15	25	35
Bending Moment (kNm)	2.5	3.75	6.25	8.75
No fibre control	0.09	0.16	0.24	0.40
Polypropylene polyethylene FRC	0.09	0.11	0.14	0.19
Hooked-end steel FRC	0.05	0.06	0.11	0.15

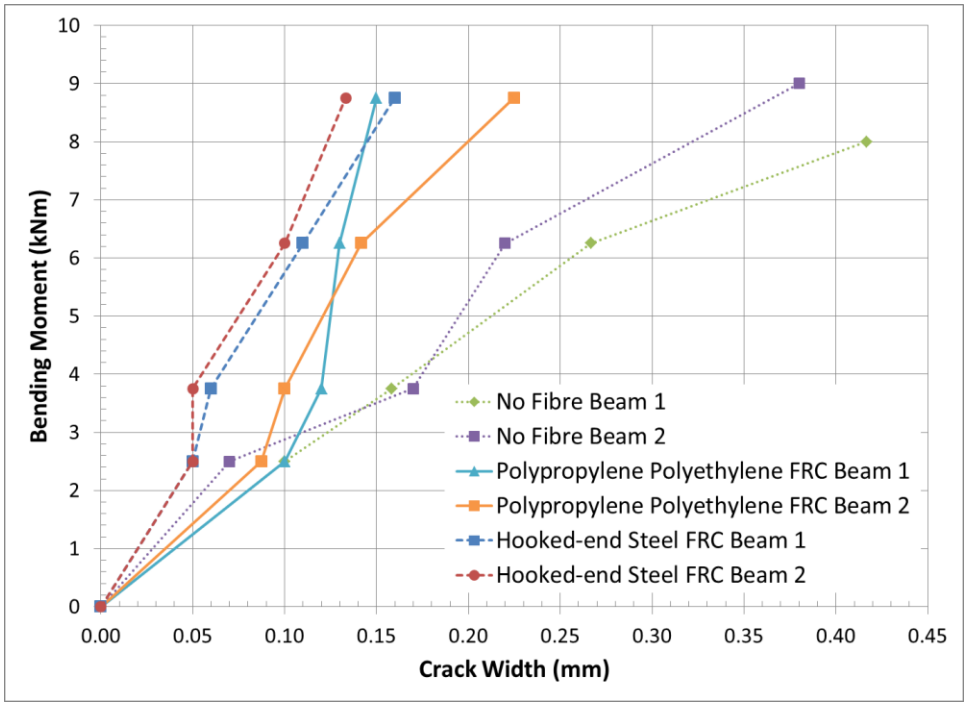

Figure 4.19 – Average crack width versus bending moment for reinforced FRC beams

As well as crack width measurements, the average crack spacing was obtained from measurements of the photographs, after testing. A load level of 15 kN or 3.75 kNm was selected because it most closely represented what a maximum service load would be in relation to the ultimate load capacity of the beams. This data is shown in Table 4.9.

Table 4.9 – Average crack spacing (mm) on reinforced FRC beams (@ M = 3.75 kNm)

No Fibre	101.1
Hooked-end steel FRC	72.5
Polypropylene polyethylene FRC	75.4

4.2.2.1. Compressive and splitting tensile strength testing

Each mixture for the reinforced FRC beam flexural testing was tested for compressive and splitting tensile strength. These data are shown in Table 4.10 and are comparable to the results of the same mixtures when they was cast to be tested in the flexural strength, shrinkage and freezing and thawing testing shown in Table 4.7.

Table 4.10 – Average 28 day compressive and splitting tensile strength for reinforced FRC mixtures

FRC type	Compressive strength (MPa)	Splitting tensile strength (MPa)
No fibre	38.83	3.70
Polypropylene polyethylene	37.79	3.99
Hooked-end steel	41.13	5.00

4.3. Material durability properties

4.3.1. Outdoor exposure strain samples

Three concrete mixtures were used to cast two blocks each to test the outdoor exposure effects on the internal strain of the FRC mixtures. The mixtures used were pre-optimization with a fibre dosage of approximately 0.5% by volume. The proportions of the mixtures used are shown in Table 3.5. One sample of each was to be exposed to road salt brine, while the other was not. Strain data were collected via internal strain gauges cast inside the blocks. Strain and temperature data were collected on the blocks starting within hours after casting of the blocks and was continued up to the point

where the samples were de-moulded and moved outside. The temperature and strain readings for the curing week are shown in Appendix H. After the samples were de-moulded they were moved outside and reconnected 3 days later. One sample of each were then filled with salt solution and the second sample with water. Figure 4.20 shows the average strains for the water exposed samples along with the average temperature measured in the samples over 96 weeks of outdoor exposure. As can be seen in Figure 4.20, the strain profile follows the temperature profile with higher strains generated in higher temperatures.

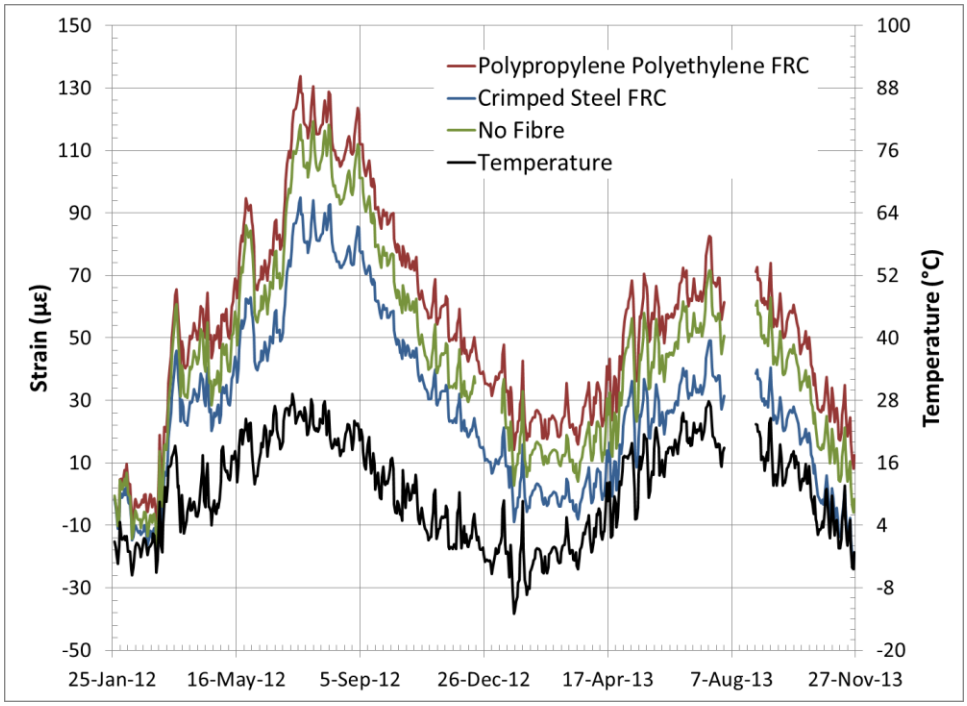

Figure 4.20 – Average strains and average temperature of outdoor exposure samples

Figure 4.21 again shows the average strain data of the water filled samples over the same 96 weeks but with the addition of the average strains of the salt filled samples. As can be seen in Figure 4.21, the salt has the effect of

increasing the strain in the sample, with the greatest effect occurring when temperatures are high.

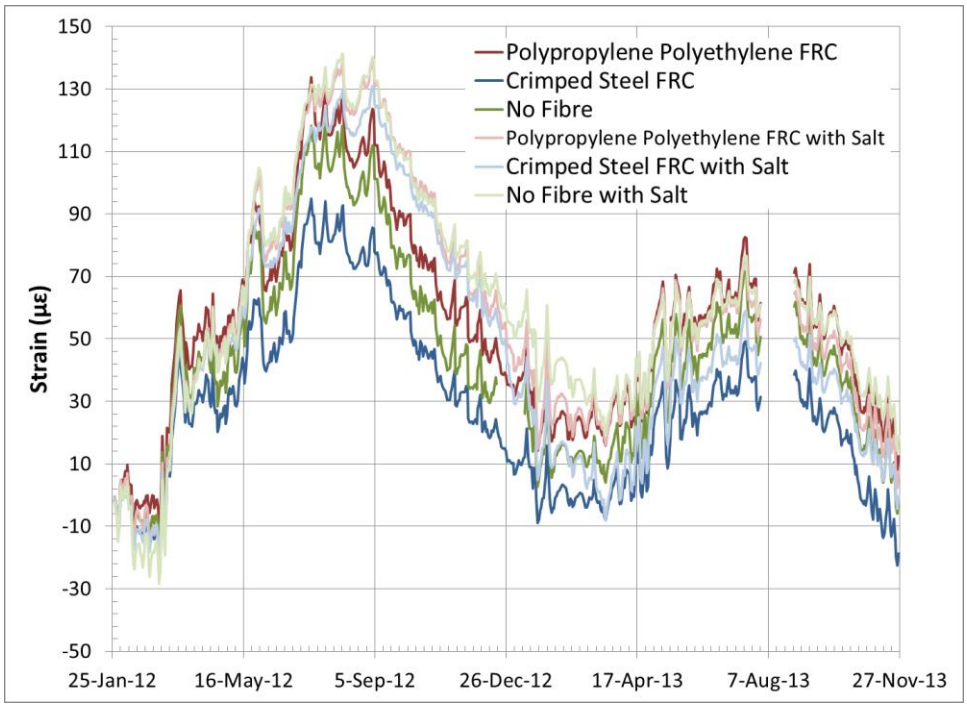

Figure 4.21 – Average strains of outdoor exposure samples with and without salt exposure

4.3.2. Linear shrinkage testing

Samples were divided into two sets as with the FRC flexural testing. The first set included the no fibre control concrete, polypropylene polyethylene FRC and the crimped steel FRC. These samples were measured up to 224 days. The second set was comprised of the hooked steel FRC, PVA FRC, deformed carbon steel FRC and the deformed stainless steel FRC. This set was cast at a later date, and because of time limitations the samples were only measured for 112 days. Shrinkage of the samples is measured verses a 400 mm (10 inch) invar steel bar and is calculated as follows:

$$\Delta L_x = \frac{CRD_x - CRD_{initial}}{G} \times 100\%$$

Where:

ΔL_x is the length change at time x (%)

CRD_x is the measured difference in length comparator reading of the sample and the gauge bar at time x (in.)

$CRD_{initial}$ is the initial measured difference in length comparator reading of the sample and the gauge bar (in.)

G is the length of the gauge bar (10 in.)

The average values for 3 samples of each concrete mixture are shown in Table 4.11.

Table 4.11 – Average linear shrinkage of FRC samples (%)

FRC type	0 Days	1 Day	7 Days	14 Days	28 Days	56 Days	112 Day	224 Day
NF	0.00	0.00	0.00	0.00	-0.01	-0.02	-0.04	-0.05
PP	0.00	0.00	0.00	-0.01	-0.02	-0.03	-0.04	-0.05
St	0.00	0.00	0.00	0.00	-0.02	-0.03	-0.04	-0.05
HS	0.00	0.00	-0.01	-0.02	-0.03	-0.04	-0.05	
PVA	0.00	0.00	-0.02	-0.03	-0.04	-0.05	-0.05	
BS	0.00	0.00	-0.02	-0.03	-0.04	-0.04	-0.06	
SS	0.00		-0.02	-0.03	-0.04	-0.04	-0.05	

The data from Table 4.11 are displayed graphically in Figure 4.22. The two sets of cast samples show a different trend but end up at a similar result at 112 days. Set one (NF, St, PP) shows a small initial increase then a downward trend where set two (HS, PVA, SS, BS) starts immediately into the downward trend. This difference may be due to a slight difference in ambient conditions at the different times of the year that the testing was done.

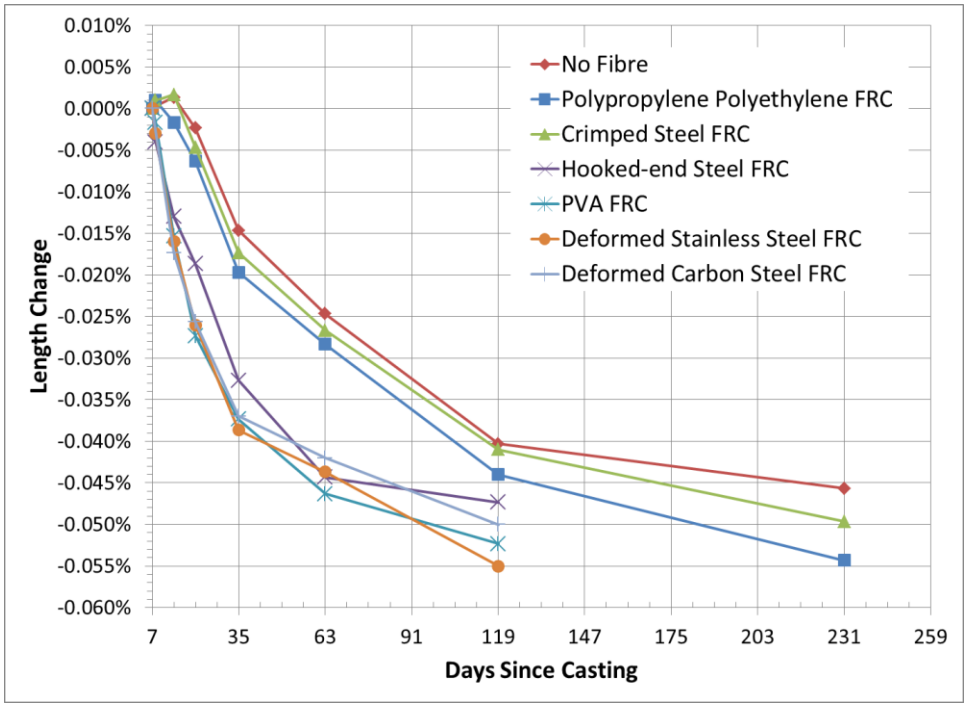

Figure 4.22 – Linear shrinkage of FRC mixtures

4.3.3. Freezing and thawing cycle testing

When casting was done for the flexural testing and shrinkage testing, samples were also cast for the freezing and thawing cycle testing. These samples were also cast and tested in two sets, with set one consisting of the no fibre control, the polypropylene polyethylene FRC and the crimped steel FRC. The second set consisted of the hooked-end steel FRC, PVA FRC, deformed stainless steel FRC and the deformed steel FRC. The first test was cast on November 13th, 14th and 15th of 2012 and cyclic testing did not begin until 6 months later on April 30th, 2013. The second set of samples was cast March 12th, 14th, 19th and 20th of 2013 and testing commenced 3 months later on June 12th, 2013. Over the period from casting to testing both sets of samples were stored in a moist curing location. Once cyclic freezing and thawing cycles began they were

continued until 300 cycles were reached. Set one reached 300 cycles in 43 days, but because of the larger number of samples in set two the cycles ran more slowly and 56 days were required to reach 300 cycles. Temperature throughout the 300 cycles for both sets is shown Appendix I. Samples were removed from the freeze-thaw chamber once a week and measurements for weight and fundamental frequency for each sample were recorded. The average mass change for each mixture in both sets is shown in Figure 4.23 with full results shown in Appendix J. It is noted that there is less variation in the mass for set two (hooked-end steel, PVA, deformed stainless steel, deformed carbon steel) because greater effort was taken to minimize evaporation between removal of the samples from the chamber to the time they were weighed.

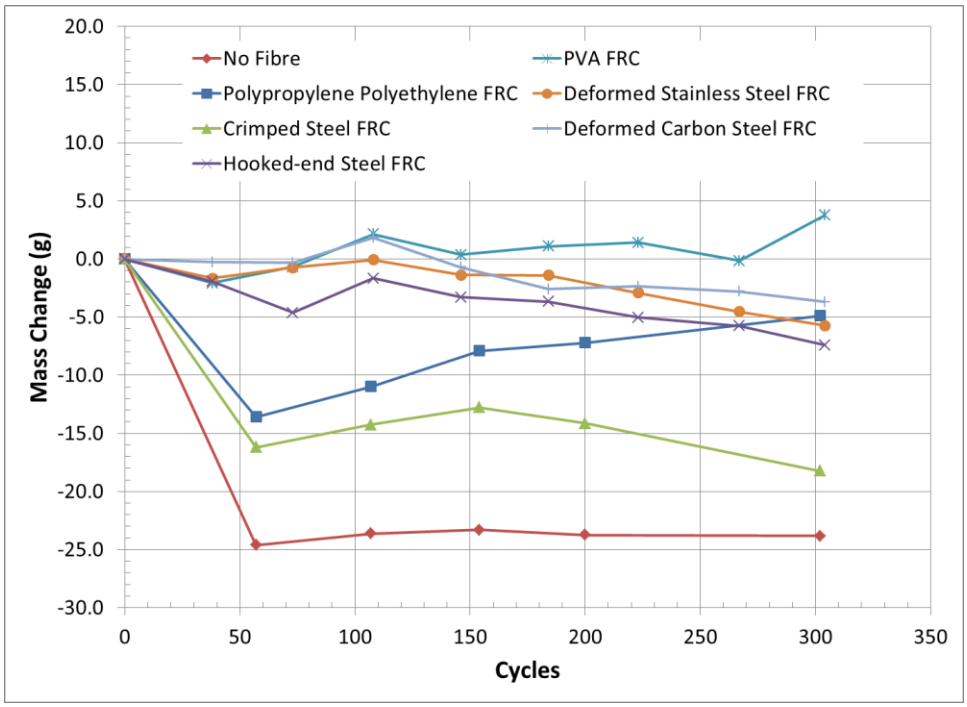

Figure 4.23 – Mass change of FRC samples in freezing and thawing tests

The second test that was conducted weekly was the measurement of fundamental frequency of the samples. From this, the relative dynamic modulus of elasticity was calculated with the formula:

$$P_c = \frac{n_0^2}{n_c^2} \times 100\%$$

Where:

P_c is the relative dynamic modulus of elasticity after c cycles of freezing and thawing (%)

n_c is the fundamental frequency after c cycles of freezing and thawing

n_0 is the fundamental frequency after 0 cycles of freezing and thawing

Figure 4.24 shows the relative dynamic modulus of elasticity over the 300 cycles of testing with full results shown in Appendix K.

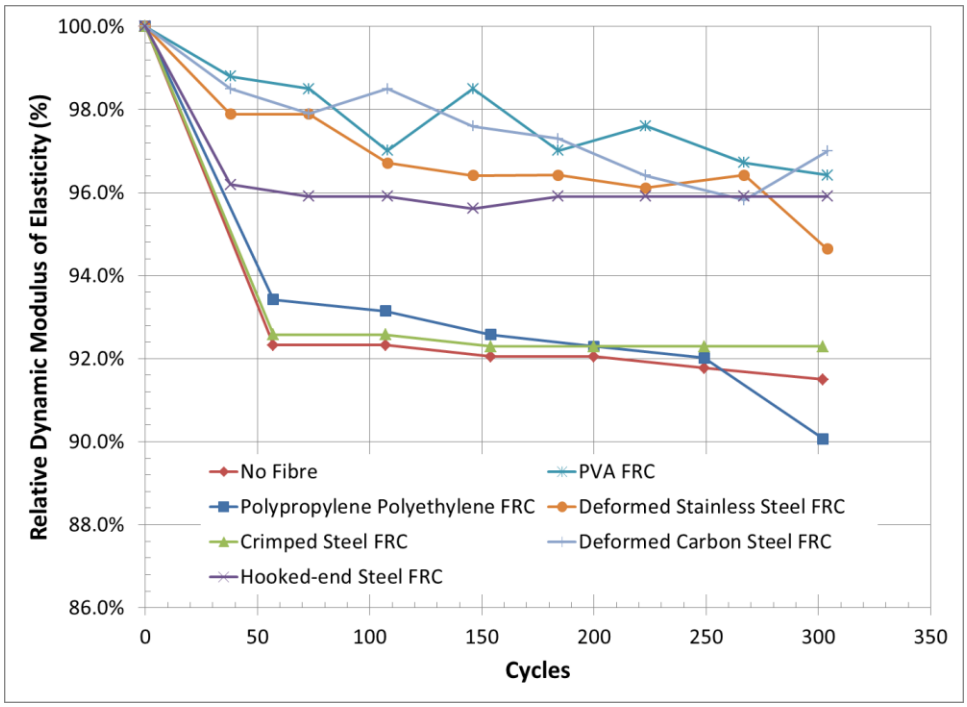

Figure 4.24 – Relative dynamic modulus of elasticity for FRC samples in freezing and thawing tests

4.3.4. Rust staining observation

It was observed that when the crimped steel FRC outdoor exposure samples were exposed to the road salt solution, they quickly developed a spotted rust stained appearance, as shown in Figure 4.25. Because of this, a test was developed to determine if the problem could be avoided with the use of stainless steel fibres.

Figure 4.25 – Rust staining on crimped steel FRC outdoor exposure sample

To test the rust staining properties of stainless verse black steel, half cylinders of FRC with the deformed stainless steel fibre and the deformed steel fibre were soaked in salt brine for 3 months and then allowed to dry. The cylinders before salt exposure are shown in Figure 4.26 with Figure 4.27 showing the cylinders after exposure.

Figure 4.26 – Rust staining samples before salt exposure (stainless steel left, carbon steel right)

Figure 4.27 – Rust staining of samples after salt exposure (stainless steel left, carbon steel right)

5. Discussion

5.1. Mix design

5.1.1. Mix optimization

The mix design optimization was carried out to achieve two goals within the project. The first was to develop the optimized mixture that was used throughout the remaining experiments and the second was to familiarize the researcher with the process and problems associated with mixing FRC. An optimized mixture was developed with a sand to gravel ratio of 1:1 and a paste percentage of 35% for all fibre types. This allowed for ease of mixing with the available equipment and good consolidation. The high paste percentage that was selected allowed for a mixture to be used that did not require any superplasticizer (high-range water-reducing agent), while still achieving a high slump value for adequate workability. Similar workability could likely be achieved by using a lower paste percentage and a dosage of superplasticizer.

5.1.1.1. Slump testing

The slump testing conducted on the fresh mixtures showed that a highly workable mixture could be achieved through the optimization method explained in Section 3.1.2. As the ratio of sand to gravel was increased, the mixture became more fluid up to a point where there was no longer sufficient paste to fully coat the increased surface area of the aggregates and the workability began to decrease. When S/G ratios ≥ 2:1 were used, the concrete mixtures took on the consistency of wet

beach sand that could be used to build a sand castle. This type of stiff dense concrete mixture could be ideal for extruded slabs but would be impossible to pour in a form containing a reinforcement cage and obtain proper consolidation without excessive vibration.

After the optimum ratio was found for each type and volume of fibre used, the paste percentage was increased until the workability of the mixture was found to be suitable. As the paste percentage increased, the workability increased greatly with little effect on the tested mechanical properties of the concrete.

Once all optimization mixtures were completed it was found that the optimal mixtures for all fibre types and dosages were in a similar range. Because of this it was decided that one set of mixture proportions could be used for all further FRC testing with similar fibres and a dosage within the 1-2% by volume range. The optimal S/G ratio was observed to be in the 1-1.5 range for most mixtures. An S/G ratio of 1 was selected for the optimized mixture because it more closely resembled the original mixture while still being within the observed optimal range. 35% paste was selected as the paste percentage for the FRC mixtures while 32.5% was used for the no fibre control mixture. This was because a high slump could be achieved without the use of any superplasticizer. This allowed the mixture to be simplified without need for additional artificial slump from a superplasticizer.

5.1.1.2. Air content testing

With the tests conducted on the fresh concrete to measure the entrained air in the FRC mixtures it was observed that the addition of fibres did increase the air content in the mixtures. It is unknown if this additional air content is true entrained air or is more likely extra entrapped air due to voids created by clumping of the fibres. Larger entrapped air voids that are often created when small clumps of fibres form in the concrete mixture are very difficult to remove even with external vibration. Because the larger entrapped air voids do not contribute to the freezing and thawing resistance of the concrete, as do the much smaller entrained air voids, this additional air content is not considered useful in the concrete. In addition very large air voids can have a negative impact on the concrete by creating weak areas in the material reducing the overall strength. Since the ASTM C231 fresh concrete pressure test [40] is not able to distinguish between the air content which is entrained air and that which is entrapped air it is unknown, from this test, how much of the air content is suitable for freezing and thawing resistance. To determine the volume of entrapped versus entrained air the ASTM C457 test for microscopic analysis of air-void systems [50] could be conducted to establish how much of this air content is considered to be useful. The mixture optimization procedure did have a noticeable effect on the air content of the concrete across all the FRCs and the control mixture. The increase in air content, when

working with the increased sand to gravel ratios, can be seen in Table 4.3. This is a known result of increasing the amount of sand [51] in any concrete mixture and could be compensated for by reducing the air entraining agent if needed. In the second half of the optimization there was no observable trend in the change in air content as the paste percentage was changed with each mixture. Although the air content would be expected to increase along with the increase in paste percentage, because the volume of air entrainer was not adjusted as the paste percentage increase the air content remained relatively unchanged.

5.1.1.3. Compressive strength testing

Although the optimization phase of the research was focused on the workability and ease of placement for the FRC mixtures, compressive strength testing was conducted on each batch of concrete made. Over the optimization process, a lower strength was observed with increased S/G ratio and paste percentage. The average compressive strength decrease was 12% at the end of the optimization for the 32.5% and 35% paste mixtures. Since the focus was on increasing the workability of the mixtures, a strength loss of this magnitude in the concrete was considered acceptable. Compressive strength can also be used as an indicator of proper consolidation in a concrete mixture. If a concrete cylinder shows significantly less strength than expected, it could be due to poor consolidation inside the cylinder even if all surfaces appear

normal. Incrementally, the strength was never significantly lower than that of the previous batch in the optimization so there is little indication of improper consolidation in the mixtures. Along with the quantitative results of the compressive tests, there was an important qualitative observation that the FRC cylinders remained fully intact once failure occurred, with only small surface cracks visible. In contrast, the control samples separated into pieces in a dual cone failure. Even after a sample of polypropylene polyethylene FRC was tested to an extreme displacement level, the parts of the cylinder remained attached and some load was still being carried when the machine reached its maximum displacement. This cylinder is shown in Figure 5.1 and, although the cylinder has clearly splintered into many pieces, it retains its general cylindrical shape whereas a standard concrete cylinder would have already been reduced to a pile of rubble at this displacement.

Figure 5.1 – Compressive cylinder tested to extreme displacement

This type of behaviour would be useful in a structural situation where the damage to the concrete would be visible, but would prevent large pieces of concrete from dislodging from the structure and falling on vehicles or people under the structure when it failed.

5.1.1.4. Splitting tensile strength testing

Similar to the compressive strength testing, the tensile strength of each mixture in the optimization was measured but, since the focus was not on optimizing for tensile strength, significant gains were not expected. As was seen with the compressive strength tests, the majority of the mixtures showed a lower tensile strength with the increased S/G ratio and paste percentages. On average the strength was only 9.2% lower than the original mixture for the 32.5% and 35% paste mixtures. This lower tensile strength was again considered acceptable because of the increased workability that was achieved in the mixtures. It is also beneficial that the optimization procedure did not have as great a negative impact on the tensile strength of the mixtures as it did on the compressive strength, as the added tensile strength of the concrete is important to the benefits of using FRC in a link slab. As with the compressive tests, the cylinders made from mixtures that included fibres remained intact after failure where the standard concrete mixtures all split in half at failure. This is shown clearly in Figure 5.2

showing a failed no fibre concrete splitting tensile cylinder and a failed polypropylene polyethylene FRC splitting tensile cylinder.

Figure 5.2 – Failed splitting tensile cylinders (left: no fibre cylinder, right: polypropylene polyethylene FRC cylinder)

This is a result of the post peak tensile strength that was further investigated with the ASTM C1609 flexural testing later in the research. Although the cylinder has reached its maximum load, it still retains enough load capacity to hold the cylinder in one piece. Because only a small range of displacement was available with the splitting tensile test apparatus it was not possible to test the FRC cylinders to a point where they would separate in two, the failure mode was considered to be similar to the control with a crack pattern that fractures both the aggregates and cement paste matrix as expected in splitting tensile testing.

5.2. Structural properties of FRC with selected fibre types

The results of the structural testing of the optimized FRC mixtures were used to evaluate the potential of the mixtures have for use in a link slab application. Tests

were selected to best determine, in the allotted time, the structural limits of the FRCs in compression, tension and flexure with and without reinforcing steel. The results of these tests not only showed which fibres gave the greatest increases in performance, but the data were also used in computer modelling done by Yu Hong [52] on how the addition of an FRC link slab would affect an overall bridge structure.

5.2.1. Flexural testing of FRC

The ASTM C1609 flexural testing was conducted on the control mixture and each of the optimized FRC mixtures with the six fibre types selected. As was expected, all FRC mixtures showed significant improvement in the sustained post-cracking flexural strength over the no fibre control mixture. Since the control mixture did not contain any additional material other than the standard concrete ingredients, once a crack formed in the matrix, the beams failed catastrophically. Although the control mixtures did fail suddenly after cracking, the peak load, or moment of rupture (MOR), was similar for the control mixture and all the FRC mixtures, as can be seen in Table 4.6, of the values of P_1 (peak load) and f_1 (MOR). This shows that although the fibres are capable of withstanding high loads, they do not strongly contribute to the flexural strength of the beam until failure of the matrix has occurred and load can be transferred to them.

Of the six fibres tested in the flexural testing, the hooked-end steel fibre created the most superior FRC mixture. As can be seen in Figure 4.9 the

hooked-end steel fibre has one of the highest peak strengths but, more importantly, maintains the highest post peak strength over the full duration of the test. This is again shown in Table 4.6 with the hooked-end steel having the highest toughness value (T_{150}) of any of the mixtures; this combined with the high peak strength results in the highest equivalent flexural strength ratio ($R_{T,150}$) as well. The hooked-end steel fibre is believed to perform so well because of its high strength and stiffness but most importantly the added anchorage that is provided by the hooked-ends keeping the fibres from slipping or pulling out when load is transferred to them.

Another important observation made from the flexural testing is the similarity between the results of the deformed stainless steel and deformed carbon steel fibre. These two fibres have identical geometric properties but have different material properties, because of the different types of steel used to make them. The resulting FRCs that were made with the two fibres showed nearly identical load deflection curves in the flexural testing while differing greatly from the two other fibres made from similar carbon steel. This suggests that the geometry of the steel fibre and how the fibres anchor in the concrete are more significant than the exact material properties of fibres.

Although the two synthetic fibres tested had a similar shape and length and were both made from a polymer material, they did not show many similarities in results of the FRC flexural testing. Both the polypropylene polyethylene FRC and the PVA FRC had peak loads in the 50-55 kN range. Both FRCs also have a steep drop off after peak load compared to the other

steel fibres, but the polypropylene polyethylene FRC seems to take-up the load at a point and holds the load constant over the remainder of the test. The PVA FRC only slows this loss of load capacity and is in the range of the lowest load capacities by $L/150$ of all the fibres tested. Overall the synthetic fibres required a large initial displacement and load drop before load is taken up by the fibres. This could be due to initial slipping of the fibre anchorage but is more likely due to the fibres stretching and deforming when load is first applied to them, due to their low stiffness. Unlike the steel fibres, the individual material properties of the polymeric fibres seem to have a significant impact on how the FRC will perform.

From examination of the samples it was seen that the failure of all six fibre types was from pull out of the fibre, not from failure or breakage. This indicates that although the stiffness of the fibre may contribute to the pre-failure response, the ultimate failure is governed by the bond that the fibres can generate with concrete.

From the results of the ASTM C1609 flexural test, the best fibre for both high peak flexural strength and sustained post peak flexural strength is the hooked-end steel fibre. Although the FRC with these fibres did not show the highest average peak flexural strength, it was less than 1.5% below the highest peak value set by the shorter deformed black steel FRC and was shown to be one of the stiffest FRC samples before cracking. After the FRC samples have cracked, the hooked-end steel FRC can carry 50% more load than the polypropylene polyethylene FRC at a deflection of 150^{th} of the span

length and nearly double the load of the next highest steel fibre at that deflection. The strong post-cracking response along with the high peak load resulted in the hooked-end steel FRC having, by a large margin, the highest toughness value of any of the FRCs tested.

5.2.2. Compression and splitting tensile strength testing

The accompanying compressive strength and splitting tensile strength cylinders cast from the same mixtures as the ASTM C1609 samples show a similar hierarchy of the FRC mixtures as in the flexural testing. The hooked-end fibres give the FRC both the highest average compressive and tensile strengths followed by the other fibre types. The deformed stainless and carbon steel FRCs again show similar properties with nearly identical average tensile strengths and average compressive strengths differing by around 5%. The two synthetic fibres in the polypropylene polyethylene FRC and the PVA FRC give nearly identically performing FRCs in both compressive and tensile testing. Although both of these fibres performed relatively well in the flexural testing they show substantially lower compressive and tensile strengths than the steel FRCs.

It is also important to note that a linear relationship between the compressive and splitting tensile strength results is observable in Figure 4.11. Normally the relationship between compressive and tensile strength in normal concrete is often considered to vary with the square root of compressive strength. However, this shows that there is a linear correlation

between the compressive and tensile strength added by the fibres to the concrete. Fibres are not expected to directly add to the compressive strength but instead increase the restraint to hold the concrete together once cracks form, resulting in higher overall compressive strength. This is the same mechanism that provided the increase in tensile strength of the concrete. Therefore, it would be expected that similar increases in tensile and compressive strength would be observed from the same FRC mixture. It can also be seen in Figure 4.11 that the control (no fibre) concrete does not lie along the same linear trend as the FRC mixtures. This is most likely explained by the difference in optimized mixture that was created in phase one. Where all FRC mixtures share the same concrete matrix, the optimized mixture for the control concrete was of a different composition with a lower paste percentage. This could have given the control mixture a higher compressive strength than some FRC mixtures but as expected it still has a substantially lower tensile strength without the added benefit of fibres.

5.2.3. Flexural testing of FRC beams with steel reinforcement

The specimens created for the flexural testing with steel reinforcement were created to simulate how the FRC mixtures would perform in as reinforced concrete structural application such as a beam or a link slab. The beams were designed with reinforcement ratios similar to known link slabs constructed in Ontario as well as a similar thickness and cover depth on the tensile surface. These beams were cast with two FRC mixtures from the ASTM C1609

flexural test along with the control no fibre concrete mixture. The two FRC mixtures used were the hooked-end steel FRC and the polypropylene polyethylene FRC because they were the best overall performers of the steel and synthetic fibres, respectively, in the previous tests. The results of the test are shown in Figure 4.12. Although this graph might at first seem to show three distinct pairs of load displacement curves, they do not correspond to the three concrete mixtures, as would be expected. The two standard concrete beams show similar responses but the first tested samples of the hooked-end steel and polypropylene polyethylene FRCs have similar curves and their respective second samples also closely align. This was probably due to the failure shape of the beams. Where the first samples, (a) and (c) in Figure 5.3, both failed in the centre of the beam, the second samples, (b) and (d) in Figure 5.3, failed close to one of the loading points, thereby offsetting the failure to one side and skewing the measured load-deflection results.

Figure 5.3 – Reinforced FRC beams at failure (top to bottom: polypropylene polyethylene FRC beams 1 (a) and 2 (b), hooked-end steel FRC beam 1 (c) and 2 (d))

Additionally the first hooked-end steel FRC beam shows significantly non-uniform spacing of cracks during the flexural test, as can be seen in Figure 5.3. Upon further investigation by sectioning the beam at the areas of low cracking and areas of high crack concentration, it was found that this beam had a highly inhomogeneous fibre distribution with some areas not containing any fibres. This can be seen in the two cross sections shown in Figure 5.4.

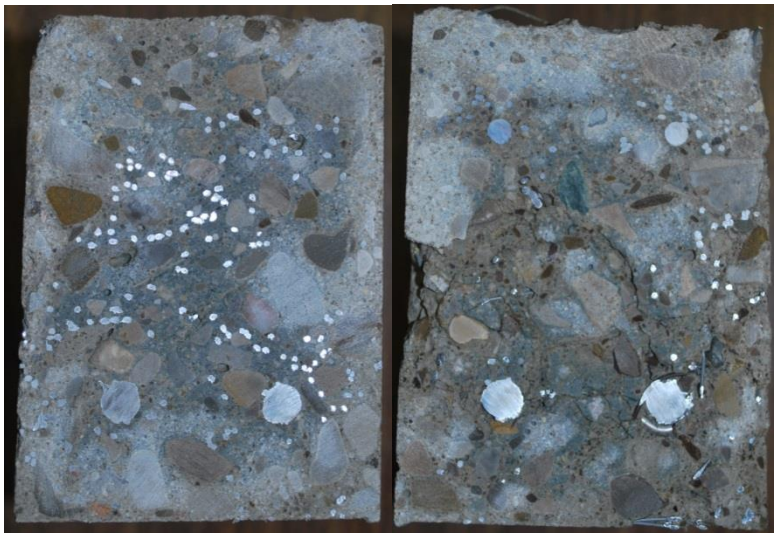

Figure 5.4 – Reinforced FRC beam cut sections from hooked-end steel FRC beam (left: normal fibre concentration, right: low fibre concentration)

This poor distribution of fibres is probably the cause of the low performance of the beam. As can be seen in the load deflection graph of Figure 4.12, both the first and second hooked-end steel beams have very similar performance up to about 25 mm of deflection where the first sample quickly begins to lose load capacity. This is a sign of the premature failure of the beam from the poor fibre distribution. This shows the importance of having a uniform distribution of fibres throughout the FRC. If one area has fewer fibres than the rest of the structure, it can change the behaviour of the whole unit. Because the weak area failed before the rest of the beam, it resulted in the beam acting like a non-FRC beam in that area having a sudden failure dropping off until the load was low enough for the remaining fibres to have an effect.

Adding fibres to the reinforced concrete beams greatly increased the post failure strength of the beams by allowing them to carry a substantial portion

of the load even after the beam would otherwise have failed. This property although useful in an extreme load or emergency situation, would not be important under everyday service loading. Normally a structure should not be exposed to such extreme loads that it would need to have a strong post failure response. Normally a concrete structure would have a service load range well below the ultimate failure load and, in this region, the addition of FRC does give two significant properties. The first of the benefits of FRC in a reinforced concrete structure is increased stiffness. As can be seen in Figure 5.5, showing the first 10 mm of deflection from the reinforced FRC beam tests, both FRC beams resulted in less deflection under the same load as the traditionally reinforced beams.

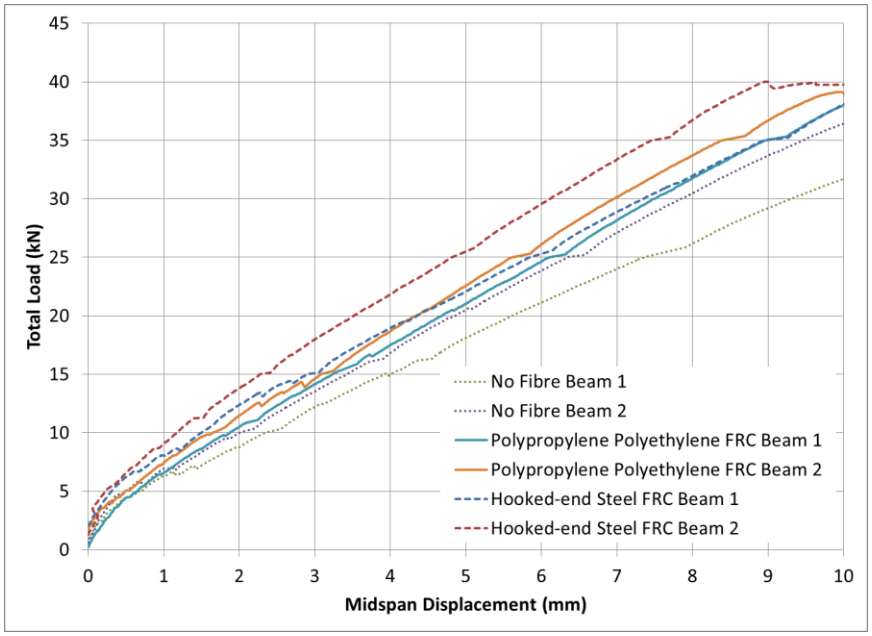

Figure 5.5 – Reinforced FRC beams load deflection up to 10 mm

Disregarding the first hooked-end steel FRC beam due to its inconsistent fibre distribution, the hooked-end steel FRC was the best performer, giving more

stiffness than the polypropylene polyethylene FRC. The second hooked-end FRC beam resulted in the lowest deflection in the pre-cracking range, at given load levels. This was in part due to it having the highest stiffness but also due to the increased cracking load that the hooked-end steel FRC beams had. Even the inconsistent first beam of the hooked-end steel showed similarly high cracking load at the beginning of the test before quickly crossing over the curve for polypropylene polyethylene FRC, due to its reduced stiffness, while still maintaining a lower deflection than the no fibre beams within the first 10 mm.

The increased stiffness of the beams is closely linked to the second major benefit of the FRC, the reduction in crack widths. When FRC is added to the beams, the crack widths are greatly reduced. The fibres bridging the cracks and restraining them, keeping small cracks from growing into large cracks, reduces the curvature and deflection of the beam increasing the overall stiffness. Table 4.8 shows the significant change in the crack widths from the control to the FRCs. An assumed maximum service load was selected for the reinforced FRC beams as 15 kN or 3.75 kNm based on it being approximately one third of the ultimate load. In the assumed service load range, the average crack width was 0.05 mm less for the polypropylene polyethylene FRC and 0.1 mm for the hooked-end steel FRC. The added restraint from the fibres keeps the cracks narrow but also increases the number of cracks that form in the FRC. This can be seen in Table 4.8 and Table 4.9 where crack spacing and crack width were measured from the photos taken at a load of 3.75 kNm. The

average crack spacing of the FRCs was around 75 mm while the no fibre beams had an average crack spacing of about 100 mm. Although, with the addition of FRC there are more cracks in the concrete, they are smaller in width and depth. This is beneficial because if the cracks are kept small enough, penetration of water and other contaminants can be reduced even if more cracks are formed in the concrete. In the case of a bridge deck link slab, reduction in cracking is one of the largest benefits of FRC. If a link slab can be made to form only small cracks under the repetitive loading and unloading they experience without using the traditional high volumes of reinforcing steel, the cost of a link slab may be reduced while also increasing the long-term durability.

5.3. Material durability properties

5.3.1. Outdoor exposure strain samples

Environmental conditions are often one of the largest effects on a concrete structure, especially structures such as bridges. To study the effects of temperature and weather exposure on FRCs, samples were cast and placed outside for almost 2 years of Southern Ontario weather. Temperatures in the area ranged from a high of 34 ºC to a low of -24 ºC [53] and the samples were exposed to rain, snow and direct sunlight throughout the course of 96 weeks. As would be expected, the samples experienced higher strains in the warm weather and lower strains in the cold periods. Initially the strains of all samples were set to zero when they were placed outside. After an initial

period, the no fibre control and the polypropylene polyethylene FRC reached a point where they began to follow a similar trend with a relatively constant offset. The polypropylene polyethylene sample developed more strain than the control samples but this is not likely to be a result of the fibres but more likely a result of the final curing of the samples and acclimatizing to the outdoor conditions differently. The crimped steel FRC underwent the same curing and acclimatization period as the other samples; however, once the other samples stabilized in relation to each other the crimped steel FRC did not. Figure 5.6 shows the absolute difference of the two FRC samples in relation to the no fibre control with the crimped steel FRC line representing a negative offset (value difference below no fiber) and the polypropylene polyethylene FRC line representing a positive offset (value difference above no fibre). As can be seen in Figure 5.6, the crimped steel FRC does not maintain a constant offset. In summer months when temperatures are warmer, the crimped steel FRC develops less strain compared to the other samples.

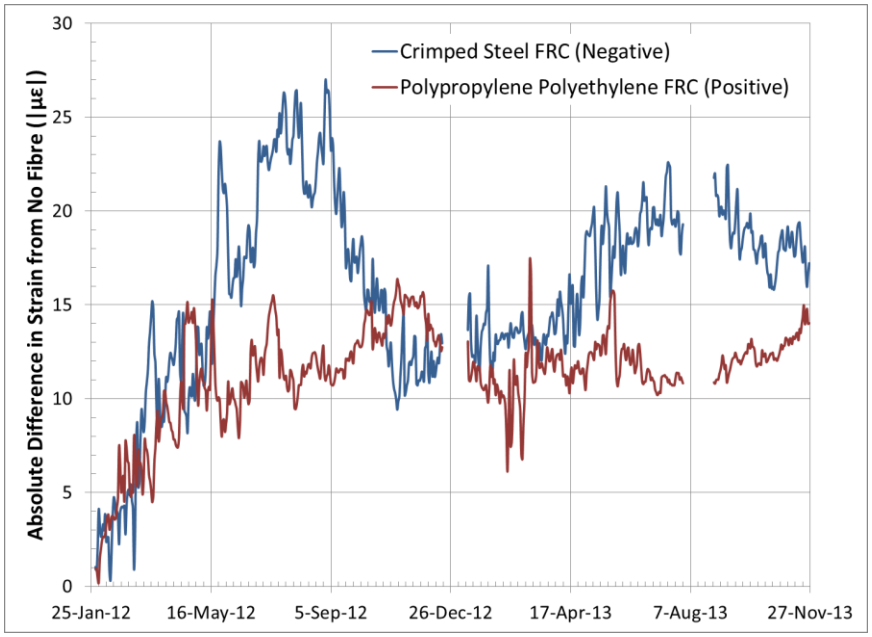

Figure 5.6 – Absolute difference in strain from no fibre control sample

When the samples are exposed to high temperature they expand as most materials do, and this increases the strain in the samples. It appears that when the crimped steel FRC sample is exposed to heat that would normally cause a large expansion of the concrete the steel fibres restrain the concrete matrix and keep the deformations low. In addition to developing less peak strain in high temperatures, the crimped steel FRC has consistently lower strain levels than the other samples. This is probably also due to the added restraint of the steel fibres not allowing the concrete to expand as much over the period of curing and acclimatization undergone by all the samples. This added restraint shown by the crimped steel fibres in the FRC would be beneficial to real world applications by reducing the thermal expansion of a structure at high temperatures.

In addition to weather conditions, another set of samples was exposed to road salt brine to simulate actual road conditions. These samples were also monitored for changes in the strain internally compared to the equivalent samples exposed only to water. The addition of the salt to the samples increased the levels of strain experienced by all the samples but the greatest effect was on the no fibre control sample that before salt, had the lowest strain but with salt, had the highest strain of the three salt exposed samples. The increased strain due to the addition of the salt ($CaCl_2$) was expected, from previous research done on similar samples, because of the formation of expansive calcium hydroxy-chloride within the material [54]. Both fibres seem to have an effect on reducing the strain caused by the added salt again by restraining the concrete and keeping it from expanding.

From this longer term test, it shows that both the synthetic and steel fibres are capable of reducing the strain levels in the FRCs compared to standard concrete. The steel fibres are more effective at controlling the strain and this should be true of the other steel fibres due to their higher stiffness. The polypropylene polyethylene fibres have a lesser effect on the internal strain of the concrete due to their lower stiffness and are not as able to restrain the concrete under high levels of expansion. Polypropylene and polyethylene may also suffer at higher temperatures due to softening of the material with the temperatures that can be observed inside concrete structures. Polypropylene has a glass transition temperature around -18^{o} C with polyethylene being around -110^{o} C [55]. Because the internal concrete

temperature is usually above both of these there is a possibility for additional softening of the material as the temperature increases. This could be disadvantageous to the polypropylene and polyethylene fibre because at high temperatures is when the highest strains occur.

5.3.2. Linear shrinkage testing

The linear shrinkage samples used for this testing were cast in two sets at different times of the year and, because of this, there is a large variation in the shrinkage readings from set to set while, within each set, the samples do not differ greatly from each other. This result suggests that the ambient conditions the samples were stored in differed, despite our best efforts to maintain similar conditions. It was observed that the ambient relative humidity (RH) in the storage location can vary from as low as 35% RH to as high as 75% RH. In addition to the highly variable ambient relative humidity, set one was stored in an airtight container. This could have retained much of the initial moisture from the samples, again, raising the RH to highly elevated levels. Using the ACI 209R-92 shrinkage model presented in ACI 209.2R-08 [56] shrinkage values were estimated for 35 days for both 35% RH and 75% RH, with calculations shown in Appendix L. The estimated shrinkage for an RH of 35% was 0.052% and 0.031% for an RH of 75%. Although, both calculations overestimate the maximum and minimum 35 day shrinkage values they do show that the difference of 0.02% shrinkage can be explained by differences in the ambient relative humidity.

In the first set, the crimped steel, the polypropylene polyethylene FRCs and the control mixture with no fibres were tested. In this test the control mixture actually resulted in the lowest shrinkage as can be seen in Figure 4.22. Although fibres are often used to control shrinkage cracking it is obvious in this test that this is not done by actually reducing the shrinkage but instead by restraining the concrete to maintain uniform shrinkage of the concrete as a whole and not allowing cracks to form as sections shrink away from each other.

The second set of samples included the FRCs made with the hooked-end steel, PVA as well as the deformed black and stainless steel fibres. All show similar shrinkage to each other again showing that the addition of fibre does not directly affect the shrinkage unrestrained concrete will undergo. The second set did undergo a larger amount of shrinkage than the first sample set and this was most likely due to the difference in interior conditions in the lab from summer to winter. As well, the storage container used for the second set was not as air tight as that used to store the first set and this could have affected the shrinkage rates of the samples. Despite this difference, it is still clear that the addition of fibres has little effect on the shrinkage of the samples when they are in an unrestrained condition and that the shrinkage rate is governed by the composition of the matrix as in normal concrete.

5.3.3. Freezing and thawing cycle testing

The samples for the cyclic freezing and thawing tests were again cast and tested in two sets with the first set consisting of the crimped steel FRC, the polypropylene polyethylene FRC and the control mixture with no fibres. This set was exposed to 300 cycles of freezing and thawing in just over 6 weeks. While working with the first set, some trouble was encountered when weighing the samples that could have contributed to significant error in the measurements. Because the samples were not weighed in the same location as the freezing and thawing cabinet, care was taken to keep the samples from losing too much moisture to evaporation during transport. Unfortunately this did not always work well. The data points collected on the fifth week of the test are an example of this, when an unforeseen delay was incurred in the time between removal of the samples from the chamber and the weighing of them. A significant amount of moisture was lost to evaporation and all samples showed a spike in mass loss. For this reason the data points from week five have been omitted from Figure 4.23. Otherwise over the 300 cycles of the test there was little change in the mass of the samples other than the loss observed from the baseline measurements to the first measurements after one week of freezing and thawing cycles. The polypropylene polyethylene FRC was seen to have a slight increase in mass over time but it is unclear if this was due to samples actually gaining mass, possibly by the fibres absorbing moisture, or if this was error in the measurement of the mass since the mass gained is only about 0.1%.

The second set of samples tested were the hooked-end steel FRC, PVA FRC, deformed stainless steel FRC and the deformed carbon steel FRC. To try to remove some of the error present in the first set of testing, these samples were submerged in water before weight measurements were taken. As a result of this, there was less mass loss in the first week of testing because the samples were closer to the moisture level that was present at the initial weigh in. Because of the larger number of samples that were tested in the second set, a greater load was placed on the freezing and thawing equipment slowing down the rate of freezing and thawing resulting in eight weeks being required to reach 300 cycles for this set. As with the previous set of freezing and thawing tests, little difference was noticed between any of the FRCs. As observed with the polypropylene polyethylene FRC, the PVA FRC seemed to gain some weight over the test. This again could have been well within the error of the test as it was only an increase of 0.05% over the duration of the test. Since this mass gain was seen in both synthetic fibres, it is likely that it is due to the fibres themselves and not the concrete surrounding them. The fibres may not be as resistant to freezing and thawing and, as they begin to breakdown, they absorb water increasing the total amount of water in the samples. If the fibres are beginning to break down, it is unknown what effect this would have on the overall strength of the sample but it is assumed that the degraded fibres would not be as beneficial as they would initially be.

In addition to the mass loss measurements for both sets of freezing and thawing samples, measurements of the relative dynamic modulus of elasticity

(MOE) were collected each week. These measurements did not appear to be affected by the moisture level of the samples and as a result all six weeks of data from set one was retained in Figure 4.24. As with the mass loss measurements, very little change was observed after the initial change in the first week of the test. A slight downward trend in the MOE was seen in the polypropylene polyethylene, deformed black and stainless steels and the PVA FRCs but it was not substantial. The no fibre control and the hooked-end and crimped steel FRCs MOE remained constant. In the last week of testing both the polypropylene polyethylene and the deformed stainless steel FRCs showed large decreases in MOE both dropping 2%. While this drop was not directly a concern it may show that the test was not long enough to capture adequate freezing and thawing damage to the samples and if the test was allowed to run longer more differentiation between the performance of the FRCs may have been observable.

5.3.4. Rust staining observation

Surface rust staining on many of the FRC samples with the various carbon steel fibre types was observed throughout the research. Although the corrosion was restricted to fibres on exposed surfaces and is considered superficial, it does cause an unsightly aesthetic. As the exposed fibres rust, they stain the concrete around them causing an orange spotted appearance on the surface of the concrete. Although this does not affect the overall structural performance of the concrete it could cause alarm to the general

public if seen on a structure. In the case of a link slab the FRC section would be covered on the top by a waterproof membrane and the asphalt road surface but would be exposed on the underside of the bridge and visible to anyone driving under the bridge. This rust staining was more predominant on samples that were exposed to road salts where samples were severely stained within six months but was also observed to a lesser extent when only exposed to water and normal outdoor conditions. Again in the case of a link slab the top surface of the slab would be protected from salt exposure by the road surface and although the underside of bridges are not directly exposed to road salts, as vehicles drive under a bridge spray can redeposit salts from the lower road surface onto the bottom of the bridge deck.

The problem of rust staining is specific to the carbon steel fibres and did not affect the stainless steel or the synthetic type fibres for obvious reasons. If the appearance of the FRC is important, either substituting a stainless steel fibre or using a comparable synthetic FRC would provide an acceptable solution.

6. Conclusions

In this research fibre-reinforced concrete has been shown to be a viable material for the construction of bridge deck link slabs in the Province of Ontario. Although the FRC mixtures examined do not have the same superior structural properties shown by the ultra-high performance fibre-reinforced concrete used in some link slabs, they do offer significant benefits at a much more widely accessible level. The goal of creating an FRC mixture with structural benefits from the addition of fibres while maintaining normal workability and using widely available fibres and concrete mixture ingredients was achieved.

6.1. Mix optimization

The ideal optimized mixture was found to be a one to one sand/gravel ratio and a paste percentage of 35% by volume was selected. The optimized FRC mixture showed excellent slump characteristics with both 1% and 2% by volume of the crimped steel and polypropylene polyethylene fibres, as a result it was believed that this would be true for other similar fibre types and dosages. A paste percentage of 35% resulted in a mixture that was highly workable and had no segregation problems without the use of any superplasticizers or water reducers. The high paste percentage would normally raise concerns about excessive shrinkage but is not expected to be a problem in the FRC due to the added fibres, which were often used for shrinkage cracking control.

6.2. Structural properties

A fibre dosage of 1.5% by volume was selected for all fibres as it was a compromise between the benefits of high fibre dosages and a lower cost mixture. Four steel fibres

and two synthetic polymer fibres were tested for structural properties. Hooked-end steel fibre was the clear leader in all structural property tests. The stiffness and strength of the steel combined with the anchorage provided by hooked-ends gave the FRC with this fibre the most beneficial properties.

The increases in the compressive and tensile strengths produced by the different fibres were linearly linked, with the steel fibres providing higher strengths than the synthetic fibres.

The ASTM C1609 flexural testing showed the hooked-end FRC preformed the best, having a high peak strength and the ability to maintain a high post-cracking load. This is beneficial to a link slab because it is inevitable that concrete will crack and the higher the load that the cracked FRC can carry, the smaller will be the cracks that do form.

When FRC was used in reinforced concrete beam both FRC mixtures were shown to be stiffer than the control beams before the ultimate load was reached but the hooked-end steel FRC had the lowest deflections, below the peak load. Both FRCs extended the post peak load capacity of the beams and extended the range of deflection that could be withstood before total failure of the beams but again the hooked-end steel FRC did this the best.

The hooked-end steel FRC did show a weakness when it comes to placement of the FRC mixture. Due to the stiff fibres getting caught in the dense steel reinforcement they were not able to evenly distribute throughout the beam. When working with steel fibres, extra care must be taken to ensure that a uniform FRC mixture reaches all

areas of the structure when casting. Failure to do so can lead to significant deficiencies in the strength and durability of the structure.

Data were also collected on the cracking of the steel reinforced FRC beams throughout the test. The hooked-end steel FRC again gave the greatest reduction in average crack width while the polypropylene polyethylene FRC gave significant reductions in crack width over the no fibre control beams as well. This is an important property for an FRC link slab because, if the crack widths in the concrete can be kept to a minimum, the penetration of water and other harmful elements can be greatly reduced improving the long-term durability of the link slab.

The results of the structural testing show that when focusing purely on structural properties of the FRC alone, the hooked-end steel fibre is the clear leader of the fibres tested. Although this is still the case when steel reinforcing bars are added, the difference between hooked-end steel and the polypropylene polyethylene FRCs was reduced significantly. This suggests that, although the fibres may not be as good when working alone to reinforce the concrete matrix, they can still contribute to the overall strength when working with steel reinforcement. Since the steel reinforcement carries the largest portion of the tensile stress in a reinforced FRC element, the fibres act as an assistant to the reinforcing bars maintaining the integrity of the concrete, keeping the bars restrained.

6.3. Durability properties

The long-term durability of an FRC material is also an important factor. Internal strain, linear shrinkage and freezing and thawing cycling tests were conducted on the

FRC mixtures throughout the research and unlike the structural properties results no mixture came out as the clear leader.

The outdoor exposure strain test was carried out on non-optimized FRC mixtures with the crimped steel and polypropylene polyethylene fibres of approximately 0.5% by volume. As the samples underwent thermal volume changes over the year it was noted that the steel fibre was better at restraining the expansion of the concrete than the synthetic fibre, due to the higher stiffness of the steel fibre.

In addition to the environmental exposure, some samples were exposed to road salt solution. Diffusion of the salt into the samples increased the strain in all the samples but both FRC types exhibited less strain increase than the no fibre concrete control sample. The difference was marginal and it was unclear if one fibre performed better than the other.

It may be concluded from the results of the linear shrinkage testing, that the selection of a higher paste percentage in the FRCs is not enough to result in a significant shrinkage problem in the curing and hardening stages, because none of the specimens tested exceeded the CSA A23.1 35 day limit of 0.04% or the Ontario Ministry of Transport specialty concrete applications limit of 0.06% [57]. Additionally, the type of fibre used was not shown to have an effect on the shrinkage of the samples.

Similarly all samples performed well in the ASTM C666 cyclic freezing and thawing testing. Both the mass loss and the relative dynamic modulus of elasticity (MOE) were relatively constant over the 300 cycle period. The synthetic FRC samples were seen to have a slight increase in mass rather than a loss as expected. This would most likely be due to the fibres themselves breaking down from the freezing and thawing and

absorbing moisture, thereby increasing the weight of the sample. If this is the case then the samples could be significantly weakened by the loss of strength that the fibres could no longer provide.

Finally, it was shown that when the stainless steel FRC was exposed to salt solution, it did not develop the spotted rusty appearance observed with the carbon steel FRCs giving the stainless steel fibres an aesthetic benefit over carbon steel fibres.

In conclusion it was demonstrated that an FRC mixture could be developed with common materials that would be beneficial to use in the construction of a link slab. With the use of an optimized mixture, consisting of equal weights of fine and coarse aggregates and a high percentage of cement paste, a consistent and reliable FRC could be created that is highly fluid allowing for easy placement and finishing. As long as care is taken to ensure that the fibres distribute evenly throughout the element, a dosage of 1.5% by volume of hooked-end macro steel fibres gives an FRC that is highly resistant to forming large cracks and shows high strength under the type of flexural loads often experienced by link slabs. Although the FRC mixtures created did not attain the high level of performance of a UHPFRC, they did provide a simpler and less costly alternative for improving the performance and durability of a link slab.

7. Recommendations for future work

To fully evaluate the properties of an FRC link slab using the FRC mixtures developed in this research some additional testing would be recommended.

7.1. Reinforced FRC flexural beam testing

When conducting the flexural testing of the reinforced FRC beams there was limited time and space, as a result only two FRC types could be tested. To fully understand the structural properties all the FRC types tested in the research should be evaluated in the reinforced FRC flexural beam test. Once all fibre types have been tested a clearer picture can be developed of what fibre types are suitable for use in an FRC link slab with traditional reinforcement.

7.2. Large-scale slab strip sections

Once the reinforced FRC flexural beam tests are completed, either all tested FRC types or a selection of the best performing FRCs should be tested in large-scale slab strip samples. The slab strip samples should be designed to closely simulate real world dimensions of a link slab within practical limits. The samples should be cast with feild procedures and have realistic reinforcing steel cages. These samples should be tested in flexural loading with measurements taken of load, deflection, crack spacing and crack widths as the loading progresses.

7.3. Fatigue testing

To establish how FRCs responds to repeated loading and unloading, cyclic fatigue testing should be considered. It is unknown if repeated loading and unloading will

decrease the effectiveness of the FRC to reduce crack size and continue to strengthen the concrete over time. This testing should be conducted on samples that include steel reinforcement. These tests could either be conducted on samples like the reinforced FRC flexural beams or if resources, space and time allow, on the large-scale slab strip style samples described above.

7.4. Investigation of environmental effects on synthetic fibres

Some of the tests conducted within the research pointed to possible deficiencies of synthetic fibres under extreme environmental conditions. Tests should be conducted to further understand how structural properties of synthetic fibres in FRCs are affected by softening at high temperatures and embrittlement at low temperatures. This testing could be conducted on compressive or splitting tensile samples in a controlled temperature setting. In addition there was some evidence that synthetic fibres degraded over time with repeated freezing and thawing. Testing of this could again be conducted with compressive or splitting tensile testing samples that had been repeatedly frozen and thawed. These tests would give a better understanding of the long-term durability of the synthetic fibres to be used in FRC link slabs.

References

[1] C. Lam, "Pulling the Teeth on Old Bridge Structures: Eliminating Bridge Expansion Joints with Concrete Link Slab," *Ontario's Transportation Technology Transfer Digest: Road Talk,* pp. Vol. 17, Issue 1, Winter 2011.

[2] A. Caner and P. Zia, "Behavior and Design of Links Slabs for Jointless Bridge Decks," *PCI Journal,* vol. 43, no. 3, pp. 68-80, May-June 1998.

[3] M. D. Lepech and V. C. Li, "Application of ECC for bridge deck link slabs," *Materials and Structures,* vol. 42, no. 9, pp. 1185-1195, July 2009.

[4] P. Rossi and N. Harrouche, "Mix design and mechanical behaviour of some steel-fibre-reinforced concretes used in reinforced concrete structures," *Materials and Structures,* vol. 23, no. 136, pp. 256-266, 1990.

[5] Ontario Ministry of Transportation, "Ontario Provincial Bridges," 29 Nov. 2013. [Online]. Available: http://www.mto.gov.on.ca/english/bridges/. [Accessed 12 Dec. 2013].

[6] E. Ulku, U. Attanayake and H. Aktan, "Jointless Bridge Deck with Link Slabs: Design for Durability," *Journal of the Transportation Research Board,* vol. 2131, no. Structures 2009, pp. 68-78, 2009.

[7] E. Ho and J. Lukashenko, "Link Slab Deck Joints," MMM Group Limited, Sep. 2011.

[8] School of Natural Resources and Environment at the University of Michigan, "Sustainable Concrete Infrastructure Materials and Systems," [Online]. Available: http://sitemaker.umich.edu/muses/muses-research/integration. [Accessed August 2013].

[9] A. Au, C. Lam, J. Au and B. Tharmabala, "Eliminating Deck Joints Using Debonded Link Slabs: Research and Field Tests in Ontario," *Journal of Bridge Engineering,* vol. 18, no. 8, pp. 768-778, Aug. 2013.

[10] Y. Y. Kim and V. C. Li, "Fatigue Response of Bridge Deck Link Slabs Designed with Ductile Engineered Cementitious Composite (ECC)," in *Proceedings of International Conference on Concrete under Severe Conditions - Environment & Loading*, Seoul, Korea, 2004.

[11] R. F. Zollo and C. D. Hays, "A Habitat of Fiber Reinforced Concrete," *Concrete International,* vol. 16, no. 6, pp. 23-26, June 1994.

[12] H. Helmink and J. E. Schibley, "Batching, Mixing, Placing, and Finishing Steel Fiber-Reinforced Floors," *Concrete international,* vol. 31, no. 7, pp. 26-28, July 2009.

[13] R. F. Zollo, "Fiber-reinforced concrete an overview after 30 years of development," *Cement and Concrete Composites,* vol. 19, no. 2, pp. 107-122, 1997.

[14] G. N. Karam, "Effect of Fiber-Fiber Interaction on the Strength Properties of Short Fiber Reinforced Cements," *Journal of Composites Technology & Research,* vol. 16, no. 2, pp. 154-160, Apr. 1994.

[15] C. X. Qian and P. Stroeven, "Development of hybrid polypropylene-steel fibre-reinforced concrete," *Cement and Concrete Research,* vol. 30, no. 1, pp. 63-69, Jan.

2000.

[16] P. Balaguru, "Contribution of fibers to crack reduction of cement composites during the initial and final setting period," *ACI Materials Journal,* vol. 91, no. 3, pp. 280-288, 1994.

[17] ACI Committee 544, "Guide for Specifying, Proportioning, and Production of Fiber-Reinforced Concrete," American Concrete Institute, Farmington Hills, MI, Nov. 2008.

[18] S. L. Billington and J. K. Yoon, "Cyclic Response of Unbonded Posttensioned Precast Columns with Ductile Fiber-Reinforced Concrete," *Journal of Bridge Engineering,* vol. 9, no. 4, pp. 353-363, July-Aug. 2004.

[19] C. D. Atis and K. Okan, "Properties of steel fiber reinforced fly ash concrete," *Construction and Building Materials,* vol. 23, no. 1, pp. 392-399, Jan. 2009.

[20] ASTM Standard C1116, 2010a, "Standard Specification for Fiber-Reinforced Concrete," ASTM International, West Conshohocken, PA, 2010, DOI: 10.1520/C1116_C1116M-10A, www.astm.org.

[21] A. M. Brandt, "Fibre reinforced cement-based (FRC) composites after over 40 years of development in building and civil engineering," *Composite Structures,* vol. 86, no. 1-3, pp. 3-9, 2008.

[22] ASTM Standard A820, 2011, "Standard Specification for Steel Fibers for Fiber-Reinforced Concrete," ASTM International, West Conshohocken, PA, 2011, DOI: 10.1520/A0820_A0820M-11, www.astm.org.

[23] M. A. Issa, M. A. Alhassan and J. C. Ramos, "Glass Fiber-Reinforced Latex-Modified Concrete," *Concrete international,* vol. 29, no. 3, pp. 48-52, Mar. 2007.

[24] S. P. Shah, "Fiber-Reinforced Concretes: A review of capabilities," *Concrete Construction,* 1 Mar. 1981.

[25] H. Krenchel and S. Shah, "Applications of Polypropylene Fibers in Scandinavia," *Concrete International,* vol. 7, no. 3, pp. 32-34, Mar. 1985.

[26] ASTM Standard D7508, 2010, "Standard Specification for Polyolefin Chopped Strands for Use in Concrete," ASTM International, West Conshohocken, PA, 2010, DOI: 10.1520/D7508_D7508M-10, www.astm.org.

[27] N. Banthia and A. Bhargava, "Permeability of stressed concrete and role of fiber reinforcement," *ACI Materials Journal,* vol. 104, no. 1, pp. 70-76, 2007.

[28] V. C. Li et al., "Interface Tailoring for Strain-Hardening Polyvinyl Alcohol-Engineered Cementitious Composite (PVA-ECC)," *ACI Materials Journal,* vol. 99, no. 5, pp. 463-472, Sept. 2002.

[29] S. Akihama, T. Suenaga and H. Nakagawa, "Carbon Fiber Reinfirced Concrete," *Concrete International,* vol. 10, no. 1, pp. 40-47, Jan. 1988.

[30] ASTM Standard D7357, 2007 (2012), "Standard Specification for Cellulose Fibers for Fiber-Reinforced Concrete," ASTM International, West Conshohocken, PA, 2012, DOI: 10.1520/D7357-07R12, www.astm.org.

[31] S. A. Hamoush and M. M. El-Hawary, "Feather Fiber Reinforced Concrete," *Concrete International,* vol. 16, no. 6, pp. 33-35, June 1994.

[32] P. N. Balaguru and S. P. Shah, "Alternative reinforcing materials for less developed

countries," *International Journal for Development Technology,* vol. 3, no. 2, pp. 87-107, 1985.

[33] G. L. Vondran, "Applications of Steel Fiber Reinforced Concrete," *Concrete International,* vol. 13, no. 11, pp. 44-49, Nov. 1991.

[34] S. Grünewald and J. C. Walraven, "Parameter-study on the influence of steel fibers and coarse aggregate content on the fresh properties of self-compacting concrete," *Cement and Concrete Research,* vol. 31, no. 12, pp. 1793-1798, 2001.

[35] B. Bakht et al., "Canadian Bridge Design Code Provisions for Fiber-Reinforced Structures," *Journal of Composites for Construction,* vol. 4, no. 1, pp. 3-15, Feb. 2000.

[36] M. A. Harding, "Mixing, Placing, and Finishing Fiber-Reinforced Concrete," *Concrete Construction,* 1 July 1996.

[37] M. Laura, Interviewee, [Interview]. 2012.

[38] ASTM Standard C39, 2012a, "Standard Test Method for Compressive Strength of Cylindrical Concrete Specimens," ASTM International, West Conshohocken, PA, 2012, DOI: 10.1520/C0039_C0039M-12A, www.astm.org.

[39] ASTM Standard C496, 2011, "Standard Test Method for Splitting Tensile Strength of Cylindrical Concrete Specimens," ASTM International, West Conshohocken, PA, 2011, DOI: 10.1520/C0496_C0496M-11, www.astm.org.

[40] ASTM Standard C231, 2010, "Standard Test Method for Air Content of Freshly Mixed Concrete by the Pressure Method," ASTM International, West Conshohocken, PA, 2010, DOI: 10.1520/C0231_C0231M-10, www.astm.org.

[41] ASTM Standard C143, 2012, "Standard Test Method for Slump of Hydraulic-Cement Concrete," ASTM International, West Conshohocken, PA, 2012, DOI: 10.1520/C0143_C0143M-12, www.astm.org.

[42] ASTM Standard C1609, 2012, "Standard Test Method for Flexural Performance of Fiber-Reinforced Concrete (Using Beam With Third-Point Loading)," ASTM International, West Conshohocken, PA, 2012, DOI: 10.1520/C1609_C1609M-12, www.astm.org.

[43] ASTM Standard C192, 2013a, "Standard Practice for Making and Curing Concrete Test Specimens in the Laboratory," ASTM International, West Conshohocken, PA, 2013, DOI: 10.1520/C0192_C0192M, www.astm.org.

[44] *Test Methods and Standard Practices for Concrete*, CSA A23.2, 2009.

[45] *Concrete materials and methods of concrete construction*, CSA A23.1, 2009.

[46] M. Mahoney , Interviewee, [Interview]. 2012.

[47] J. G. McCants, Interviewee, [Interview]. 2012.

[48] *Method of Test for Linear Shrinkage of Concrete*, MTO Test Method LS-435, 2001.

[49] ASTM Standard C666, 2003 (2008), "Standard Test Method for Resistance of Concrete to Rapid Freezing and Thawing," ASTM International, West Conshohocken, PA, 2008, DOI: 10.1520/C0666_C0666M-03R08, www.astm.org.

[50] ASTM Standard C457, 2012, "Standard Test Method for Microscopical Determination of Parameters of the Air-Void System in Hardened Concrete," ASTM International, West Conshohocken, PA, 2008, DOI: 10.1520/C0457_C0457M-12, www.astm.org.

[51] Portland Cement Association, "Control of Air Content in Concrete," *Concrete Technology Today,* vol. 19, no. 1, pp. 1-8, Apr. 1998.

[52] Y. Hong, “Analysis and Design of Link Slabs in Jointless Bridges with Fibre-Reinforced Concrete,” M.S. thesis, Dept. Civil and Envromental Eng., Univ. Waterloo, Waterloo, ON, 2014.

[53] University of Waterloo, "University of Waterloo Weather Station," [Online]. Available: http://weather.uwaterloo.ca/.

[54] M. Cremasco, “Analysis of the Effects of Anti-Icing Agents on the Mechanical Properties of Concrete,” M.S. thesis, Dept. Mech. and Mechatronics Eng., Univ. Waterloo,Waterloo, ON, 2012.

[55] W. D. Callister, Materials Science and Engineering: An Introduction, New York: John Wiley & Sons, Inc., 2007.

[56] ACI Committee 209, "Guide for Modeling and Calculating Shrinkage and Creep in Hardened Concrete," American Concrete Institute, Farmington Hills, MI, May 2008.

[57] Ready Mixed Concrete Association of Ontario, "Concrete Producer Guidelines for MTO Concrete Projects," 1 October 2010. [Online]. Available: http://www.rmcao.org/sites/default/files/Concrete%20Producer%20Guidelines%20for%20MTO%20Projects_0.pdf. [Accessed September 2012].

Appendices

Appendix A – Mixture proportions for optimization mixtures

Table A.0.1 – Concrete mixture proportions for S/G ratio optimization (per cubic metre)

	Units	No fibre				1% Polypropylene polyethylene FRC				1% Crimped steel FRC	
S/G ratio		0.7	**1**	1.5	2	0.7	1	**1.5**	2	0.7	**1**
Gravel	kg	1053	**895**	716	597	1042	886	**709**	591	1042	**886**
Sand	kg	737	**895**	1074	1193	730	886	**1063**	1181	730	**886**
GU cement	kg	266	**266**	266	266	263	263	**263**	263	263	**263**
Slag	kg	89	**89**	89	89	88	88	**88**	88	88	**88**
Fibre	kg	0	**0**	0	0	10	10	**10**	10	77	**77**
Air entrainer	mL	237	**237**	237	237	235	235	**235**	235	235	**235**
Superplasticizer	mL	476	**476**	476	476	300	300	**300**	300	1048	**1048**
Total water	L	159	**159**	159	159	157	157	**157**	157	157	**157**
Slump	mm	30	**45**	0	0	0	3	**5**	0	0	**35**

	Units	1% Crimped steel FRC		2% Polypropylene polyethylene FRC				2% Crimped steel FRC			
S/G ratio		1.5	2	0.7	1	**1.5**	2	**0.7**	1	1.5	2
Gravel	kg	709	591	1032	877	**702**	585	**983**	835	668	557
Sand	kg	1063	1181	722	877	**1053**	1169	**688**	835	1002	1114
GU cement	kg	263	263	261	261	**261**	261	**295**	295	295	295
Slag	kg	88	88	87	87	**87**	87	**99**	99	99	99
Fibre	kg	77	77	20	20	**20**	20	**147**	147	147	147
Air entrainer	mL	235	235	232	232	**232**	232	**232**	232	232	232
Superplasticizer	mL	1048	1048	1850	1850	**1850**	1850	**619**	619	619	619
Total water	L	157	157	156	156	**156**	156	**176**	176	176	176
Slump	mm	0	0	0	NA	**0**	NA	**130**	90	70	60

Selected mixtures shown in **Bold.**

Table A.0.2 – Concrete mixture proportions for paste percentage optimization (per cubic metre)

	Units	No fibre				1% Polypropylene polyethylene FRC				1% Crimped steel FRC	
Paste %		26.75	30.0	32.5	35.0	26.75	30.0	32.5	35.0	26.75	30.0
Gravel	kg	895	859	828	798	709	677	653	629	886	847
Sand	kg	895	859	828	798	1063	1016	980	944	886	847
GU cement	kg	266	295	319	344	263	295	320	345	263	295
Slag	kg	89	99	107	115	88	99	107	115	88	99
Fibre	kg	0	0	0	0	10	10	9	9	77	74
Air entrainer	mL	237	237	237	237	235	235	235	235	235	235
Superplasticizer	mL	476	528	572	616	900	1009	1093	1177	1048	1174
Total water	L	159	175	190	204	157	176	190	204	157	175
Slump	mm	0	70	175	0	0	40	90	180	30	150

	Units	1% Crimped steel FRC		2% Polypropylene polyethylene FRC				2% Crimped steel FRC			
Paste %		32.5	35.0	26.75	30.0	32.5	35.0	26.75	30.0	32.5	35.0
Gravel	kg	817	787	702	668	644	620	1032	983	946	911
Sand	kg	817	787	1053	1002	966	930	722	688	662	638
GU cement	kg	320	344	261	296	320	345	261	295	321	345
Slag	kg	107	115	87	99	107	115	87	99	107	116
Fibre	kg	71	68	20	19	18	18	154	147	141	136
Air entrainer	mL	235	235	232	232	232	232	232	232	232	232
Superplasticizer	mL	1271	0	1100	1248	1352	1456	925	1048	1138	1226
Total water	L	190	204	156	176	190	204	155	176	190	205
Slump	mm	230	180	0	20	NA	140	5	120	170	185

Appendix B – Salt solution analysis

Table A.0.3 – Analysis of salt solutions

	K	Mg	Ca	Fe	Na	Sr	Cl	Br	SO_4
Unit	mg/L	mg/L	mg/L	mg/L	mg/L	mg/L	mg/L	mg/L	mg/L
NaCl	275	49.6	534	4.78	103000	5.26	169000	< 50	1390
$CaCl_2$	7500	< 10	134000	1.14	4490	2450	245000	3140	83.4

Appendix C – Compressive strength testing results for optimization mixtures

Table A.0.4 – Compressive strength testing results for no fibre S/G optimization mixtures

Mix	S/G Ratio	Sample	MPa	MPa (avg)	Standard Deviation	kN	kN (avg)
1	0.7	a	52.46	53.08	2.46	412.04	416.88
		b	50.98			400.41	
		c	55.79			438.19	
2	1.0	a	46.40	49.57	2.78	364.46	389.31
		b	50.72			398.33	
		c	51.59			405.16	
3	1.5	a	57.88	56.21	1.48	454.58	441.45
		b	55.05			432.36	
		c	55.70			437.41	
4	2.0	a	33.70	51.34	1.13	264.65	403.22
		b	52.14			409.48	
		c	50.55			396.96	

*Red values not counted in average

Table A.0.5 – Compressive strength testing results for 1% polypropylene polyethylene FRC S/G optimization mixtures

Mix	S/G Ratio	Sample	MPa	MPa (avg)	Standard Deviation	kN	kN (avg)
1	0.7	a	58.19	58.46	1.31	457.02	459.12
		b	59.87			470.25	
		c	57.30			450.08	
2	1.0	a	51.29	52.42	1.65	402.85	411.67
		b	54.31			426.54	
		c	51.65			405.62	
3	1.5	a	52.04	52.64	0.69	408.76	413.42
		b	53.39			419.33	
		c	52.48			412.16	
4	2.0	a	50.06	50.89	0.94	393.13	399.71
		b	51.90			407.66	
		c	50.72			398.34	
5	2.5	a	43.03	43.36	0.47	337.97	340.58
		b	43.70			343.19	

Table A.0.6 – Compressive strength testing results for 1% crimped steel FRC S/G optimization mixtures

Mix	S/G Ratio	Sample	MPa	MPa (avg)	Standard Deviation	kN	kN (avg)
1	0.7	a	65.65	64.09	1.97	515.58	503.39
		b	61.87			485.96	
		c	64.76			508.64	
2	1.0	a	55.64	54.66	1.10	437.01	429.29
		b	53.48			420.01	
		c	54.86			430.85	
3	1.5	a	60.65	59.65	0.87	476.33	329.14
		b	59.11			464.25	
		c	59.19			46.85	
4	2.0	a	58.55	58.27	0.65	459.85	457.64
		b	57.52			451.76	
		c	58.74			461.30	

Table A.0.7 – Compressive strength testing results for 2% polypropylene polyethylene FRC S/G optimization mixtures

Mix	S/G Ratio	Sample	MPa	MPa (avg)	Standard Deviation	kN	kN (avg)
1	0.7	a	41.78	37.59	4.08	328.18	295.23
		b	33.63			264.09	
		c	37.36			293.42	
3	1.5	a	53.30	48.69	4.00	418.60	382.41
		b	46.11			362.19	
		c	46.66			366.45	

Table A.0.8 – Compressive strength testing results for 2% crimped steel FRC S/G optimization mixtures

Mix	S/G Ratio	Sample	MPa	MPa (avg)	Standard Deviation	kN	kN (avg)
1	0.7	a	45.93	45.98	0.04	360.74	361.09
		b	45.99			361.17	
		c	46.01			361.37	
2	1.0	a	41.82	42.61	0.90	328.49	334.65
		b	42.41			333.10	
		c	43.59			342.35	
3	1.5	a	42.80	42.46	0.81	336.19	333.47
		b	41.53			326.19	
		c	43.04			338.03	
4	2.0	a	41.36	40.90	0.40	324.86	321.21
		b	40.68			319.49	
		c	40.65			319.28	

Table A.0.9 – Compressive strength testing results for no fibre paste % optimization mixtures

Mix	Paste %	Sample	MPa	MPa (avg)	Standard Deviation	kN	kN (avg)
1	0.2675	a	59.15	57.92	1.52	464.57	454.89
		b	56.21			441.50	
		c	58.39			458.60	
2	0.3	a	54.22	53.82	0.35	425.83	422.68
		b	53.55			420.59	
		c	53.68			421.63	
3	0.325	a	50.97	51.01	1.04	400.31	400.64
		b	49.99			392.65	
		c	52.07			408.97	

Table A.0.10 – Compressive strength testing results for 1% polypropylene polyethylene FRC paste % optimization mixtures

Mix	Paste %	Sample	MPa	MPa (avg)	Standard Deviation	kN	kN (avg)
1	0.2675	a	49.41	50.70	1.61	388.04	398.20
		b	52.50			412.38	
		c	50.19			394.17	
2	0.3	a	50.43	50.52	0.60	396.07	396.82
		b	49.98			392.56	
		c	51.16			401.83	
4	0.325	a	46.54	48.06	1.31	365.49	377.44
		b	48.86			383.79	
		c	48.77			383.04	
3	0.35	a	47.51	47.48	1.09	373.16	372.93
		b	46.38			364.27	
		c	48.56			381.37	

Table A.0.11 – Compressive strength testing results for 1% crimped steel FRC paste % optimization mixtures

Mix	Paste %	Sample	MPa	MPa (avg)	Standard Deviation	kN	kN (avg)
1	0.2675	a	54.74	55.11	1.01	429.88	432.80
		b	54.33			426.74	
		c	56.25			441.78	
2	0.3	a	50.54	50.30	1.39	396.91	395.08
		b	48.82			383.37	
		c	51.56			404.97	
4	0.325	a	50.66	50.93	0.87	397.83	400.02
		b	50.23			394.52	
		c	51.91			407.70	
3	0.35	a	55.28	53.39	1.66	434.20	419.34
		b	52.70			413.90	
		c	52.19			409.94	

Table A.0.12 – Compressive strength testing results for 2% polypropylene polyethylene FRC paste % optimization mixtures

Mix	Paste %	Sample	MPa	MPa (avg)	Standard Deviation	kN	kN (avg)
1	0.2675	a	53.30	48.69	4.00	515.58	503.39
		b	46.11			485.96	
		c	46.66			508.64	
2	0.3	a	48.57	49.57	1.47	437.01	429.29
		b	51.26			420.01	
		c	48.88			430.85	
4	0.35	a	41.02	40.57	1.94	459.85	457.64
		b	42.24			451.76	
		c	38.44			461.30	

Table A.0.13 – Compressive strength testing results for 2% crimped steel FRC paste % optimization mixtures

Mix	Paste %	Sample	MPa	MPa (avg)	Standard Deviation	kN	kN (avg)
1	0.2675	a	45.60	45.13	1.11	358.11	354.43
		b	43.86			344.48	
		c	45.93			360.71	
2	0.3	a	43.28	41.27	1.77	339.93	324.12
		b	39.96			313.83	
		c	40.56			318.60	
3	0.325	a	39.48	38.87	2.50	310.06	305.24
		b	36.12			283.63	
		c	41.00			322.03	
4	0.35	a	42.03	41.02	1.86	330.09	322.16
		b	42.16			331.10	
		c	38.87			305.29	

Appendix D – Splitting tensile strength testing results for optimization mixtures

Table A.0.14 – Splitting tensile strength testing results for no fibre FRC S/G optimization mixtures

Mix	S/G Ratio	Sample	L	kN	MPa	MPa (avg)
1	0.7	a	202.0	136.4	4.30	4.32
		b	202.0	130.7	4.12	
		c	202.0	143.7	4.53	
2	1	a	202.0	146.1	4.61	4.18
		b	204.0	104.4	3.26	
		c	201.0	147.7	4.68	
3	1.5	a	200.0	116.3	3.70	4.16
		b	199.0	126.2	4.04	
		c	199.0	148.6	4.75	
4	2	a	199.0	109.9	3.51	3.83
		b	200.0	125.0	3.98	
		c	200.0	126.0	4.01	

Table A.0.15 – Splitting tensile strength testing results for 1% polypropylene polyethylene FRC S/G optimization mixtures

Mix	S/G Ratio	Sample	L	kN	MPa	MPa (avg)
1	0.7	a	200.0	157.9	5.03	4.98
		b	201.0	156.0	4.94	
2	1.0	a	199.0	155.8	4.98	4.82
		b	201.0	146.7	4.65	
3	1.5	a	200.0	155.7	4.96	5.43
		b	201.3	186.9	5.91	
4	2.0	a	200.7	146.3	4.64	4.96
		b	201.2	167.0	5.28	
5	2.5	a	198.0	143.6	4.62	4.93
		b	204.0	168.0	5.24	

Table A.0.16 – Splitting tensile strength testing results for 1% crimped steel FRC S/G optimization mixtures

Mix	S/G Ratio	Sample	L	kN	MPa	MPa (avg)
1	0.7	a	200.0	224.2	7.14	7.15
		b	200.0	240.9	7.67	
		c	200.0	209.0	6.65	
2	1	a	200.0	164.3	5.23	5.72
		b	200.0	183.7	5.85	
		c	200.0	191.5	6.10	
3	1.5	a	200.0	265.5	8.45	6.93
		b	200.0	225.2	7.17	
		c	200.0	162.8	5.18	
4	2	a	200.0	197.9	6.30	5.84
		b	200.0	172.5	5.49	
		c	200.0	179.6	5.72	

Table A.0.17 – Splitting tensile strength testing results for 2% polypropylene polyethylene FRC S/G optimization mixtures

Mix	S/G Ratio	Sample	L	kN	MPa	MPa (avg)
1	0.7	a	207.0	132.2	4.06	4.53
		b	207.0	150.9	4.64	
		c	204.0	156.9	4.90	
3	1.5	a	195.0	155.6	5.08	5.26
		b	202.0	161.0	5.07	
		c	200.0	176.9	5.63	

Table A.0.18 – Splitting tensile strength testing results for 2% crimped steel FRC S/G optimization mixtures

Mix	S/G Ratio	Sample	L	kN	MPa	MPa (avg)
1	0.7	a	201.0	164.5	5.21	5.49
		b	199.0	182.4	5.84	
		c	200.0	170.8	5.44	
2	1	a	200.0	161.6	5.14	5.15
		b	200.0	167.0	5.32	
		c	200.0	156.8	4.99	
3	1.5	a	201.0	170.5	5.40	5.52
		b	204.0	174.4	5.44	
		c	200.0	179.5	5.71	
4	2	a	200.0	133.9	4.26	4.68
		b	200.0	157.0	5.00	
		c	200.0	150.2	4.78	

Table A.0.19 – Splitting tensile strength testing results for no fibre FRC paste % optimization mixtures

Mix	Paste %	Sample	L	kN	MPa	MPa (avg)
1	0.2675	a	200.0	133.9	4.26	3.90
		b	200.0	120.2	3.83	
		c	200.0	113.1	3.60	
2	0.3	a	200.0	122.0	3.88	3.88
		b	200.0	123.0	3.91	
		c	200.0	120.7	3.84	
3	0.325	a	201.0	146.3	4.63	4.24
		b	203.0	126.2	3.96	
		c	199.0	129.4	4.14	

Table A.0.20 – Splitting tensile strength testing results for 1% polypropylene polyethylene FRC paste % optimization mixtures

Mix	Paste %	Sample	L	kN	MPa	MPa (avg)
1	0.2675	a	198.0	160.0	5.14	5.08
		b	199.0	158.9	5.08	
		c	199.0	156.9	5.02	
2	0.3	a	199.0	127.1	4.06	4.63
		b	200.0	159.4	5.07	
		c	201.0	149.9	4.75	
4	0.325	a	198.0	157.1	5.05	4.60
		b	200.0	134.3	4.27	
		c	200.0	141.0	4.49	
3	0.35	a	199.0	145.8	4.66	4.58
		b	195.5	141.5	4.61	
		c	199.5	139.8	4.46	

Table A.0.21– Splitting tensile strength testing results for 1% crimped steel FRC paste % optimization mixtures

Mix	Paste %	Sample	L	kN	MPa	MPa (avg)
1	0.2675	a	200.0	181.1	5.77	5.87
		b	200.0	183.5	5.84	
		c	200.0	188.4	6.00	
2	0.3	a	200.0	139.0	4.43	4.98
		b	200.0	187.8	5.98	
		c	199.0	142.1	4.55	
4	0.325	a	200.0	172.1	5.48	5.68
		b	200.0	184.5	5.87	
		c	200.0	178.9	5.69	
3	0.35	a	202.0	165.4	5.21	5.34
		b	202.0	164.1	5.17	
		c	202.0	178.4	5.62	

Table A.0.22 – Splitting tensile strength testing results for 2% polypropylene polyethylene FRC paste % optimization mixtures

Mix	Paste %	Sample	L	kN	MPa	MPa (avg)
1	0.2675	a	195.0	155.6	5.08	5.26
		b	202.0	161.0	5.07	
		c	200.0	176.9	5.63	
2	0.3	a	204.0	164.3	5.13	5.06
		b	204.0	162.3	5.06	
		c	204.0	160.1	5.00	
4	0.35	a	204.0	137.7	4.30	4.28
		b	204.0	143.0	4.46	
		c	204.0	131.1	4.09	

Table A.0.23 – Splitting tensile strength testing results for 2% crimped steel FRC paste % optimization mixtures

Mix	Paste %	Sample	L	kN	MPa	MPa (avg)
1	0.2675	a	200.0	196.0	6.24	5.93
		b	200.0	189.3	6.03	
		c	200.0	173.9	5.54	
2	0.3	a	198.0	181.0	5.82	5.42
		b	196.0	162.7	5.29	
		c	204.0	164.9	5.15	
3	0.325	a	200.0	168.4	5.36	5.44
		b	200.0	168.4	5.36	
		c	199.0	174.8	5.59	
4	0.35	a	202.0	173.1	5.46	5.29
		b	204.0	168.8	5.27	
		c	203.0	164.4	5.15	

Appendix E – Numerical results for ASTM C1609 flexural testing

Table A.0.24 – Numerical results for ASTM C1609 flexural testing

	Units	NF1	NF2	NF3	PP1	PP2	PP3
P_1	kN	39.30	42.50	45.10	53.91	48.48	49.62
P_{600}	kN	NA	NA	NA	15.49	19.90	1.70
P_{150}	kN	NA	NA	NA	15.53	17.15	11.03
f_1	MPa	5.32	5.76	6.11	7.30	6.57	6.72
f_{600}	MPa	NA	NA	NA	2.10	2.70	0.23
f_{150}	MPa	NA	NA	NA	2.10	2.32	1.49
T_{150}	J	NA	NA	NA	52.55	58.87	32.38
R_{t150}		NA	NA	NA	31.98%	39.85%	21.41%

	Units	St1	St2	St3	HS1	HS2	HS3
P_1	kN	50.30	48.91	48.92	56.21	57.29	52.99
P_{600}	kN	26.41	18.72	26.05	45.36	43.33	45.72
P_{150}	kN	16.07	9.20	13.44	25.84	21.02	27.67
f_1	MPa	6.81	6.63	6.63	7.61	7.76	7.18
f_{600}	MPa	3.58	2.54	3.53	6.14	5.87	6.19
f_{150}	MPa	2.18	1.25	1.82	3.50	2.85	3.75
T_{150}	J	73.63	49.15	70.54	116.84	105.54	116.64
R_{t150}		48.02%	32.97%	47.30%	68.19%	60.44%	72.21%

	Units	SS1	SS2	SS3	BS1	BS2	BS3
P_1	kN	55.02	52.70	51.11	54.03	59.19	55.70
P_{600}	kN	31.69	27.84	26.16	29.03	24.90	36.06
P_{150}	kN	6.47	4.89	6.17	5.99	3.58	6.17
f_1	MPa	7.45	7.14	6.92	7.32	8.02	7.55
f_{600}	MPa	4.29	3.77	3.54	3.93	3.37	4.89
f_{150}	MPa	0.88	0.66	0.84	0.81	0.48	0.84
T_{150}	J	59.36	55.12	54.20	59.85	52.49	67.52
R_{t150}		35.40%	34.31%	34.80%	36.34%	29.10%	39.77%

	Units	PVA1	PVA2
P_1	kN	53.49	54.85
P_{600}	kN	28.30	32.29
P_{150}	kN	7.79	7.70
f_1	MPa	7.25	7.43
f_{600}	MPa	3.83	4.37
f_{150}	MPa	1.06	1.04
T_{150}	J	68.05	69.70
R_{t150}		41.74%	41.70%

Appendix F – Compressive and splitting tensile strength testing results for ASTM C1609 flexural testing mixtures

Table A.0.25 – Compressive strength testing results for ASTM C1609 flexural testing mixtures

Mix	Sample	MPa	MPa (avg)
NF	1	44.71	42.76
	2	45.93	
	3	37.65	
St	1	43.03	43.89
	2	42.39	
	3	46.26	
PP	1	42.07	41.31
	2	40.47	
	3	41.41	
HS	1	48.26	48.90
	2	51.09	
	3	47.36	
PVA	1	40.24	41.02
	2	40.96	
	3	41.87	
SS	1	45.19	45.70
	2	45.02	
	3	46.90	
BS	1	49.74	48.32
	2	50.76	
	3	44.46	

Table A.0.26 – Splitting tensile strength testing results for ASTM C1609 flexural testing mixtures

Mix	Sample	L	kN	MPa	MPa (avg)
NF	1	203.0	102.8	3.22	3.81
	2	204.0	141.4	4.41	
	3	202.0	120.3	3.79	
St	1	200.0	161.8	5.15	5.21
	2	198.0	168.1	5.41	
	3	199.0	158.3	5.06	
PP	1	199.0	150.0	4.80	4.50
	2	201.0	138.8	4.40	
	3	202.0	136.9	4.32	
HS	1	199.0	194.2	6.21	6.34
	2	198.0	194.8	6.26	
	3	200.0	205.6	6.54	
PVA	1	200.0	133.1	4.24	4.59
	2	200.0	154.4	4.91	
	3	200.0	145.5	4.63	
SS	1	201.0	184.5	5.84	5.55
	2	200.0	155.6	4.95	
	3	200.0	183.8	5.85	
BS	1	200.0	173.4	5.52	5.54
	2	200.0	165.6	5.27	
	3	200.0	182.9	5.82	

Appendix G – Crack width measurements for reinforced FRC beam testing

Table A.0.27 – Crack width measurements for no fibre reinforced beam 1

Load (kN)	10	15	25
Moment (kNm)	2.5	3.75	6.25
Crack 1	0.10	0.20	0.30
Crack 2	0.10	0.20	0.20
Crack 3	0.10	0.15	0.30
Crack 4	0.10	0.15	0.35
Crack 5	0.10	0.10	0.25
Crack 6	0.10	0.15	0.20

Table A.0.28 – Crack width measurements for no fibre reinforced beam 2

Load (kN)	10	15	25
Moment (kNm)	2.5	3.75	6.25
Crack 1	0.05	0.15	0.30
Crack 2	0.10	0.20	0.30
Crack 3	0.05	0.20	0.20
Crack 4	0.10	0.20	0.20
Crack 5	0.05	0.10	0.10

Table A.0.29 – Crack width measurements for reinforced polypropylene polyethylene FRC beam 1

Load (kN)	10	15	25	35
Moment (kNm)	2.5	3.75	6.25	8.75
Crack 1	0.10	0.10	0.15	0.15
Crack 2	0.10	0.10	0.10	0.15
Crack 3	0.10	0.15	0.15	0.15
Crack 4	0.10	0.15	0.15	0.15
Crack 5	0.10	0.10	0.10	0.15

Table A.0.30 – Crack width measurements for reinforced polypropylene polyethylene FRC beam 2

Load (kN)	10	15	25	35
Moment (kNm)	2.5	3.75	6.25	8.75
Crack 1	0.05	0.10	0.15	0.20
Crack 2	0.10	0.10	0.15	0.20
Crack 3	0.10	0.10	0.10	0.20
Crack 4	0.10	0.10	0.20	0.30
Crack 5	-	0.10	0.10	0.20
Crack 6	-	0.10	0.15	0.25

Table A.0.31 – Crack width measurements for reinforced hooked-end steel FRC beam 1

Load (kN)	10	15	25	35
Moment (kNm)	2.5	3.75	6.25	8.75
Crack 1	0.05	0.05	0.15	0.15
Crack 2	0.05	0.10	0.10	0.15
Crack 3	0.05	0.05	0.10	0.30
Crack 4	-	0.05	0.10	0.10
Crack 5	-	0.05	0.10	0.10

Table A.0.32 – Crack width measurements for reinforced hooked-end steel FRC beam 2

Load (kN)	10	15	25	35
Moment (kNm)	2.5	3.75	6.25	8.75
Crack 1	0.05	0.05	0.10	0.10
Crack 2	0.05	0.05	0.05	0.20
Crack 3	-	0.05	0.15	0.20
Crack 4	-	0.05	0.10	0.10
Crack 5	-	0.05	0.10	0.10
Crack 6	-	0.05	0.10	0.10

Appendix H – Temperature and strain measurements for curing week of outdoor exposure samples

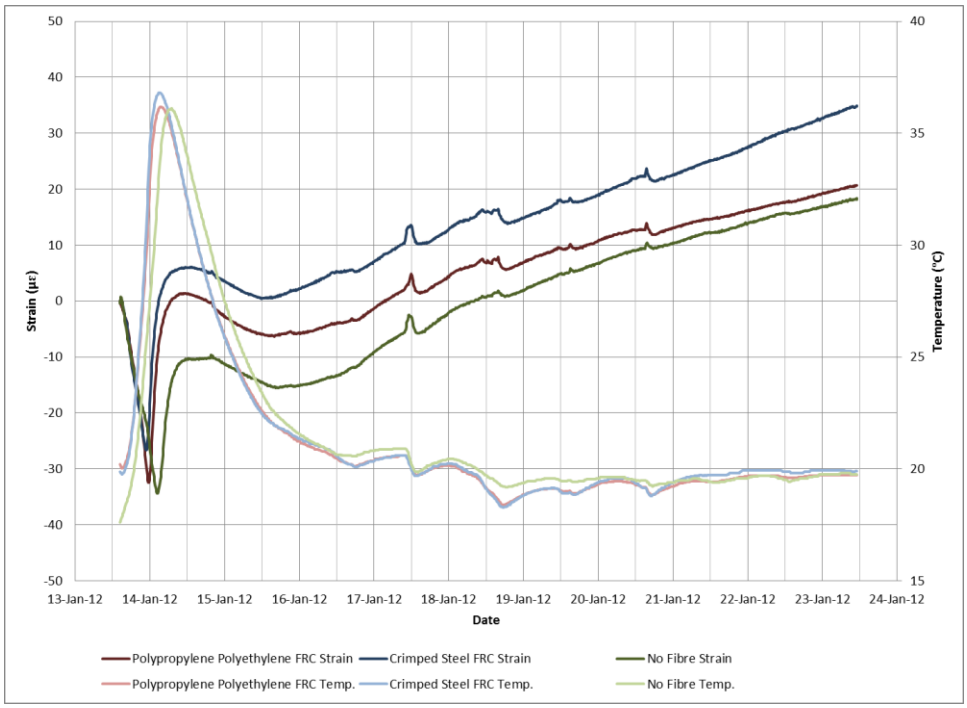

Figure A.1 – Temperature and strain measurements for curing week of outdoor exposure samples

Appendix I – Temperature cycles for cyclic freezing and thawing testing

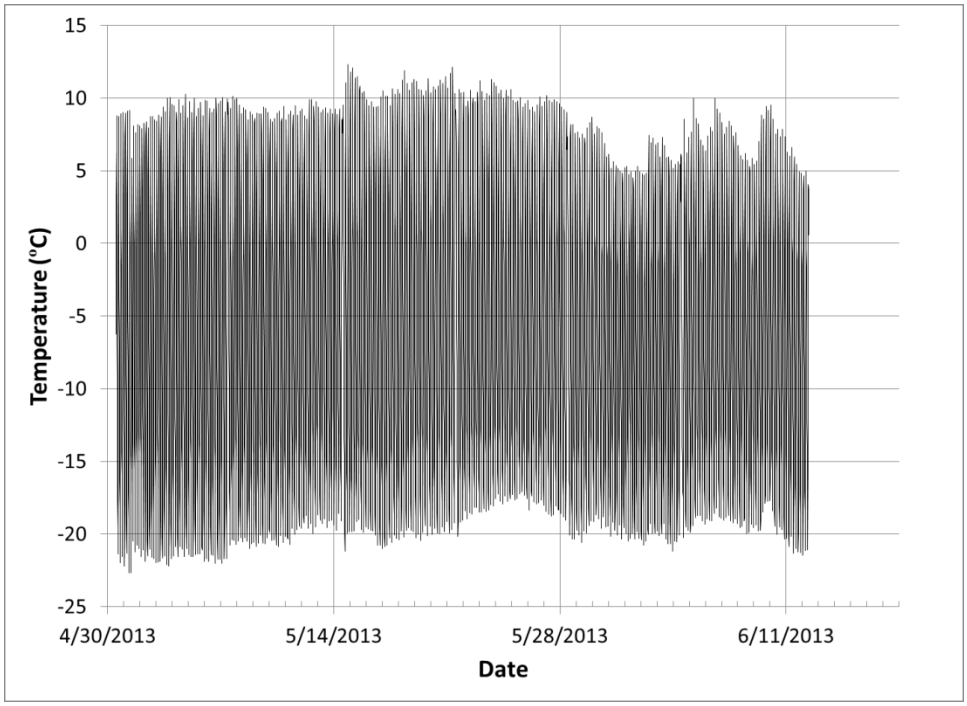

Figure A.2 – Temperature cycles for set one of cyclic freezing and thawing testing

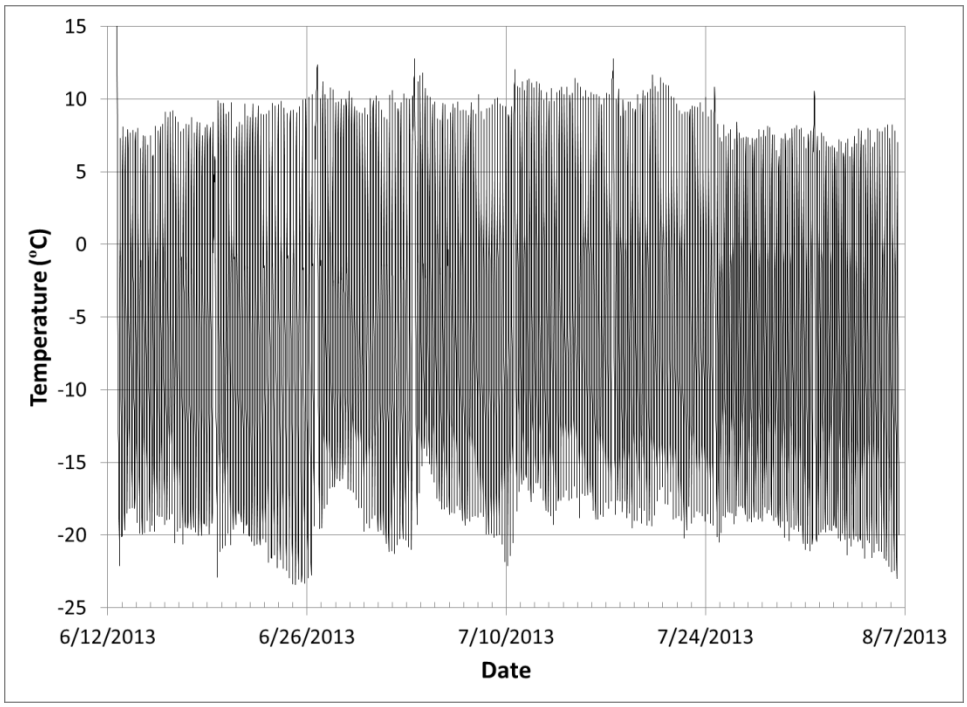

Figure A.3 – Temperature cycles for set two of cyclic freezing and thawing testing

Appendix J – Mass change of samples for cyclic freezing and thawing testing

Table A.0.33 – Mass change of samples for set one of cyclic freezing and thawing testing

Days	Cycles	NF	PP	St
0	0	0.00	0.00	0.00
7	57	-24.60	-13.60	-16.20
14	107	-23.63	-10.97	-14.27
21	154	-23.30	-7.90	-12.77
28	200	-23.73	-7.20	-14.13
35	249	-31.43	-12.53	-24.00
43	302	-23.83	-4.90	-18.23

Table A.0.34 – Mass change of samples for set two of cyclic freezing and thawing testing

Days	Cycles	HS	PVA	SS	BS
0	0	0.00	0.00	0.00	0.00
7	38	-1.93	-2.07	-1.67	-0.27
14	73	-4.63	-0.67	-0.73	-0.33
21	108	-1.67	2.13	-0.07	1.83
28	146	-3.30	0.37	-1.37	-0.70
35	184	-3.67	1.10	-1.40	-2.60
42	223	-5.03	1.40	-2.90	-2.37
49	267	-5.77	-0.17	-4.53	-2.80
57	304	-7.40	3.77	-5.73	-3.70

Appendix K – Relative dynamic modulus of elasticity of samples for cyclic freezing and thawing testing

Table A.0.35 – Relative dynamic modulus of elasticity of samples for set one of cyclic freezing and thawing testing

Days	Cycles	NF	PP	St
0	0	100.00%	100.00%	100.00%
7	57	92.33%	93.42%	92.57%
14	107	92.33%	93.14%	92.57%
21	154	92.05%	92.58%	92.29%
28	200	92.05%	92.30%	92.29%
35	249	91.77%	92.02%	92.29%
42	302	91.49%	90.07%	92.29%

Table A.0.36 – Relative dynamic modulus of elasticity of samples for set two of cyclic freezing and thawing testing

Days	Cycles	HS	PVA	SS	BS
0	0	100.00%	100.00%	100.00%	100.00%
7	38	96.19%	98.80%	97.89%	98.49%
14	73	95.91%	98.50%	97.89%	97.89%
21	108	95.91%	97.01%	96.71%	98.49%
28	146	95.61%	98.50%	96.41%	97.59%
35	184	95.91%	97.01%	96.41%	97.30%
42	223	95.91%	97.60%	96.11%	96.41%
49	267	95.91%	96.72%	96.41%	95.81%
57	304	95.91%	96.41%	94.64%	97.00%

Appendix L – ACI 209.2R-92 shrinkage model calculations [56]

Volume = 1603125 mm^3
Surface Area = 96750 mm^2
V/S = 16.75 mm
$f = 26e^{1.42x10^{-2}(V/S)} = 32.897$

$\gamma_{sh,tc}$ = 1.0 – 7 days wet curing
$\gamma_{sh,RH}$ = 0.635 – RH 75%
$\gamma_{sh,RH}$ = 1.043 – RH 35%
$\gamma_{sh,vs}$ = 1.109 – V/S
$\gamma_{sh,s}$ = 1.051 – 100 mm slump (assumed)
$\gamma_{sh,\psi}$ = 1.15 – 50% fine aggregate ratio
$\gamma_{sh,c}$ = 1.03 – 459 kg/m^3 cementitious material
$\gamma_{sh,\alpha}$ = 1.0 – Air content (1.0 minimum value)

$\gamma_{sh} = \gamma_{sh,tc}\ \gamma_{sh,RH}\ \gamma_{sh,vs}\ \gamma_{sh,s}\ \gamma_{sh,\psi}\ \gamma_{sh,c}\ \gamma_{sh,\alpha}$

<u>RH 75%</u>
γ_{sh} = 0.877
$\varepsilon_{shu} = 780\gamma_{sh} \times 10^{-6}$ = 0.00068406 mm/mm
α = 1.0
t = 35 days
t_c = 7 days

$$\varepsilon_{sh}(t, t_c) = \frac{(t - t_c)^{\alpha}}{f + (t - t_c)^{\alpha}} \varepsilon_{shu}$$

ε_{sh} (35,7) = 0.031%

<u>RH 35%</u>
γ_{sh} = 1.44
$\varepsilon_{shu} = 780\gamma_{sh} \times 10^{-6}$ = 0.0011232 mm/mm
α = 1.0
t = 35 days
t_c = 7 days

$$\varepsilon_{sh}(t, t_c) = \frac{(t - t_c)^{\alpha}}{f + (t - t_c)^{\alpha}} \varepsilon_{shu}$$

ε_{sh} (35,7) = 0.052%